

LEARNING EXTREMAL GRAPHICAL STRUCTURES IN HIGH DIMENSIONS

BY SEBASTIAN ENGELKE^{1,a}, MICHAËL LALANCETTE^{2,b} AND STANISLAV VOLGUSHEV^{2,c}

¹Research Center for Statistics, University of Geneva [a](mailto:sebastian.engelke@unige.ch)sebastian.engelke@unige.ch

²Department of Statistical Sciences, University of Toronto [b](mailto:lalancette@utstat.toronto.edu)lalancette@utstat.toronto.edu; [c](mailto:stanislav.volgushev@utoronto.ca)stanislav.volgushev@utoronto.ca

Extremal graphical models encode the conditional independence structure of multivariate extremes. For the popular class of Hüsler–Reiss models, we propose a majority voting algorithm for learning the underlying graph from data through L^1 regularized optimization. We derive explicit conditions that ensure consistent graph recovery for general connected graphs. A key statistic in our method is the empirical extremal variogram. We prove non-asymptotic concentration bounds for this quantity that hold for general multivariate Pareto distributions and are of independent interest.

1. Introduction. Motivated by extreme value theory, the univariate tail of a random variable can be well described by parametric generalized extreme value and Pareto distributions. For effective quantification of the risk related to floods (Keef et al., 2013), heatwaves (Engelke et al., 2019) or financial crises (Zhou, 2010), understanding the interplay between many different risk factors becomes crucial. Mathematically this amounts to an analysis of the tail dependence between components of a random vector $\mathbf{X} = (X_1, \dots, X_d)$, which can become arbitrarily complex in larger dimensions d . Sparsity or dimension reduction are then required to obtain statistically sound and practically feasible methods; see Engelke and Ivanovs (2021) for a review of recent developments.

One popular approach to obtaining interpretable dependence models for a random vector \mathbf{X} in high dimensions relies on graphical modeling (Lauritzen, 1996). Conditional independence relations between pairs of variables are described by the absence of edges in a graph $G = (V, E)$ with node set $V = \{1, \dots, d\}$ and edges $E \subset V \times V$. Graphical models are particularly well studied for multivariate normal distributions where conditional independence relations are encoded as zeroes in the precision matrix (Lauritzen, 1996, Chapter 5).

For distributions arising in the setting of extreme value analysis, graphical modeling is more challenging. Broadly speaking, there are two main approaches to modeling asymptotically dependent extremes. The first approach considers component-wise maxima of blocks of random vectors and leads to the notion of max-stable distributions; we refer the reader to Beirlant et al. (2004, Chapter 8) and de Haan and Ferreira (2006, Chapter 6). For such distributions, Gissibl and Klüppelberg (2018), Klüppelberg and Lauritzen (2019) and Améndola et al. (2022) study max-linear models on directed acyclic graphs. The distributions considered in this line of work do not have densities, and a general result by Papastathopoulos and Strokorb (2016) shows that there exist no non-trivial density factorization of max-stable distributions on graphical structures.

The second approach relies on multivariate Pareto distributions, which arise as limits of conditional distributions of \mathbf{X} given that at least one its components is large (Rootzén and Tajvidi, 2006; Rootzén et al., 2018). While multivariate Pareto distributions inherit certain

MSC2020 subject classifications: Primary 60G70, 62H22; secondary 62G30 .

Keywords and phrases: Multivariate Pareto distribution, Peaks over threshold modeling, Hüsler-Reiss distribution, Graphical lasso, Neighborhood selection.

structural properties such as homogeneity from their definition through limits, their class is still very flexible and too large to allow for efficient and interpretable inference in high dimensions. Classical conditional independence is not suited for these distributions since they are not supported on a product space. [Engelke and Hitz \(2020\)](#) overcome this challenge by introducing new notions of conditional independence and extremal graphical models. They show that these definitions naturally link to density factorizations and enable efficient inference on extremal graphical models; see also [Asenova et al. \(2021\)](#). Certain extremal graphical structures are known to arise as the extremes of regularly varying Markov trees ([Segers, 2020](#)) and Markov random fields on block graphs ([Asenova and Segers, 2021](#)).

The underlying graph plays a key role in graphical modeling. This graph is typically unknown and needs to be estimated in a data driven way. One may consider different levels of generality for the class of graph structures. [Figure 1](#) shows four different graphs from a simple tree structure, over decomposable graphs, and up to the most general case of possibly non-decomposable graphs. In general, estimating more complex graphs requires more assumptions on the underlying distribution. In the non-extreme world, two important cases correspond to graphical models on trees, which can be estimated non-parametrically ([Liu et al., 2011](#)), and multivariate normal distributions, for which general graphs can be estimated through the corresponding precision matrix; see [Meinshausen and Bühlmann \(2006\)](#), [Yuan and Lin \(2007\)](#) and [Friedman et al. \(2008\)](#) among many others.

To date, we are aware of only two approaches to estimating extremal graph structures, both of which are only applicable to fairly simple graphs or have other limitations. In their application to river discharge data, [Engelke and Hitz \(2020\)](#) use an ad-hoc forward selection method where edges are added one after the other to create a simple block graph (second from the left in [Figure 1](#)). Block graphs are decomposable and the intersection of the cliques are only allowed to be single nodes. As such, they are fairly close to tree structures and have too limited flexibility for general applications. This was also noted in several discussion contributions in [Engelke and Hitz \(2020\)](#), pointing out the need for estimation techniques for more general graphs. In addition to these limitations, the forward selection procedure is a heuristic method that does not guarantee consistent structure recovery. [Engelke and Volgushev \(2020\)](#) study structure estimation of extremal tree models. They introduce the extremal variogram and show that it can be used in a minimum spanning tree algorithm for consistent tree recovery in a completely non-parametric way.

For more general graphs, such as the two graphs on the right of [Figure 1](#), no methods that guarantee consistent graph recovery exist in the world of extremes. In the present paper, we propose a general methodology to learn arbitrary graphs for the class of Hüsler–Reiss distributions ([Hüsler and Reiss, 1989](#)). Those distributions share many attractive properties of multivariate normal distributions and have been widely used in modeling multivariate and spatial extremes (e.g., [Davison et al., 2012](#); [Engelke et al., 2015](#)). They are parametrized by a $d \times d$ -dimensional variogram matrix Γ , which can be shown to contain the underlying graph structure. More precisely, [Engelke and Hitz \(2020\)](#) show that for any $m \in V$, the Farris transform $\Sigma^{(m)} \in \mathbb{R}^{d \times d}$ ([Farris et al., 1970](#)) with entries

$$(1.1) \quad \Sigma_{ij}^{(m)} = \frac{1}{2} (\Gamma_{im} + \Gamma_{jm} - \Gamma_{ij}), \quad i, j \in V,$$

encodes information about the extremal conditional independence structure through sparsity patterns in the entries and row-sums of $(\Sigma_{\setminus m, \setminus m}^{(m)})^{-1}$.

In the present paper, we develop a structure learning algorithm that leverages this information and leads to consistent recovery of arbitrary graphs. Due to the special nature of Hüsler–Reiss distributions, the entire graph structure cannot be recovered from the zero pattern of a single matrix $(\Sigma_{\setminus m, \setminus m}^{(m)})^{-1}$, and estimators across all values of $m \in V$ need to be

combined. Our approach therefore uses a majority voting algorithm to combine estimated sub-graphs for all $m \in V$, which are obtained from base learners. In principle, any base learner can be used, and we provide a thorough theoretical investigation for two of the most popular choices: neighborhood selection (Meinshausen and Bühlmann, 2006) and graphical lasso (Yuan and Lin, 2007; Friedman et al., 2008). We prove that consistent graph recovery is possible even when the dimension grows exponentially in the number of extreme samples.

A key difficulty in our analysis lies in the fact that, in practice, we only observe realizations whose tail can be approximated by a Hüsler–Reiss distribution, rather than from the latter, limiting model itself. Hence, estimators of the variogram matrix Γ use only the largest observations from a sample, which need to be transformed marginally. An additional difficulty arises from the special structure of the extremal variogram, which makes standard concentration results in the extremes literature (Goix et al., 2015; Clémençon et al., 2021; Lhaut et al., 2021) inapplicable. A substantial part of our theoretical contribution is therefore devoted to derive concentration bounds for an empirical estimator of Γ . Our bounds provide a crucial ingredient for the proof of consistent graph recovery in increasing dimensions. The results are also of broader interest in multivariate extremes beyond the case of Hüsler–Reiss distributions. For instance, the tail bounds we derive play a crucial role in the theoretical developments in Engelke and Volgushev (2020) and we expect that they can be leveraged elsewhere.

The rest of the paper is organized as follows. Section 2 contains necessary background information on multivariate extreme value distributions in general and Hüsler–Reiss distributions in particular. The estimation methodology is described in detail in Section 3. Section 4 contains all theoretical results while finite-sample performance of the proposed methods is illustrated in a simulation study in Section 5. Illustrations on two real data sets are provided in Section 6, and potential extensions and directions for future work are described in Section 7. Some additional numerical results as well as all proofs are delegated to the Supplementary Material. All references to sections, results, equations, etc. starting with the letter ‘‘S’’ are pointing to this supplement.

The methods of this paper are implemented in the R package `graphicalExtremes` and all numerical results and figures can be reproduced using the code on https://github.com/sebastian-engelke/extremal_graph_learning.

Notation. Throughout the paper we use the following notation. For square matrices A with real eigenvalues, let $\lambda_{\min}(A)$ denote the smallest eigenvalue of A . The notation $\|\mathbf{x}\|_{\infty}$ and $\|A\|_{\infty}$ is used to denote the element-wise sup-norm of vectors \mathbf{x} and matrices A . $\|A\|_p$ denotes the L^p/L^p operator norm of a (not necessarily square) matrix A . For a natural number $d \geq 1$ let $[d] := \{1, \dots, d\}$. For vectors $\mathbf{x} = (x_1, \dots, x_d)^{\top} \in \mathbb{R}^d$ (or similarly for random vectors $\mathbf{X} = (X_1, \dots, X_d)^{\top}$) and subsets $J = \{j_1, \dots, j_k\} \subseteq [d]$, define the vector $\mathbf{x}_J := (x_{j_1}, \dots, x_{j_k})^{\top}$ where $j_1 < j_2 < \dots < j_k$. Vectors with all entries 1 and 0 are denoted with $\mathbf{1}$ and $\mathbf{0}$, respectively; the dimension will be clear from the context. Inequalities between

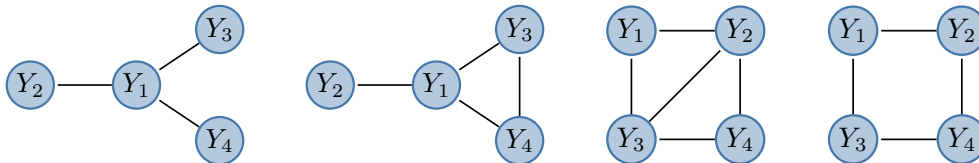


FIG 1. Four graph structures on the node set $V = \{1, \dots, 4\}$. From left to right: tree graph, block graph, decomposable graph, non-decomposable graph.

vectors are understood component-wise. The notation $\mathbf{x}_{\setminus J}$ is used to denote the vector $\mathbf{x}_{V \setminus J}$, and if $J = \{j\}$ we also write $\mathbf{x}_{\setminus j}$. We use similar notations to index rows and columns of matrices A .

2. Background.

2.1. *Multivariate Pareto distributions and domains of attraction.* Let $\mathbf{Y} = (Y_j : j \in V)$ be a d -dimensional random vector indexed by $V = \{1, \dots, d\}$ with support contained in the space $\mathcal{L} = \{\mathbf{y} \geq 0 : \|\mathbf{y}\|_\infty > 1\}$. The random vector \mathbf{Y} is said to have a multivariate Pareto distribution if $\mathbb{P}(Y_1 > 1) = \dots = \mathbb{P}(Y_d > 1)$ and if it satisfies the homogeneity property

$$(2.1) \quad \mathbb{P}(\mathbf{Y} \in tA) = t^{-1} \mathbb{P}(\mathbf{Y} \in A), \quad t \geq 1,$$

where for any Borel subset $A \subset \mathcal{L}$ we define $tA = \{t\mathbf{y} : \mathbf{y} \in A\}$ (Rootzén and Tajvidi, 2006). The homogeneity implies that for any $i \in V$ the univariate conditional margin satisfies $\mathbb{P}(Y_i \leq x \mid Y_i > 1) = 1 - 1/x$ for $x \geq 1$, that is, $Y_i \mid Y_i > 1$ follows a standard Pareto distribution. The class of multivariate Pareto distributions is very rich and contains parametric sub-families such as the extremal logistic (Tawn, 1990) and Dirichlet distributions (Coles and Tawn, 1991). Of particular interest in the present paper is the family of Hüsler–Reiss distributions (Hüsler and Reiss, 1989). Those distributions are often considered as the Gaussian distributions of extremes and will be described in Section 2.3 in detail.

Multivariate Pareto distributions arise as natural models in the study of multivariate extreme events, since they are the only possible limits of so-called threshold exceedances. To formalize this, consider a random vector $\mathbf{X} = (X_j : j \in V)$ in \mathbb{R}^d with eventually continuous marginal distributions F_i and define $F(\mathbf{x}) = (F_1(x_1), \dots, F_d(x_d))$. If for some random vector \mathbf{Y} the limit relation

$$(2.2) \quad \lim_{q \downarrow 0} \mathbb{P}(F(\mathbf{X}) \leq 1 - q/\mathbf{x} \mid F(\mathbf{X}) \not\leq 1 - q) = \mathbb{P}(\mathbf{Y} \leq \mathbf{x}),$$

holds at all continuity points $\mathbf{x} \in \mathcal{L}$ of $\mathbb{P}(\mathbf{Y} \leq \cdot)$, we say that \mathbf{X} is in the domain of attraction of \mathbf{Y} .

In this case, the limit \mathbf{Y} is necessarily a multivariate Pareto distribution, and conversely any multivariate Pareto distribution appears as a limit; see Engelke and Volgushev (2020, Proposition 6) for a more formal statement. Note that the margins of \mathbf{X} are standardized via a marginal transformation, so this is really an assumption on the extremal dependence structure of \mathbf{X} . The notation $F(\mathbf{X}) \not\leq 1 - q$ means that at least one component of the vector $F(\mathbf{X})$ exceeds $1 - q$, equivalently at least one component X_j of \mathbf{X} exceeds its high marginal quantile $F_j^{-1}(1 - q)$, $j \in V$. The above limit can thus be interpreted as a model for realizations of \mathbf{X} with at least one extreme component.

There are several other popular objects that are routinely used to describe tails of multivariate random vectors. For instance, one can show that (2.2) implies existence of the limit

$$(2.3) \quad L(\mathbf{x}) = \lim_{q \downarrow 0} q^{-1} \mathbb{P}(F(\mathbf{X}) \not\leq 1 - q\mathbf{x}), \quad \mathbf{x} \in [0, \infty)^d.$$

The function L is called the stable tail dependence function of \mathbf{X} and is a popular object in the study of multivariate extremes (Huang, 1992; Einmahl et al., 2012; Fougères et al., 2015). The link between the distribution of \mathbf{Y} and L is given by the relation

$$L(\mathbf{x}) = \frac{\mathbb{P}(\mathbf{Y} \not\leq 1/\mathbf{x})}{\mathbb{P}(Y_1 > 1)}, \quad \mathbf{x} \in \mathcal{L}.$$

2.2. *Extremal graphical models.* Since the support space \mathcal{L} of a multivariate Pareto distribution \mathbf{Y} is not a product space, the set of auxiliary random vectors $\mathbf{Y}^{(m)} = (\mathbf{Y} \mid Y_m > 1)$, $m \in V$, plays an important role in the analysis. In fact, they are the basis for the definition of conditional independence for the random vector \mathbf{Y} in [Engelke and Hitz \(2020\)](#). For disjoint sets $A, B, C \subset V$, we say that \mathbf{Y}_A is conditionally independent of \mathbf{Y}_C given \mathbf{Y}_B if the usual conditional independence holds for all auxiliary vectors:

$$\forall m \in V : \mathbf{Y}_A^{(m)} \perp\!\!\!\perp \mathbf{Y}_C^{(m)} \mid \mathbf{Y}_B^{(m)}.$$

In this case, we speak of extremal conditional independence and denote it by $\mathbf{Y}_A \perp_e \mathbf{Y}_C \mid \mathbf{Y}_B$.

In graphical modeling, conditional independence is connected to graph structures to define sparse probabilistic models ([Lauritzen, 1996](#)). An undirected graph $G = (V, E)$ is a set of nodes $V = \{1, \dots, d\}$ and a collection of edges $E \subset V \times V$ of unordered pairs of distinct nodes. With the notion of extremal conditional independence, we define an extremal graphical model as a multivariate Pareto distribution \mathbf{Y} that satisfies the pairwise Markov property,

$$Y_i \perp_e Y_j \mid \mathbf{Y}_{\setminus\{i,j\}}, \text{ if } (i, j) \notin E.$$

When \mathbf{Y} possesses a positive continuous density, the graph G is necessarily connected. In this case, the pairwise Markov property is equivalent to the stronger global Markov property ([Lauritzen, 1996](#), Chapter 3). If G is in addition decomposable, then the density factorizes on the graph into lower-dimensional densities, and inference is considerably more efficient thanks to the sparsity; see [Engelke and Hitz \(2020\)](#) for details.

A summary statistic for extremal dependence in \mathbf{Y} that will turn out to be useful for graph structure learning is the extremal variogram ([Engelke and Volgushev, 2020](#)). The extremal variogram rooted at node $m \in V$ is defined as the matrix $\Gamma^{(m)}$ with entries

$$(2.4) \quad \Gamma_{ij}^{(m)} = \mathbb{V}\text{ar} \left\{ \log Y_i^{(m)} - \log Y_j^{(m)} \right\}, \quad i, j \in V,$$

whenever the right-hand side exists and is finite. For an extremal graphical model on a tree, for any $m \in V$, the minimum spanning tree with weights $\Gamma_{ij}^{(m)}$, $i, j \in V$, recovers the underlying tree structure corresponding to extremal conditional independence. This can be exploited for non-parametric consistent tree recovery without distributional assumptions ([Engelke and Volgushev, 2020](#)). Extremal variograms will also play a crucial role in learning general extremal graph structures.

2.3. *Hüsler–Reiss distributions.* Let \mathcal{S}_0^d be the set of symmetric $d \times d$ -matrices with zero diagonal and non-negative entries. A conditionally negative definite matrix $\Gamma \in \mathcal{S}_0^d$ is defined by the property that $\mathbf{x}^\top \Gamma \mathbf{x} \leq 0$ for all $\mathbf{x} \in \mathbb{R}^d$ with $\mathbf{x}^\top \mathbf{1} = 0$. If the inequality is strict except for $\mathbf{x} = \mathbf{0}$, then Γ is in the cone $\mathcal{C}^d \subset \mathcal{S}_0^d$ of strictly conditionally negative definite matrices, which we will also call variogram matrices. Let further \mathcal{P}^{d-1} denote the space of symmetric, strictly positive definite $(d-1) \times (d-1)$ -matrices.

The family of d -dimensional Hüsler–Reiss (Pareto) distributions consists of multivariate Pareto distributions parametrized by $\Gamma \in \mathcal{C}^d$ ([Hüsler and Reiss, 1989](#)). For each $m \in V$, the Farris transform ([Farris et al., 1970](#)) is a function $\varphi_m : \mathcal{C}^d \rightarrow \varphi_m(\mathcal{C}^d)$ that maps a given Γ to the matrix $\Sigma^{(m)}$ by the mapping in (1.1). The image $\varphi_m(\mathcal{C}^d)$ consists of all matrices $\Sigma^{(m)} \in \mathbb{R}^{d \times d}$ whose m th row and column contain zeros, and such that the submatrix $\Sigma_{\setminus m, \setminus m}^{(m)}$ is an element of \mathcal{P}^{d-1} and thus invertible. Let $\Theta^{(m)}$ be obtained by inverting that submatrix and adding back the row and column of zeros in the m th position, i.e., $\Theta^{(m)} \in \mathbb{R}^{d \times d}$ is defined by

$$(2.5) \quad \Theta_{\setminus m, \setminus m}^{(m)} = (\Sigma_{\setminus m, \setminus m}^{(m)})^{-1},$$

and $\Theta_{im}^{(m)} = \Theta_{mi}^{(m)} = 0$, $i \in V$. We note that the Farris transform φ_m is a bijection with inverse $\varphi_m^{-1} : \varphi_m(\mathcal{C}^d) \rightarrow \mathcal{C}^d$ given by the mapping

$$(2.6) \quad \Sigma \mapsto \mathbf{1} \text{diag}(\Sigma)^\top + \text{diag}(\Sigma) \mathbf{1}^\top - 2\Sigma.$$

This mapping is the same for every $m \in V$ and can be extended to the space of all positive semi-definite symmetric matrices Σ , in which case we call it the inverse Farris transform φ^{-1} .

The density of a Hüsler–Reiss distributed \mathbf{Y} with parameter matrix $\Gamma \in \mathcal{C}^d$ exists, and for any $m \in V$ it can be expressed as

$$(2.7) \quad f_{\mathbf{Y}}(\mathbf{y}) \propto y_m^{-2} \left(\prod_{i \neq m} y_i^{-1} \right) \exp \left\{ -\frac{1}{2} \tilde{\mathbf{y}}^\top \Theta^{(m)} \tilde{\mathbf{y}} \right\},$$

where $\tilde{\mathbf{y}} = \log \mathbf{y} - \mathbf{1} \log y_m + \Gamma_{Vm}/2$. The matrix $\Sigma^{(m)}$ is the covariance matrix of a transformation of the auxiliary random vector given by $(\log\{Y_i^{(m)}/Y_m^{(m)}\} : i \in V)$. From this it is easy to see that extremal variograms in (2.4) at nodes m are given by $\varphi_m^{-1}(\Sigma^{(m)})$, $m \in V$, and therefore they are all equal to the parameter matrix of the Hüsler–Reiss distribution, that is, $\Gamma = \Gamma^{(1)} = \dots = \Gamma^{(d)}$.

The importance of the matrices $\Sigma^{(m)}$ and $\Theta^{(m)}$ comes from the fact that the latter contains the graphical structure of the Hüsler–Reiss distribution \mathbf{Y} in its sparsity pattern. Indeed, for any fixed node $m \in V$ and $i \neq j$, [Engelke and Hitz \(2020, Proposition 3\)](#) show that

$$(2.8) \quad Y_i \perp_e Y_j \mid \mathbf{Y}_{\setminus\{i,j\}} \iff \begin{cases} \Theta_{ij}^{(m)} = 0, & \text{if } i, j \neq m, \\ \sum_{\ell=1}^d \Theta_{i\ell}^{(m)} = 0, & \text{if } j = m. \end{cases}$$

Relation (2.8) provides the key to learning general graphs for Hüsler–Reiss distributions through estimating sparse versions of $\Theta^{(m)}$.

The following equivalent parametrization of the Hüsler–Reiss distribution was proposed by [Hentschel \(2021\)](#); see also [Röttger et al. \(2021\)](#) for details. Consider the $d \times d$ matrix Θ with entries

$$(2.9) \quad \Theta_{ij} = \Theta_{ij}^{(m)}, \quad i, j \neq m,$$

and note that it is well-defined since $\Theta_{ij}^{(m)} = \Theta_{ij}^{(m')}$ for $i, j \notin \{m, m'\}$ by [Engelke and Hitz \(2020, Lemma 1\)](#). The matrix Θ is symmetric, positive semi-definite with rank $d - 1$, and it has zero row sums $\Theta \mathbf{1} = 0$. Let $P = I_d - \mathbf{1} \mathbf{1}^\top / d$. Then there is a one-to-one correspondence between the parameter matrix Γ and the matrix Θ given by $\Theta = (P(-\Gamma/2)P)^+$, where A^+ is the Moore–Penrose pseudoinverse of a matrix A . The matrix Θ uniquely defines the Hüsler–Reiss distribution since the parameter matrix can be recovered through the inverse Farris transform in (2.6) by $\Gamma = \varphi^{-1}(\Theta^+)$. Moreover, it contains the graphical structure through the simple relation

$$(2.10) \quad Y_i \perp_e Y_j \mid \mathbf{Y}_{\setminus\{i,j\}} \iff \Theta_{ij} = 0.$$

The matrix Θ is therefore called the Hüsler–Reiss precision matrix of \mathbf{Y} .

3. Learning Hüsler–Reiss graphical models.

3.1. *EGLearn: a majority voting algorithm.* For a Hüsler–Reiss distribution, in view of (2.8), a sparse estimate of $\Theta^{(m)}$ contains information on the conditional independence structure between nodes i, j where $i, j \neq m$. This is equivalent to the presence or absence of edges in the corresponding extremal graphical model $G = (V, E)$ that are not related to the m th node. This fact can be exploited by obtaining a sparse estimate of $\Theta^{(m)}$, which establishes

a link to the problem of sparse precision matrix estimation and allows us to borrow tools from the Gaussian graphical models literature. In our case, it is natural to combine estimated sparsity patterns across different values of m to infer extremal conditional independence for all possible values of $i, j \in V$. We propose to do this through a majority voting algorithm.

More formally, for a given $m \in V$ and estimator $\hat{\Gamma}$ of the variogram matrix Γ , consider an arbitrary algorithm \mathcal{A} , called base learner in what follows, that takes the submatrix $\hat{\Sigma}_{\setminus m, \setminus m}^{(m)}$, $\hat{\Sigma}^{(m)} := \varphi_m(\hat{\Gamma})$, as input and returns an estimator of the set of non-zero entries of $\Theta_{\setminus m, \setminus m}^{(m)}$. The output of this algorithm, denoted by $\hat{Z}^{(m)}$, will be represented as a $(d-1) \times (d-1)$ matrix with entries 1 in positions where $\Theta_{\setminus m, \setminus m}^{(m)}$ is estimated to be non-zero, and entries 0 elsewhere. This matrix is assumed to be symmetric. Two examples of possible base learner algorithms are neighborhood selection (Meinshausen and Bühlmann, 2006) and graphical lasso (Yuan and Lin, 2007; Friedman et al., 2008); they are formally introduced in Section 3.2 below. The base learner \mathcal{A} may require the choice of tuning parameters, as is the case for neighborhood selection and the graphical lasso, which can be fixed or data-dependent.

Augmenting the matrix $\hat{Z}^{(m)}$ with a row and column of zeros in the m th position, we obtain a $d \times d$ matrix $\tilde{Z}^{(m)}$. The entries of $\tilde{Z}^{(m)}$ outside its m th row and column are now considered as votes in favor or against certain edges in the graph G . Running the algorithm for each $m \in V$ results in d such matrices. Those are then combined into a final graph estimator $\hat{G} = (V, \hat{E})$ using majority voting: an edge (i, j) , $i \neq j$, is included in the final graph if and only if a 1 appears in position (i, j) of more than half of the $d-2$ matrices $\tilde{Z}^{(m)}$, $m \notin \{i, j\}$. The reason for excluding $\tilde{Z}^{(i)}$ and $\tilde{Z}^{(j)}$ from the voting for edge (i, j) is that by (2.8), zeroes in the m th row and column of $\Theta^{(m)}$ are not informative about conditional independence in \mathbf{Y} . The steps described above are summarized in the following algorithm.

Input: variogram estimate $\hat{\Gamma}$, base learner algorithm \mathcal{A}
Output: extremal graph estimate $\hat{G} = (V, \hat{E})$

- 1 initialize $\hat{G} := (V, \emptyset)$
- 2 **for** $m \in V$ **do**
- 3 obtain a $(d-1) \times (d-1)$ matrix $\hat{Z}^{(m)}$ from algorithm \mathcal{A} with $\hat{\Sigma}_{\setminus m, \setminus m}^{(m)}$ as input
- 4 obtain $\tilde{Z}^{(m)}$ by augmenting $\hat{Z}^{(m)}$ with a row and column of zeros in the m th position
- 5 **for** $i, j \in V$, $i < j$ **do**
- 6 **if** $\frac{1}{d-2} \#\{m \in V \setminus \{i, j\} : \tilde{Z}_{ij}^{(m)} = 1\} > \frac{1}{2}$ **then**
- 7 add an edge in \hat{E} between nodes i and j

Algorithm 1: EGlearn: algorithm for learning general extremal graphical models.

Figure 2 shows an illustration of the majority voting algorithm where the true underlying graph $G = (V, E)$ is the non-decomposable graph on the right-hand side of Figure 1. In this example, the algorithm would output the true graph $\hat{G} = G$ since exactly the true edges appear in the majority of the cases.

An alternative method that, based on (2.8), not only uses the information in $\Theta^{(m)}$ on nodes $i, j \in V$, but jointly enforces sparsity also on edges related to the m th node, turns out to be more involved and is discussed in Section 7.

3.2. Base learners for sparsity estimation. Two classical methods from Gaussian graphical modeling to obtain sparse estimators of precision matrices are neighborhood selection (Meinshausen and Bühlmann, 2006) and the graphical lasso (Yuan and Lin, 2007). The original

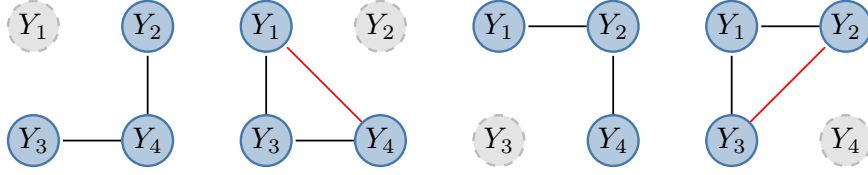


FIG 2. Illustration of the majority voting algorithm when the true underlying graph is the non-decomposable graph on the right-hand side of Figure 1. Left to right: graphical representation of the estimated matrices $\tilde{Z}^{(m)}$, where the gray node Y_m is not considered in the m th step, $m = 1, \dots, 4$; black and red edges indicate correctly and incorrectly estimated edges, respectively.

theoretical guarantees for consistent recovery of the sparsity pattern rely on Gaussian data and empirical covariances as input. Since the input estimator $\hat{\Sigma}_{\setminus m, \setminus m}^{(m)}$ for the base learner \mathcal{A} in our EGlearn in Algorithm 1 uses neither Gaussian data nor the empirical covariance, we discuss in this section how the assumptions of sparse estimators for Gaussian distributions can be relaxed. Related observations were made in Liu et al. (2012) for data that have a Gaussian copula but are not marginally Gaussian and Loh and Wainwright (2013) for discrete graphical models.

Throughout this section, we let $A \in \mathbb{R}^{p \times p}$ denote a symmetric, positive definite matrix and we are interested in the sparsity pattern of its inverse $B = A^{-1}$. We aim to use neighborhood selection and graphical lasso as the base learner algorithm \mathcal{A} in the framework of our EGlearn in Algorithm 1. In this case, in the m th step of the algorithm, the matrix A equals $\Sigma_{\setminus m, \setminus m}^{(m)}$ with $p = d - 1$, and the interest is in the sparsity pattern of $B = \Theta_{\setminus m, \setminus m}^{(m)}$.

3.2.1. Neighborhood selection. Neighborhood selection was originally proposed by Meinshausen and Bühlmann (2006) for estimating Gaussian graphical models. Although the motivation in Meinshausen and Bühlmann (2006) relies on properties of multivariate normal distributions and their conditional independence, the underlying principle can be used to estimate the sparsity pattern of the inverse of a general symmetric matrix. Indeed, for the positive definite matrix $A \in \mathbb{R}^{p \times p}$ with inverse B , we have the representation

$$\frac{-B_{\setminus \ell, \setminus \ell}}{B_{\ell \ell}} = (A_{\setminus \ell, \setminus \ell})^{-1} A_{\setminus \ell, \ell} = \arg \min_{\beta \in \mathbb{R}^{p-1}} \{ -2A_{\ell, \setminus \ell} \beta + \beta^\top A_{\setminus \ell, \setminus \ell} \beta \}, \quad \ell = 1, \dots, p.$$

The first equation follows from matrix computations using block inversion formulae (see, for instance, Lauritzen, 1996, Equation (C.4)) and the second from computing the gradient of the minimization problem. Hence, given access to an estimator \hat{A} , the sparsity pattern in $B_{\setminus \ell, \ell}$ can be estimated through the zero entries of

$$(3.1) \quad \hat{\theta} := \arg \min_{\theta \in \mathbb{R}^{p-1}} \{ -2\hat{A}_{\ell, \setminus \ell} \theta + \theta^\top \hat{A}_{\setminus \ell, \setminus \ell} \theta + \rho_\ell \|\theta\|_1 \},$$

where ρ_ℓ denotes a penalty parameter and the L^1 penalty is used for enforcing sparse solutions. The set $\hat{n}e(\ell)$ of indices of non-zero entries in $\hat{\theta}$ is then taken as an estimate of the non-zero pattern in the ℓ th row of B . The procedure is repeated for each variable ℓ . Since the matrix B is symmetric, pairs $(i, j), (j, i)$ are added to the estimated set of non-zero entries if and only if $i \in \hat{n}e(j)$ or $j \in \hat{n}e(i)$; see Algorithm 2 below.

To link the above approach to neighborhood selection as proposed in Meinshausen and Bühlmann (2006), assume that $\hat{\Sigma}$ is the sample covariance matrix of $\mathbf{W}_1, \dots, \mathbf{W}_n$, a sample

from a p -dimensional Gaussian distribution. Then regressing the variables $W_{1,\ell}, \dots, W_{n,\ell}$ on $\mathbf{W}_{1,\setminus\ell}, \dots, \mathbf{W}_{n,\setminus\ell}$ via the lasso amounts to solving the problem

$$\arg \min_{\beta \in \mathbb{R}^{p-1}} \left\{ \frac{1}{n} \sum_{i=1}^n (W_{i,\ell} - \beta^\top \mathbf{W}_{i,\setminus\ell})^2 + \rho_\ell \|\beta\|_1 \right\} = \arg \min_{\beta \in \mathbb{R}^{p-1}} \left\{ -2\widehat{\Sigma}_{\ell,\setminus\ell} \beta + \beta^\top \widehat{\Sigma}_{\ell,\setminus\ell} \beta + \rho_\ell \|\beta\|_1 \right\},$$

where the left-hand side in the equation above was originally considered in [Meinshausen and Bühlmann \(2006\)](#).

Input: Matrix $\widehat{A} \in \mathbb{R}^{p \times p}$, penalty parameters $(\rho_\ell)_{\ell=1,\dots,p}$
Output: Estimate \widehat{Z} of sparsity pattern of A^{-1}

- 1 initialize \widehat{Z} as a matrix of zeros
- 2 **for** $\ell = 1, \dots, p$ **do**
- 3 $\widehat{\theta} := \arg \min_{\theta \in \mathbb{R}^{p-1}} \{ -2\widehat{A}_{\ell,\setminus\ell} \theta + \theta^\top \widehat{A}_{\ell,\setminus\ell} \theta + \rho_\ell \|\theta\|_1 \}$
- 4 $\widehat{\text{ne}}(\ell) := \{j = 1, \dots, p : \theta_j \neq 0\}$
- 5 **for** $i = 1, \dots, p, j \neq i$ **do**
- 6 **if** $i \in \widehat{\text{ne}}(j)$ **or** $j \in \widehat{\text{ne}}(i)$ **then**
- 7 set $\widehat{Z}_{ij} = \widehat{Z}_{ji} = 1$

Algorithm 2: Sparsity pattern estimation through neighborhood selection.

3.2.2. *Graphical lasso.* As an alternative to running node-wise regressions as required for neighborhood selection, [Yuan and Lin \(2007\)](#) suggested to estimate the precision matrix $B = A^{-1}$ via penalized maximum likelihood, with a penalty on the off-diagonal, element-wise L^1 norm of the matrix:

$$(3.2) \quad \arg \min_{Q \in \mathcal{P}^{p-1}} \left\{ -\log \det Q + \text{tr}(\widehat{A}Q) + \rho \|Q\|_{1,\text{off}} \right\}, \quad \|Q\|_{1,\text{off}} := \sum_{i \neq j} |Q_{ij}|,$$

where \widehat{A} denotes an estimator of the matrix A . The name “graphical lasso” was subsequently given to the algorithm that efficiently solves this problem ([Friedman et al., 2008](#)).

In the original procedure of [Yuan and Lin \(2007\)](#), \widehat{A} denotes the sample covariance matrix of an i.i.d. sample of $N(0, A)$ random vectors. Subsequently, [Ravikumar et al. \(2011\)](#) proved that Gaussianity is not needed and the sparsity pattern of precision matrices can be recovered consistently as long as the data used to compute the empirical covariance matrix satisfy certain tail properties. A close look at the analysis of [Ravikumar et al. \(2011\)](#) further reveals that there is nothing special about empirical covariance matrices. More precisely, under certain technical conditions, the optimization in (3.2) yields an estimator of A^{-1} with the correct sparsity pattern, provided that \widehat{A} is any estimator of A that is close to A in element-wise sup-norm. These claim will be made precise in Proposition S2 of the Supplementary Material.

3.3. *The empirical extremal variogram.* The extremal variogram matrix $\Gamma^{(m)}$ rooted at node m is defined in (2.4) for a general, not necessarily Hüsler–Reiss, multivariate Pareto distribution \mathbf{Y} . In typical applications we do not observe data from \mathbf{Y} but rather from \mathbf{X} in the domain of attraction of \mathbf{Y} in the sense of (2.2). A simple computation then implies that

$$P(\mathbf{Y}^{(m)} \leq \mathbf{x}) = \lim_{q \downarrow 0} \mathbb{P} \left(\frac{q}{1 - F(\mathbf{X})} \leq \mathbf{x} \mid F_m(X_m) > 1 - q \right).$$

Let $(\mathbf{X}_t := (X_{t1}, \dots, X_{td}) : t \in [n])$ be a sample of independent copies of \mathbf{X} . Denoting by \widetilde{F}_i the left-continuous empirical distribution function of X_{1i}, \dots, X_{ni} , the sample

$$\left\{ \frac{k}{n} \frac{1}{1 - \widetilde{F}(\mathbf{X}_t)} : \widetilde{F}_m(X_{tm}) > 1 - k/n \right\},$$

with $\tilde{F}(\mathbf{x}) := (\tilde{F}_1(x_1), \dots, \tilde{F}_d(x_d))$, is an approximate sample from $\mathbf{Y}^{(m)}$ if k/n is sufficiently small. This motivates the empirical extremal variogram rooted at node m (Engelke and Volgushev, 2020), defined through

$$\hat{\Gamma}_{ij}^{(m)} := \widehat{\text{Var}}\left(\log(1 - \tilde{F}_i(X_{ti})) - \log(1 - \tilde{F}_j(X_{tj})) : \tilde{F}_m(X_{tm}) > 1 - k/n\right),$$

where $\widehat{\text{Var}}$ denotes the empirical variance with scaling equal to k^{-1} , the inverse of the sample size.

When \mathbf{Y} has a Hüsler–Reiss Pareto distribution, the population variograms $\Gamma^{(m)}$, $m \in V$, are all equal to the parameter matrix Γ . We therefore combine the estimators into the empirical (extremal) variogram

$$(3.3) \quad \hat{\Gamma} := \frac{1}{d} \sum_{m \in V} \hat{\Gamma}^{(m)}.$$

Concentration properties of this estimator will be derived in Section 4.2.

4. Consistent extremal graph recovery and concentration of empirical variograms.

In this section we provide theoretical guarantees for Algorithm 1 to correctly recover the true extremal graph G when either neighborhood selection or graphical lasso are used as base learners. Our main results on consistent graph recovery are collected in Section 4.1.

A key technical ingredient of the corresponding proofs is a general concentration bound for the empirical extremal variogram; see Theorem 3. This result is obtained under general domain of attraction conditions and does not require the limiting multivariate Pareto distribution to be from the Hüsler–Reiss family. This finding is of independent interest. For instance, the theory of high-dimensional extremal tree recovery in Engelke and Volgushev (2020) relies on Theorem 3 from the present paper.

As a second ingredient, we establish guarantees on the estimators provided by neighborhood selection and graphical lasso when the input matrices are not empirical covariances of i.i.d. Gaussian data. This is a straightforward consequence of the analysis in Ravikumar et al. (2011) for the graphical lasso but requires more work for neighborhood selection, since classical arguments in Meinshausen and Bühlmann (2006) explicitly rely on properties of the multivariate normal distribution. We provide a formal statement (Proposition S1) and a complete proof (Section S3) in the Supplementary Material.

4.1. *Consistent recovery of Hüsler–Reiss graphical models.* We start by collecting technical assumptions which are needed for graph recovery in the Hüsler–Reiss case. Throughout this subsection, assume that \mathbf{Y} is a Hüsler–Reiss Pareto distribution on \mathbb{R}^d with parameter matrix $\Gamma \in \mathcal{C}^d$ that is an extremal graphical model on the connected graph $G = (V, E)$. Recall the definitions of the precision matrix Θ and the matrices $\Sigma^{(m)}$ and $\Theta^{(m)}$ in Section 2.3.

Our first assumption is a second order condition that essentially controls the speed of convergence in (2.3). For notational reasons, it turns out to be more convenient to work with slightly different versions of the probabilities appearing in (2.3).

ASSUMPTION 1 (Extended second order). The marginal distribution functions F_1, \dots, F_d are continuous and there exist constants $\xi > 0$ and $K < \infty$ independent of d such that for all triples of distinct indices $J = (i, j, m)$ and $q \in (0, 1]$,

$$(4.1) \quad \sup_{\mathbf{x} \in [0, q^{-1}]^2 \times [0, 1]} \left| q^{-1} \mathbb{P}(F_J(\mathbf{X}_J) > 1 - q\mathbf{x}) - \frac{\mathbb{P}(\mathbf{Y}_J > 1/\mathbf{x})}{\mathbb{P}(\mathbf{Y}_1 > 1)} \right| \leq Kq^\xi,$$

where $F_J(\mathbf{x}_J) = (F_i(x_i), F_j(x_j), F_m(x_m))$.

This formulation differs from classical second order conditions in that the supremum is taken over sets that grow with q . For Hüsler–Reiss distributions it is implied by a standard second order condition on bounded sets (see Assumption 3 in the next section) which is routinely imposed in theoretical developments for multivariate extreme value theory (Einmahl et al., 2012; Fougères et al., 2015; Engelke and Volgushev, 2020); see Proposition 1 in Section 4.2 for details.

Depending on whether we use neighborhood selection or graphical lasso as base learners in Algorithm 1, additional assumptions are needed on the matrices $\Sigma^{(m)}$ that parametrize the limiting model Y . We start by discussing neighborhood selection.

Let s denote the maximal degree, that is, the largest number of edges connected to any node, of the graph G . For $m, \ell \in V$, $m \neq \ell$, define the set of all nodes, except for node m , that are connected to node ℓ as

$$S_{m,\ell} := \{i \in V \setminus \{m, \ell\} : \Theta_{i\ell} \neq 0\} \subset V \setminus \{m\}$$

and its complement $S_{m,\ell}^c$ taken in $V \setminus \{m\}$. Define the quantities $\theta_{\min}^{\text{ns}} := \min_{i,\ell:\Theta_{i\ell} \neq 0} |\Theta_{i\ell}| / \Theta_{\ell\ell}$ and

$$\begin{aligned} \lambda &:= \min_{m,\ell \in V, m \neq \ell} \lambda_{\min}(\Sigma_{S_{m,\ell}, S_{m,\ell}}^{(m)}), \\ \kappa &:= \max_{m,\ell \in V, m \neq \ell} \left\| \left\| \Sigma_{S_{m,\ell}, S_{m,\ell}}^{(m)} \right\| \right\|_{\infty}, \\ \vartheta &:= \max_{m,\ell \in V, m \neq \ell} \left\| \left\| (\Sigma_{S_{m,\ell}, S_{m,\ell}}^{(m)})^{-1} \right\| \right\|_{\infty}. \end{aligned}$$

Additionally, consider the neighborhood selection incoherence parameter

$$(4.2) \quad \eta^{\text{ns}} := \min_{m,\ell \in V, m \neq \ell} \eta_{m,\ell}^{\text{ns}}, \quad \eta_{m,\ell}^{\text{ns}} := 1 - \left\| \left\| \Sigma_{S_{m,\ell}, S_{m,\ell}}^{(m)} (\Sigma_{S_{m,\ell}, S_{m,\ell}}^{(m)})^{-1} \right\| \right\|_{\infty}.$$

Incoherence parameters of this sort are known to be a crucial ingredient for support recovery via the lasso (Zhao and Yu, 2006; Meinshausen and Bühlmann, 2006). In our theory below we will assume that η^{ns} is strictly positive; a technical relaxation to requiring sufficiently many $\eta_{m,\ell}^{\text{ns}}$ being positive is shown in the proof of Theorem 1.

The majority voting in Algorithm 1 applies the base learner algorithm to d distinct problems, namely for every $m \in V$. Using neighborhood selection as the base learner in turn requires the choice of $d - 1$ tuning parameters, resulting in a total of $d(d - 1)$ tuning parameters $\rho_{m,\ell}^{\text{ns}}$, $m \in V, \ell \in [d - 1]$, where $\rho_{m,1}^{\text{ns}}, \dots, \rho_{m,d-1}^{\text{ns}}$ correspond to the tuning parameters in the m th step of Algorithm 1. Define $\rho_{\min}^{\text{ns}} := \min_{m,\ell} \rho_{m,\ell}^{\text{ns}}$ and $\rho_{\max}^{\text{ns}} := \max_{m,\ell} \rho_{m,\ell}^{\text{ns}}$.

THEOREM 1. *Suppose that Assumption 1 holds and that $\eta^{\text{ns}} > 0$. Let $G^{\text{ns}}(\widehat{\Gamma})$ denote the estimated graph obtained through neighborhood selection in Algorithm 1 with penalty parameters $\rho_{m,\ell}^{\text{ns}}$. Then, as soon as*

$$\|\widehat{\Gamma} - \Gamma\|_{\infty} < C^{\text{ns}} := \frac{2}{3} \min \left\{ \frac{\lambda}{2s}, \frac{\eta^{\text{ns}}}{4\vartheta(1 + \kappa\vartheta)s}, \frac{\theta_{\min}^{\text{ns}} - \vartheta\rho_{\max}^{\text{ns}}}{2\vartheta(1 + \kappa\vartheta)}, \frac{\rho_{\min}^{\text{ns}}\eta^{\text{ns}}}{8(1 + \kappa\vartheta)^2} \right\},$$

we have $G^{\text{ns}}(\widehat{\Gamma}) = G$.

Assuming that $k \geq n^{\zeta}$ for some $\zeta > 0$, $\log d = o(k/(\log k)^8)$ and the quantities $\lambda, \kappa, \vartheta, \eta^{\text{ns}}$ are bounded away from zero and infinity, we have

$$\mathbb{P}(G^{\text{ns}}(\widehat{\Gamma}) = G) \rightarrow 1, \quad n \rightarrow \infty,$$

provided that $\rho_{\max}^{\text{ns}} < \theta_{\min}^{\text{ns}}/(2\vartheta)$ and $(k/n)^{\xi}(\log(n/k))^2 + \sqrt{\log d}/\sqrt{k} = o(\min(\rho_{\min}^{\text{ns}}, s^{-1}))$.

In the statement of the second part of the above theorem, we sacrificed generality for the sake of simplicity. Combining the first statement with the general concentration bounds on $\max_{m \in V} \|\widehat{\Gamma}^{(m)} - \Gamma^{(m)}\|_\infty$, which we derive in Section 4.2, one can obtain lower bounds on the probability of correct graph recovery that are explicit in all constants appearing above. We have opted against providing such explicit expressions because the resulting terms are lengthy and do not add much in terms of interpretability. In the same vein, the quantities $\lambda, \kappa, \vartheta, s, \eta^{\text{ns}}$ are for simplicity taken as the worst case over m, ℓ . It is possible to introduce versions of $\lambda, \kappa, \vartheta, s, \eta^{\text{ns}}$ that depend on m, ℓ . This would allow for sharper but more complex results; in particular, the incoherence parameters $\eta_{m,1}^{\text{ns}}, \dots, \eta_{m,d-1}^{\text{ns}}$ would need to be non-negative for only half of the values $m \in V$. The precise form of this statement is immediate from a close look at the proof in Section S2 of the Supplementary Material.

For interpreting the second part of the above theorem, note that $r_{k,n} := (k/n)^\xi (\log(n/k))^2 + (k^{-1} \log d)^{1/2}$ is the order at which $\|\widehat{\Gamma} - \Gamma\|_\infty$ concentrates with $(k/n)^\xi (\log(n/k))^2$ corresponding to the bias and $(k^{-1} \log d)^{1/2}$ to the stochastic part; see Theorem 3 and the discussion right after for additional details. The quantity $\theta_{\min}^{\text{ns}}$ can be interpreted as minimal signal strength among edges that are present in the graph. In order for such edges to be recovered with high probability, we need a minimal signal condition $\theta_{\min}^{\text{ns}} \gg r_{k,n}$. Similarly, the maximal edge degree s must satisfy $s^{-1} \gg r_{k,n}$. In general, such conditions on minimal signal and maximal edge degrees are unavoidable for consistent graph recovery. Conditions that are similar in spirit were also imposed in Meinshausen and Bühlmann (2006) for neighborhood selection and Ravikumar et al. (2011) for the graphical lasso.

We next discuss guarantees on structure recovery assuming graphical lasso as the base learner in Algorithm 1. Define the set of edges in the graph excluding edges containing node m , and augmented by self loops, by

$$S_m := \{(i, j) : i, j \in V \setminus \{m\}, \Theta_{ij} \neq 0\},$$

as well as its complement S_m^c taken in $(V \setminus \{m\})^2$. Let $\Omega^{(m)} := \Sigma^{(m)} \otimes \Sigma^{(m)}$ and define the quantities $\theta_{\min}^{\text{gl}} := \min_{i \neq j: \Theta_{ij} \neq 0} |\Theta_{ij}|$, $\kappa_\Sigma := \max_m \|\Sigma^{(m)}\|_\infty$ and $\kappa_\Omega := \max_m \|\Omega_{S_m, S_m}^{(m)}\|_\infty^{-1}$. The incoherence parameter for graphical lasso is defined as

$$(4.3) \quad \eta^{\text{gl}} := \min_{m \in V} \eta_m^{\text{gl}}, \quad \eta_m^{\text{gl}} := 1 - \left\| \Omega_{S_m^c, S_m}^{(m)} (\Omega_{S_m, S_m}^{(m)})^{-1} \right\|_\infty.$$

Similarly to neighborhood selection, such incoherence parameters play a crucial role in guarantees for consistent support recovery by the Gaussian graphical lasso (Ravikumar et al., 2011).

Using graphical lasso as the base learner in Algorithm 1 requires the choice of d tuning parameters $\rho_1^{\text{gl}}, \dots, \rho_d^{\text{gl}}$, one for each graphical lasso that is applied in the m th step of the loop. Define $\rho_{\min}^{\text{gl}} := \min_{m \in V} \rho_m^{\text{gl}}$ and $\rho_{\max}^{\text{gl}} := \max_{m \in V} \rho_m^{\text{gl}}$.

THEOREM 2. *Suppose that Assumption 1 holds and that $\eta^{\text{gl}} > 0$. Let $G^{\text{gl}}(\widehat{\Gamma})$ denote the estimated graph obtained through the graphical lasso as base learner in Algorithm 1 with penalty parameters $\rho_1^{\text{gl}}, \dots, \rho_d^{\text{gl}}$. Then, as soon as*

$$\|\widehat{\Gamma} - \Gamma\|_\infty < C^{\text{gl}} := \frac{2}{3} \min \left\{ \min_{i, m \in V, i \neq m} \Sigma_{ii}^{(m)}, \frac{\eta^{\text{gl}} \rho_{\min}^{\text{gl}}}{8}, \frac{1}{\chi_0 s} - \rho_{\max}^{\text{gl}}, \frac{\theta_{\min}^{\text{gl}}}{4\kappa_\Omega} - \rho_{\max}^{\text{gl}} \right\},$$

for $\chi_0 := 6\kappa_\Sigma \kappa_\Omega (1 \vee (9\kappa_\Sigma^2 \kappa_\Omega / \eta^{\text{gl}}))$, we have $G^{\text{gl}}(\widehat{\Gamma}) = G$.

Assuming that $k \geq n^\zeta$ for some $\zeta > 0$, $\log d = o(k/(\log k)^8)$ and the quantities $\min_{i \neq m} \Sigma_{ii}^{(m)}$, κ_Σ , κ_Ω , η^{gl} are bounded away from zero and infinity, we have

$$\mathbb{P}(G^{\text{gl}}(\widehat{\Gamma}) = G) \rightarrow 1, \quad n \rightarrow \infty,$$

provided that $\rho_{\max}^{\text{gl}} < (2\chi_0 s)^{-1} \wedge (\theta_{\min}^{\text{gl}}/8\kappa\Omega)$ and $(k/n)^\xi (\log(n/k))^2 + \sqrt{\log d}/\sqrt{k} = o(\rho_{\min}^{\text{gl}})$.

Similarly to the statements in Theorem 1, we opted for simplicity over generality. It is possible to obtain sharper statements for the second part by combining the statement in the first part with concentration results on the empirical variogram. Moreover, it suffices if a majority of the incoherence parameters $\eta_1^{\text{gl}}, \dots, \eta_d^{\text{gl}}$ are non-negative.

One important difference between the assumptions for consistent graph estimation via neighborhood selection and graphical lasso lies in the definition of corresponding incoherence parameters. While there are no general results stating that one parameter is always smaller than the other, simulations indicate that in the models we considered, the neighborhood selection incoherence parameter is more likely to be positive; see Section 5 for additional details. This is in line with the discussion in Ravikumar et al. (2011, Sections 3.1.1, 3.1.2) who show that in two examples, conditions required for consistent graph recovery via neighborhood selection are weaker than those required for graphical lasso.

Similarly to $\theta_{\min}^{\text{ns}}$, the quantity $\theta_{\min}^{\text{gl}}$ corresponds to a minimal signal strength condition. Both quantities are of the same order provided that all diagonal entries of $\Theta^{(m)}$ are bounded away from zero and infinity for all m . In Theorem 2, we find that assuming all other parameters fixed, $\theta_{\min}^{\text{gl}} \gg r_{k,n}$ and $s^{-1} \gg r_{k,n}$ are required for consistent graph recovery with graphical lasso as the base learner. This matches the requirements when neighborhood selection is the base learner; see the discussion following Theorem 1.

4.2. Concentration of the empirical variogram. In this section we present concentration results on the empirical extremal variogram $\widehat{\Gamma}^{(m)}$ in (4.3) when the data \mathbf{X} is in the domain of attraction of an arbitrary multivariate Pareto distribution \mathbf{Y} with extremal variogram matrices $\Gamma^{(m)}$, $m \in V$.

We first introduce some additional notation and technical assumptions. Define the R -function by

$$(4.4) \quad R(\mathbf{x}) = \lim_{q \downarrow 0} q^{-1} \mathbb{P}(F(\mathbf{X}) > 1 - q\mathbf{x}), \quad \mathbf{x} \in [0, \infty)^d.$$

This function can be recovered from the stable tail dependence function L appearing in (2.3) through simple manipulations with the inclusion-exclusion formula; for $d = 2$, their relationship simplifies to $R(x, y) = x + y - L(x, y)$. Additionally, we have $R(\mathbf{x}) = \mathbb{P}(\mathbf{Y} > 1/\mathbf{x})/\mathbb{P}(Y_1 > 1)$. The R -function is a popular object in describing multivariate extreme value distributions and turns out to be convenient for our theoretical analysis. In what follows, for $J \subset V$, let R_J denote the R -function corresponding to \mathbf{Y}_J . When J is a pair or a triple, we write R_{ij} and R_{ijm} for $R_{\{i,j\}}$ and $R_{\{i,j,m\}}$.

Assumption 1 is already sufficient to derive tail concentration bounds for the empirical extremal variogram, but sharper results are possible if the function R has pairwise densities satisfying a certain bound.

ASSUMPTION 2 (Bounds on densities). For each $i, j \in V, i \neq j$ the functions R_{ij} have mixed partial derivatives r_{ij} satisfying

$$r_{ij}(x, y) := \frac{\partial^2}{\partial x \partial y} R_{ij}(x, y) \leq \frac{K(\beta)}{x^\beta y^{1-\beta}}, \quad (x, y) \in (0, \infty)^2,$$

for constants $K(\beta)$ and every $\beta \in [-\varepsilon, 1 + \varepsilon]$, for some some $\varepsilon > 0$.

REMARK 1. Lemma S3 in the Supplementary Material shows that Assumption 2 is satisfied by any non-degenerate Hüsler–Reiss distribution; the value ε therein can be chosen arbitrarily large and the constant $K(\beta)$ will additionally depend on Γ . In addition, it is trivial to check that the assumption holds if the functions r_{ij} satisfy

$$r_{ij}(x, 1-x) \leq K_r(x(1-x))^\varepsilon, \quad x \in (0, 1),$$

for some positive constants K_r and ε .

We are now ready to state the main result in this section.

THEOREM 3. *Let Assumption 1 hold and $\zeta \in (0, 1]$ be arbitrary. There exist positive constants C , c and M only depending on K , ξ and ζ such that for any $k \geq n^\zeta$ and $\lambda \leq \sqrt{k}/(\log n)^4$,*

$$\mathbb{P}\left(\max_{m \in V} \|\widehat{\Gamma}^{(m)} - \Gamma^{(m)}\|_\infty > C \left\{ \left(\frac{k}{n}\right)^\xi (\log(n/k))^2 + \frac{(\log(n/k))^2(1+\lambda)}{\sqrt{k}} \right\}\right) \leq Md^3 e^{-c\lambda^2}.$$

If in addition Assumption 2 holds, there exists a positive constant \bar{C} only depending on K , ξ , ζ , ε and $K(\beta)$ such that for any k and λ as above,

$$\mathbb{P}\left(\max_{m \in V} \|\widehat{\Gamma}^{(m)} - \Gamma^{(m)}\|_\infty > \bar{C} \left\{ \left(\frac{k}{n}\right)^\xi (\log(n/k))^2 + \frac{1+\lambda}{\sqrt{k}} \right\}\right) \leq Md^3 e^{-c\lambda^2}.$$

This theorem is the main technical result of our paper, and the proof turns out to be surprisingly involved; especially when establishing the sharper bound under Assumption 2. A major difficulty stems from the use of empirical distribution functions to normalize the margins. As mentioned previously, this result is of general interest in structure learning for extremes. It provides a crucial ingredient in the analysis of tree learning in Engelke and Volgushev (2020) and should also prove useful in other settings such as estimation of extreme value distributions under total positivity constraints as in Röttger et al. (2021).

The term $(k/n)^\xi (\log(n/k))^2$ appearing in the upper bound above results from an upper bound on the bias in estimating $\Gamma^{(m)}$ due to the fact that we only observe data from the domain of attraction of Y , rather than from the distribution of Y directly. The second term involving λ in both cases arises from the stochastic error. We note that k corresponds to the effective number of observations used for estimation of $\Gamma^{(m)}$, and in that sense the term λ/\sqrt{k} appearing in the second tail bound corresponds to the typical \sqrt{k} convergence rates in extreme value theory.

We close this section by discussing the relation between Assumption 1 and standard second order conditions on bounded sets.

ASSUMPTION 3 (Second order). The marginal distributions F_1, \dots, F_d are continuous and there exist positive constants K', ξ' such that for all $J \subset V$, $|J| \in \{2, 3\}$ and $q \in (0, 1]$,

$$(4.5) \quad \sup_{\mathbf{x} \in [0,1]^{|J|}} \left| q^{-1} \mathbb{P}(F_J(\mathbf{X}_J) > 1 - q\mathbf{x}) - R_J(\mathbf{x}) \right| \leq K' q^{\xi'}.$$

As we show below, this condition together with an assumption on the tails of R_{ij} implies the stronger Assumption 1 and vice versa.

ASSUMPTION 4 (Tail). There exist positive constants K_T, ξ_T such that for all $i \neq j \in V$ and $q \in (0, 1]$,

$$(4.6) \quad 1 - R_{ij}(q^{-1}, 1) \leq K_T q^{\xi_T}.$$

The relation between the above conditions is summarized in the following proposition.

PROPOSITION 1. *If Assumption 1 holds then Assumption 3 holds with $K' = 2K$, $\xi' = \xi$ and Assumption 4 holds with $K_T = K$, $\xi_T = \xi$. Conversely, if Assumption 3 holds with K' , ξ' and Assumption 4 holds with K_T , ξ_T , then Assumption 1 holds with $K = (K' + 2K_T)$, $\xi = \xi' \xi_T / (1 + \xi' + \xi_T)$.*

Note that multivariate Hüsler–Reiss distributions satisfy Assumption 4 for any $\xi' > 0$ provided that all entries of the matrix Γ are bounded away from zero and infinity (see Lemma S3 in the Supplementary Material). Therefore, for Hüsler–Reiss distributions Assumption 1 holds as soon as Assumption 3 is satisfied for a strictly larger exponent ξ' . Theorems 1 and 2 thus hold under the more standard Assumption 3 only.

5. Simulations.

5.1. *Simulation setup.* We conduct several simulation studies to compare the performance and properties of different structure learning methods for extremal graphs. Two classes of Hüsler–Reiss distributions \mathbf{Y} are chosen as the true extremal graphical model. They are described below by first sampling a random graph structure $G = (V, E)$ and then generating a random parameter matrix Γ that factorizes on that graph. Using the exact method of Dombry et al. (2016), we then simulate n samples of a max-stable random vector \mathbf{X} associated to \mathbf{Y} (cf., Rootzén et al., 2018), whose copula is

$$(5.1) \quad \mathbb{P}(F(\mathbf{X}) \leq \mathbf{x}) = \exp\{-L(-\log \mathbf{x})\}, \quad \mathbf{x} \in [0, \infty)^d,$$

where L is the stable tail dependence function of \mathbf{Y} in (2.3). It is shown in Section S5.7 of the Supplementary Material that this distribution satisfies Assumption 3 with $\xi' = 1$. Hence by Proposition 1 and Lemma S3, it satisfies Assumption 1 with any $\xi < 1$. In particular, it is in the domain of attraction of \mathbf{Y} .

As the first random graph $G = (V, E)$ we consider the Barabasi–Albert model denoted by $\text{BA}(d, q)$, which is a preferential attachment model with d nodes and a degree parameter $q \in \mathbb{N}$ (Albert and Barabási, 2002). Figure 3 shows two examples in dimension $d = 100$, one for degree $q = 1$, which is a tree, and one for degree $q = 2$. In order to randomly generate a valid Hüsler–Reiss parameter matrix Γ on G , we use the scheme in Ying et al. (2021) to sample a weighted graph Laplacian matrix. The latter can be used as a Hüsler–Reiss precision matrix Θ , which then corresponds uniquely to a variogram matrix; see Section 2.3. More precisely, we sample for every undirected edge $\{i, j\} \in E$ of G an independent uniform random variable $U_{ij} \sim \text{Unif}[2, 5]$, and define the matrix $W \in \mathbb{R}^{d \times d}$ by

$$W_{ij} = W_{ji} := \begin{cases} U_{ij} & \text{if } \{i, j\} \in E, \\ 0 & \text{otherwise.} \end{cases}$$

Let D be the diagonal degree matrix with entry D_{ii} given by the i th row sum of W , $i \in V$. The matrix $\Theta = D - W$ is called the weighted Laplacian matrix over the graph G and is a valid Hüsler–Reiss precision matrix (Röttger et al., 2021).

We note that this construction always results in a precision matrix satisfying

$$(5.2) \quad \Theta_{ij} \leq 0, \quad i, j \in V, i \neq j.$$

By Röttger et al. (2021, Lemma 4.5) this implies that the corresponding Hüsler–Reiss distribution is EMTP_2 , a notion of positive dependence for multivariate Pareto distributions. While encountered frequently in multivariate extreme value models (see Röttger et al., 2021, Section 4), such positive dependence is not present in all Hüsler–Reiss distributions.

As a second model for G and Γ we therefore consider a setup where $\Theta_{ij} > 0$ for some $i, j \in V$. Note that in this case there is no easy construction method similar to the Laplacian above. Instead, we consider a graph with n_C fully connected cliques C_1, \dots, C_{n_C} , each consisting of n_N nodes. We assume that the only intersections of these cliques are between C_j and C_{j+1} , $j = 1, \dots, n_C - 1$, and that each intersection consists of a single node. This results in a block graph G and a block-like structure of the precision matrix Θ (Hentschel, 2021); see the right-hand side of Figure 3 for a block graph with $n_C = 10$ and $n_N = 4$. On this extremal graph structure, it suffices to specify Γ_{C_j, C_j} on each clique C_j , and the remaining entries are implied by the conditional independence structure (Engelke and Hitz, 2020, Proposition 4). Following Hentschel (2021), we can construct a valid Γ_{C_j, C_j} matrix by taking any $(n_N \times n_N)$ -dimensional covariance matrix S and projecting it by PSP , where $P = I_d - \mathbf{1}\mathbf{1}^\top/d$; see Section 2.3. For each clique we generate independently a correlation matrix S following the method in Joe (2006), whose off-diagonal entries have marginal Beta($\alpha - 1 + n_N/2, \alpha - 1 + n_N/2$) distributions rescaled to $(-1, 1)$, where $\alpha > 0$ is a parameter. We denote this block model for Γ by $\text{BM}(n_C, n_N, \alpha)$. It has dimension $d = n_N + (n_C - 1)(n_N - 1)$ and is parametrized by the number of cliques n_C , the number of nodes n_N per clique, and the parameter α governing the dependence inside the cliques. Figure 7 shows the proportion of positive off-diagonal entries of the Hüsler–Reiss precision matrix Θ corresponding to the block graph model $\text{BM}(6, 4, \alpha)$ for different α values. It can be seen that for increasing α , less positive values appear and the model becomes closer to EMTP_2 .

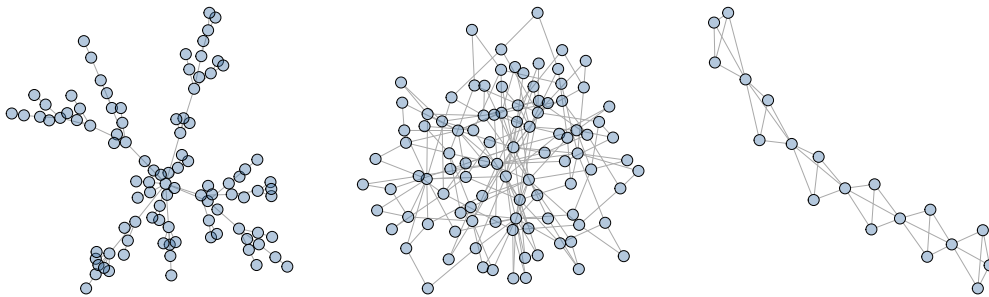


FIG 3. Realizations of the Barabasi–Albert models $\text{BA}(100, 1)$ (left) and $\text{BA}(100, 2)$ (center) in dimensions $d = 100$, and of the block graph model $\text{BM}(6, 4, \alpha)$ in dimension $d = 19$.

5.2. *Competing methods and evaluation.* We apply several methods for structure estimation to the simulated data. All methods are based on the empirical extremal variogram $\widehat{\Gamma}$ defined in (3.3). For a given sample size n , this estimator uses only the k largest exceedances in each variable. Throughout the simulation study, we choose $k = \lfloor n^{0.7} \rfloor$, which satisfies the assumptions for our theory. We refer to Engelke and Volgushev (2020, Section 5) for a detailed study of the choice of k in the framework of structure learning for extremal trees, which applies in the same manner here. In practice, k can be chosen based on stability plots of the estimated entries of $\widehat{\Gamma}$, similar to the Hill plot (e.g., Drees et al., 2000).

The first estimator of the extremal graph structure G is the extremal minimum spanning tree T_{mst} introduced in Engelke and Volgushev (2020). For a given estimate $\widehat{\Gamma}$ of the extremal variogram, it is defined as

$$(5.3) \quad T_{\text{mst}} = \arg \min_{T=(V,E)} \sum_{(i,j) \in E} \widehat{\Gamma}_{ij},$$

where the minimum is taken over all tree structures T . In [Engelke and Volgushev \(2020\)](#) it is shown to consistently recover an underlying tree even in high dimensions. By construction, this always results in a tree and hence cannot be consistent for more general graphs.

A second method is that introduced in [Röttger et al. \(2021\)](#) who obtain an EMTP₂ estimator of Θ as the solution of the convex problem

$$(5.4) \quad -\log \det^* \Theta + \frac{1}{2} \operatorname{tr} \widehat{\Gamma} \Theta$$

over all Hüsler–Reiss precision matrices and under the EMTP₂ constraint (5.2). This method sometimes introduces sparsity, but it is important to note that it is not designed for structure estimation. While [Röttger et al. \(2021\)](#) show consistency of this estimator for the entries of Γ in a fixed-dimensional setting, there are no guarantees for consistent graph recovery of G , even if the true model is EMTP₂. The method should thus not be considered as a direct competitor but is included for comparison.

In Section 3.1 we introduced our `EGlearn` algorithm that uses majority voting for structure estimation of general extremal graphical models. It can either be combined with neighborhood selection or graphical lasso as the base learning method. Both methods depend on collections of tuning parameters, which are denoted as $\rho_{m,\ell}^{\text{ns}}$ and ρ_m^{gl} , respectively, $m \in V$, $\ell \in [d-1]$. We first set them all to the same value ρ to obtain a path of estimated graphs indexed by ρ , ranging from dense to sparse graphs for increasing values of ρ ; see Figure 4 for typical paths for the two base learners. As a benchmark, we consider an oracle version of our estimator by selecting ρ to minimize the evaluation metric (5.5) below.

In practice, we need to select the amount of sparsity of the graph structure in a data driven way. We discuss automatic tuning of `EGlearn` with neighborhood selection as the base learner, since it turns out to be superior to the graphical lasso alternative in all the settings that we consider. At the m th step of the algorithm, d different lasso regressions are produced by solving (3.1) with $\widehat{A} := \widehat{\Sigma}_{\setminus m, \setminus m}^{(m)}$. For each m and ℓ , we define a residual sum of squares as

$$\text{RSS}_{m,\ell}(\theta) := k \left(\widehat{A}_{\ell\ell} - 2\widehat{A}_{\ell,\setminus\ell}\theta + \theta^\top \widehat{A}_{\setminus\ell,\setminus\ell}\theta \right);$$

if \widehat{A} was a sample covariance matrix based on k observations, this expression would be the residual sum of squares when regressing the ℓ th variable on the others. Among a path of solutions $\widehat{\theta}$ of (3.1) indexed by the choice of $\rho_{m,\ell}^{\text{ns}}$, the AIC, BIC and MBIC tuning strategies select the value $\widehat{\theta}$ minimizing

$$\text{RSS}_{m,\ell}(\widehat{\theta}) + 2\|\widehat{\theta}\|_0, \quad \text{RSS}_{m,\ell}(\widehat{\theta}) + (\log k)\|\widehat{\theta}\|_0, \quad \text{RSS}_{m,\ell}(\widehat{\theta}) + (\log k)(\log \log(d-1))\|\widehat{\theta}\|_0,$$

respectively, where $\|\widehat{\theta}\|_0$ is the number of non-zero elements in $\widehat{\theta}$. They are motivated by the traditional Akaike and Bayesian information criteria (see [Bühlmann and van de Geer, 2011](#), Section 2.6), and by an extension of the latter to high-dimensional models developed in [Wang et al. \(2009\)](#).

In order to compare an estimated graph $\widehat{G} = (V, \widehat{E})$ with the true underlying graph $G = (V, E)$, we use as evaluation metric the F -score. It is defined as

$$(5.5) \quad F = \frac{|E \cap \widehat{E}|}{|E \cap \widehat{E}| + \frac{1}{2}(|E^c \cap \widehat{E}| + |E \cap \widehat{E}^c|)},$$

where for a set of edges E , the set E^c denotes all possible undirected edges on $V \times V$ except for those in E .

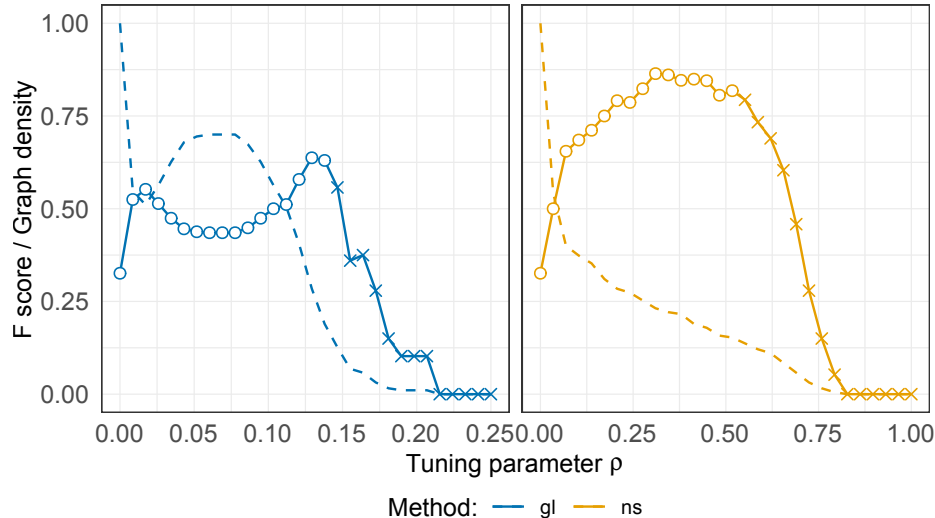


FIG 4. Paths for EGlearn with graphical lasso (left) and neighborhood selection (right) as a function of the common tuning parameter ρ , fitted to data from the $\text{BA}(20, 2)$ model with $k = 5d$. Circles indicate that the estimated graph \hat{G} is connected, and crosses correspond to disconnected graphs. Dashed lines show the density of the graph, that is, the proportion of existing edges in \hat{G} out of all $d(d-1)/2$ possible edges.

5.3. Results. The first set of simulations assesses the performance in terms of the F -score of the different methods described in the previous section. We simulate n samples from the Hüsler–Reiss distribution generated according to the Barabasi–Albert model $\text{BA}(d, q)$ of degrees $q \in \{1, 2\}$ and in dimensions $d = \{20, 50, 100\}$. For each value of d and q , we simulate three different sample sizes n such that the number of exceedances satisfy $k/d \in \{0.5, 1, 2.5\}$ and $k/d \in \{0.5, 1, 5\}$ for the models with $q = 1$ and $q = 2$, respectively. The case of $k/d = 0.5$ is a high-dimensional setting since the number of effective samples is smaller than the dimension. The different methods are then applied based on the empirical variogram $\hat{\Gamma}$ as described above using $k = \lfloor n^{0.7} \rfloor$ exceedances in each variable. Figure 4 shows typical paths of F -scores and densities of estimated graphs by EGlearn with the two base learners.

The results for dimensions 20 and 100 are shown in Figures 5 and 6 as boxplots of the F -scores for 100 repetitions of each experiment; see Section S1.1 of the Supplementary Material for similar results in dimension $d = 50$. The minimum spanning tree in (5.3) outperforms the other methods when the underlying model is indeed a tree ($q = 1$). This is expected since this approach takes advantage of the special structure of a tree. For the more general Barabasi–Albert graph with degree $q = 2$ the minimum spanning tree is no longer consistent and even with larger sample sizes the F -scores stay bounded below a certain level. The EMTP_2 estimator does not recover the graph structure well. As discussed in the previous section, this is not surprising, since there are no guarantees concerning structure estimation in this method, even if the true model is EMTP_2 .

Turning to the methods that are designed to estimate extremal graphical structures for general graphs G , we first observe that EGlearn with graphical lasso as the base learner does not perform well on any of the simulations, even with the oracle value for the penalty parameter ρ . This is surprising since the graphical lasso for Gaussian distributions is a well established method; we discuss this phenomenon in more detail below. On the other hand, EGlearn with neighborhood selection performs very well and seems to consistently recover the graph in all of the setups for large enough sample sizes.

Since the EGlearn with graphical lasso is generally not consistent even with oracle tuning parameter, we only consider data driven selection of the tuning parameters in the case of

neighborhood selection. Figures 5 and 6 show the performance of this method for model selection based on the AIC, BIC and MBIC as described in Section 5.2. We observe that AIC does not work well for selection of the penalization parameter. This is to be expected since the AIC does not result in consistent model selection even in classical settings (Arlot and Celisse, 2010). On the other hand, BIC and MBIC behave similarly and both produce structure estimates that are fairly close to the oracle estimator.

We next run simulations with Hüsler–Reiss distributions generated according to the block model $\text{BM}(6, 4, \alpha)$, which results in $d = 19$ nodes in the graph. For the dependence parameter we choose a sequence of values $\alpha \in \{0.1, 1, 2, 10, 20\}$. As before we use $k = \lfloor n^{0.7} \rfloor$ exceedances and we simulate two different sample sizes n such that $k/d \in \{2, 10\}$. The results for 100 repetitions are shown in Figure 7. The top right panel shows boxplots of the F -scores for the oracle EGlearn with graphical lasso and neighborhood selection as a function of α . We observe that, again, EGlearn with graphical lasso base learner does not seem to be consistent since even with the larger sample size the F -scores do not improve much. On the contrary, EGlearn with neighborhood selection performs well especially for larger sample sizes, suggesting consistency of the method. We further observe that in general, smaller values of α correspond to more difficult estimation problems. Note that this corresponds to the case of higher proportions of positive entries Θ_{ij} in the Hüsler–Reiss precision matrix (top left panel of Figure 7).

To understand this behavior and the related phenomenon that the graphical lasso as base learner does not seem to work well, we take a closer look at the assumptions for consistent structure recovery by EGlearn in Theorems 1 and 2. For a given parameter matrix Γ , a crucial requirement for consistency with both base learners is the positivity of the incoherence parameters η^{ns} and η^{gl} , respectively. The bottom panels of Figure 7 show boxplots of these parameters for the generated block models. All incoherence parameters η^{ns} for neighborhood selection are positive and thus, Theorem 1 guarantees consistent graph recovery. We also note that as α increases, so does η^{ns} , and the graph recovery results improve. This is in line with our theory; the expression of C^{ns} in Theorem 1 suggests that a higher η^{ns} increases the probability of graph recovery. On the other hand, all incoherence parameters η^{gl} are negative and Theorem 2 is not applicable. More generally, for all the simulation settings we have considered, the neighborhood selection incoherence parameter η^{ns} is much more likely to be positive than its graphical lasso equivalent η^{gl} . It thus appears that the assumption of Theorem 1 is significantly weaker than that of Theorem 2. This is also consistent with results in the literature of Gaussian structure learning (Ravikumar et al., 2011, Sections 3.1.1, 3.1.2).

Since Hüsler–Reiss graphical models are not defined on disconnected graphs (Engelke and Hitz, 2020), subsequent inference for Γ on \hat{G} requires that the estimated graph is connected. Theorems 1 and 2 ensure that the paths obtained by EGlearn include the true, connected graph with high probability. In finite samples with data-driven choice of the penalty parameter, it can however happen that the selected graph is disconnected. Focusing again on the case of neighborhood selection, we observe that in all our simulations, the estimated paths are monotone in the sense that the graphs are nested for increasing penalty parameters; see for instance the right panel of Figure 4. If the selected graph is disconnected, we therefore propose to use the sparsest connected graph, that is, the connected graph corresponding to the largest penalty parameter ρ . Table S1 in Section S1.2 of the Supplementary Material shows that the performance loss in terms of F -score due to this strategy is negligible, except for very sparse models such as trees, where sometimes disconnected graphs \hat{G} may be selected that are very similar to G . See the discussion and simulations therein for more details.

Note that the same strategy would not be sensible for EGlearn with graphical lasso, since the path of the graph density is not monotone; see the left panel of Figure 4.

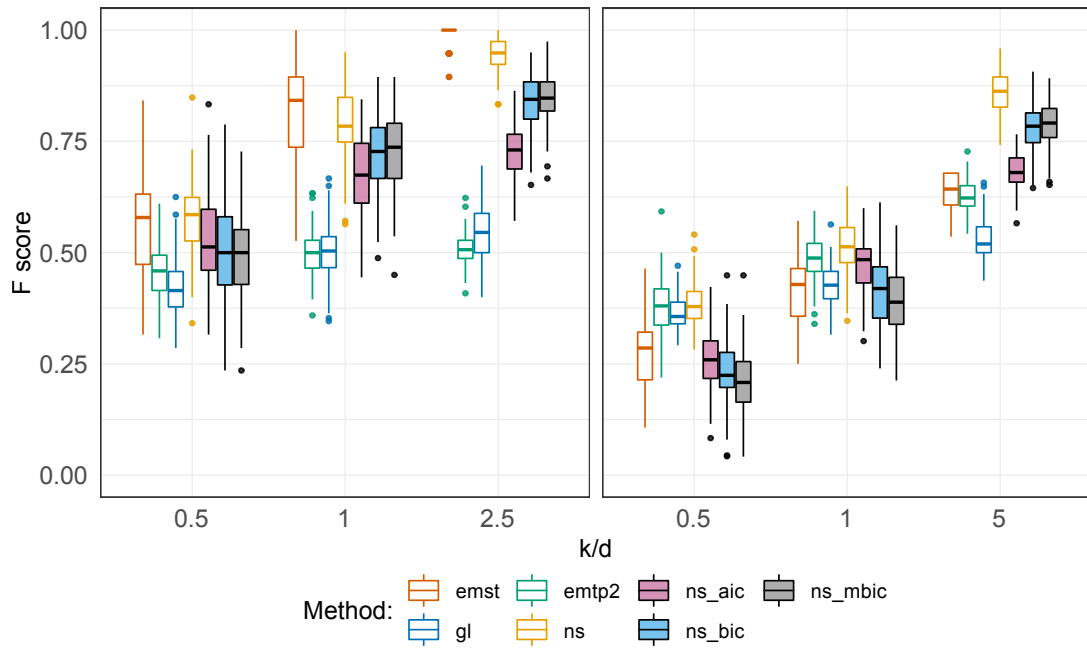


FIG 5. Boxplots of 100 repetitions of the F -scores of different methods fitted to data from the model $BA(d, q)$ of degree $q = 1$ (left) and $q = 2$ (right) and in dimension $d = 20$.

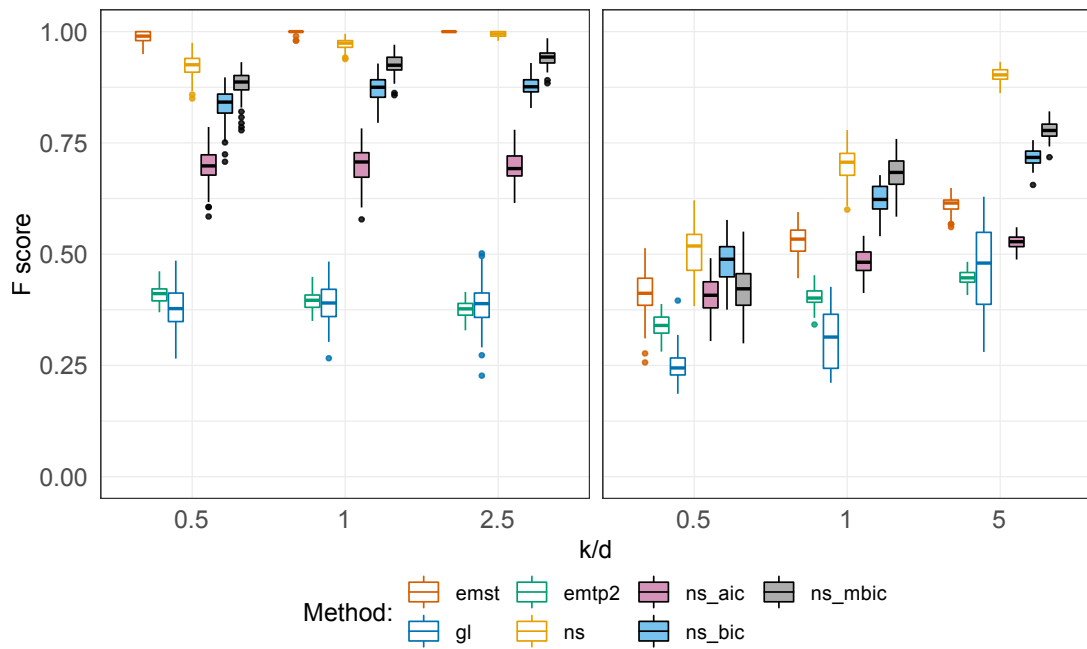


FIG 6. Boxplots of 100 repetitions of the F -scores of different methods fitted to data from the model $BA(d, q)$ of degree $q = 1$ (left) and $q = 2$ (right) and in dimension $d = 100$.

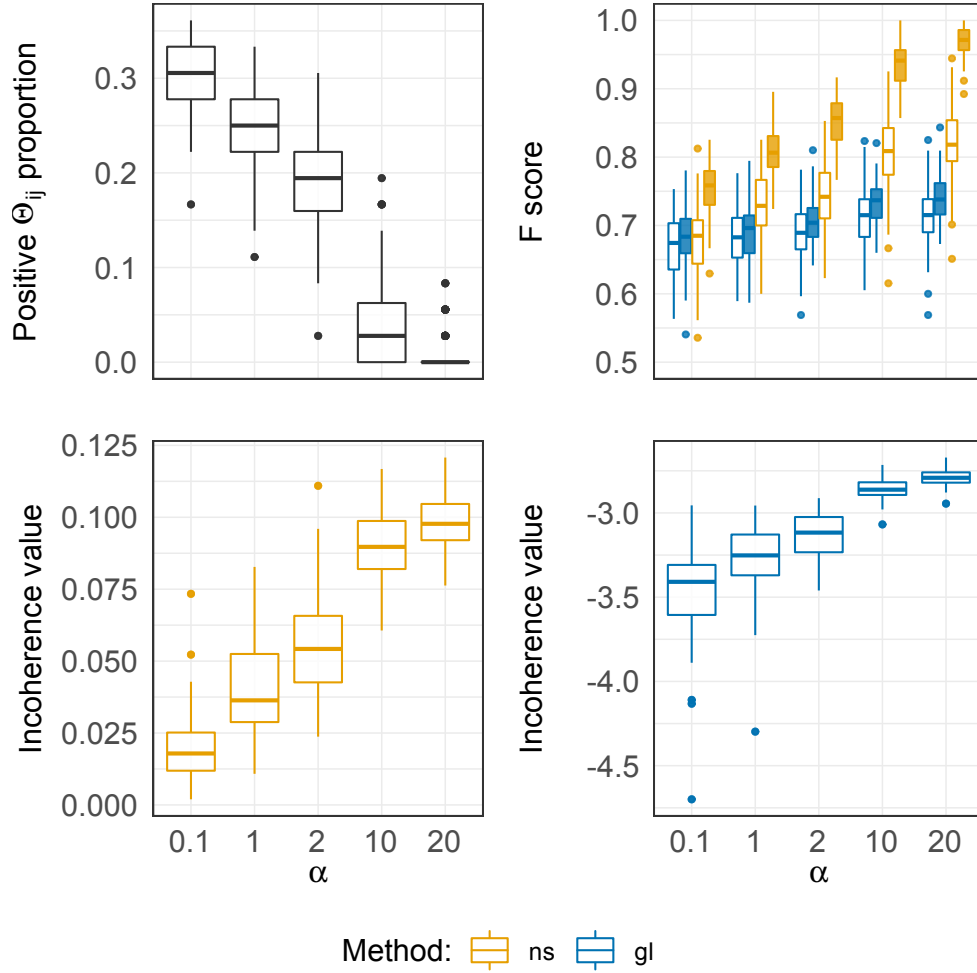


FIG 7. Top left: proportion of positive off-diagonal entries of the Hüsler–Reiss precision matrix Θ of the model $\text{BM}(6, 4, \alpha)$; top right: performance of EGlearn with neighborhood selection and graphical lasso with $k = 2d$ and $k = 10d$ for empty and filled boxes, respectively; bottom: incoherence parameters η^{ns} for neighborhood selection (left) and η^{gl} for graphical lasso (right)

6. Applications. We apply our EGlearn algorithm to a hydrological data set related to flood risk assessment and to a financial data set related to systemic risk. We focus on learning the extremal graph structures; for comments on how the estimated graphs can be used for subsequent inference we refer to the cited papers and to the discussion in Section 7.

The first data set was introduced in [Asadi et al. \(2015\)](#) and has been used as a benchmark in multivariate extremes for dependence modeling ([Engelke and Hitz, 2020](#); [Röttger et al., 2021](#)) and causal inference ([Mhalla et al., 2020](#); [Gnecco et al., 2021](#); [Tran et al., 2021](#)). It contains daily discharge measurements at $d = 31$ stations in the upper Danube basin over 50 years. We follow the original paper and use the pre-processed data containing $n = 428$ observations after a declustering of the d time series. The n samples can be considered as independent observations from a d -dimensional random vector \mathbf{X} , and we are interested in understanding the extremal dependence structure of \mathbf{X} . A certain amount of information can be deduced from the physical properties of the river network; the flow connections are shown in the left panel of Figure 8. It is reasonable to expect that extremal dependence is strong along these connections. Due to other meteorological processes such as precipitation, there

might be additional dependence between flood events that are not entirely explained by the flow connections.

We first compute the empirical variogram $\hat{\Gamma}$ with $k = \lfloor n^{0.7} \rfloor = 69$, which corresponds to how k is chosen in our simulation studies. We then use `EGlearn` with neighborhood selection as the base learner, a suitable grid of penalty parameters ρ and input variogram estimate $\hat{\Gamma}$. The graph structure selected based on the MBIC criterion is shown in the right panel of Figure 8. The graph selected by the BIC is almost identical, while the AIC graph is considerably denser; we do not show the latter since the AIC is not suited for structure recovery as seen in the simulations in Section 5. We first observe that the estimated graph contains almost all the flow connections as edges, confirming the water flow as main source of extremal dependence. It is however not connected since the stations 23–27 are separated from the rest of the network. Considering the geographical map of the river basin (Asadi et al., 2015, Figure 1), these are the only stations in the North of the Danube river, which are not fed by rainfall over the Alps. Even though not covered by our theory, the graph suggests independence of floods at these and the remaining stations; see also Mhalla et al. (2020) and Tran et al. (2021). We note that a graph learned by excluding these 5 stations is very similar to the corresponding subgraph of the one in the right panel of Figure 8, and is indeed connected.

While the information criteria provide a good heuristic for selecting a unique graphical model, the whole path of estimated graphs corresponding to all penalty parameters ρ offers a more complete view on the structure of the data. Given a sparsity level of interest, one can choose a model among this path with the desired properties. While the MBIC graph is fairly sparse and close to the flow connection tree in Figure 8, we report in Section S1.3 of the Supplementary Material three estimated graphs for smaller ρ parameters that are much denser. Those graphs are fully connected and they are significantly more complex than the block graphs obtained by the more restrictive method in Engelke and Hitz (2020).

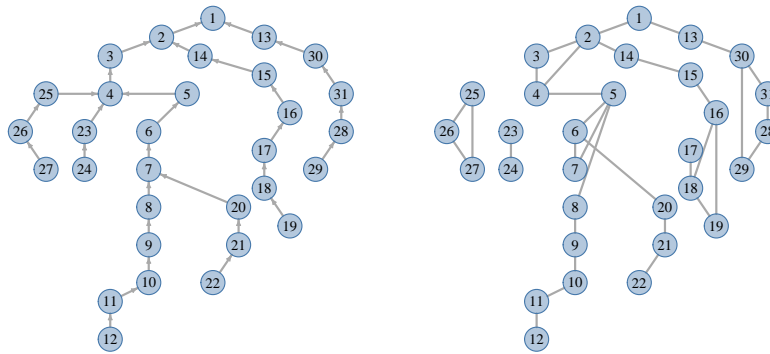


FIG 8. *The physical flow connection tree (left) and the selected graph by MBIC estimated by `EGlearn` (right) for the Danube data set.*

As a second data set we consider $n = 3790$ daily observations of spot foreign exchange rates between 2005 and 2020 of $d = 26$ currencies expressed in terms of the British Pound sterling (Engelke and Volgushev, 2020). As in the latter paper, we pre-process the data to obtain the absolute values of de-garched daily log-returns, that is, we are considering extremes of the log-returns in both directions.

Figure 9 shows the minimum spanning tree obtained in Engelke and Volgushev (2020). As in the previous application, we compute the empirical variogram $\hat{\Gamma}$ using $k = \lfloor n^{0.7} \rfloor = 319$. In order to allow for more general graphs than trees, we apply `EGlearn` with neighborhood

selection as the base learner, a suitable grid of penalty parameters ρ and input variogram estimate $\hat{\Gamma}$. The right panel of Figure 9 shows the graph selected by the MBIC. The estimated graph is connected and is much denser than a tree, suggesting that the dependencies in the extremes are considerably stronger than could have been explained by the minimum spanning tree approach.

As discussed previously, an alternative way to select the graph structure is to look for a desired sparsity level in the estimated path. In Section S1.3 of the Supplementary Material, we report three such estimated graphs that are considerably sparser than the MBIC graph. An advantage of sparse graphs is that they allow for better interpretation in the context of the application. For instance, in our case, a notable feature of all estimated models is that there are many connections within the cluster of South Asian currencies, suggesting a strong degree of dependence between the currencies of these countries.

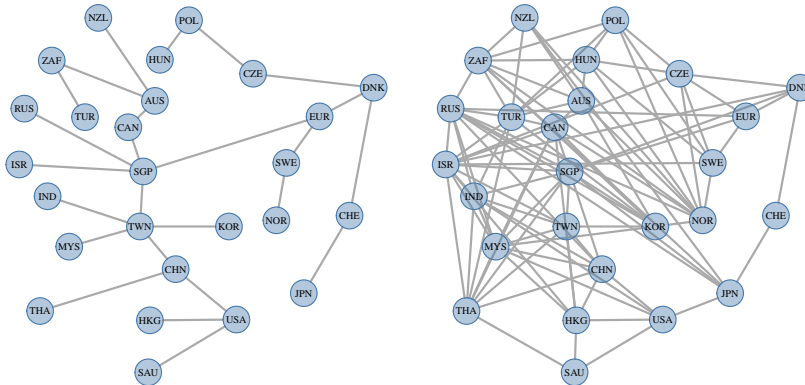


FIG 9. The minimum spanning tree (left) and the selected graph by MBIC estimated by *EGlearn* (right) for the exchange rates data set; the list of currencies with their respective abbreviations are shown in Table S2 in Supplementary Material S1.4.

7. Extensions and future work. In the present paper, we have introduced a general methodology for estimating Hüsler–Reiss graphical models through *EGlearn* and provided a thorough theoretical analysis of the resulting procedure. This is the first principled approach for estimating extremal graphical models on arbitrary graphs, and there are many questions warranting further investigation.

A first direction is a systematic exploration of alternative base learners in *EGlearn*. We have focused on the two most popular and classical approaches, but many more possible choices exist; see [Drton and Maathuis \(2017, Chapter 3\)](#) and the references cited therein for a partial overview of the recent literature with a focus on graphical modeling.

Similarly, in this paper we have used the empirical extremal variogram, but different estimators of the variogram matrix Γ could be considered. For instance, one could consider method of moments or M-estimators for extremes ([Einmahl et al., 2008, 2012](#); [Lalancette et al., 2021](#)).

In view of the characterization of extremal conditional independence for Hüsler–Reiss distributions in (2.8), there are alternatives to the *EGlearn* algorithm for structure learning of extremal graphical models. Indeed, a promising direction for future research is to consider methods that simultaneously penalize the entries and row sums of $\Theta^{(m)}$. More precisely, for an arbitrary $m \in V$, one may attempt to estimate $\Theta^{(m)}$ by solving the doubly penalized graphical

lasso problem

$$(7.1) \quad \arg \min_{\substack{\Theta^{(m)} \in \mathcal{S}^d \\ \Theta_{mV}^{(m)} = \mathbf{0}}} \left\{ -\log \det^* \Theta^{(m)} + \text{tr}(\widehat{\Sigma}^{(m)} \Theta^{(m)}) + \rho \sum_{i \neq j} \sum |\Theta_{ij}^{(m)}| + 2\rho \sum_i \left| \sum_j \Theta_{ij}^{(m)} \right| \right\},$$

where $\widehat{\Sigma}^{(m)}$ is defined as $\varphi_m(\widehat{\Gamma})$ for some estimate $\widehat{\Gamma}$ of the extremal variogram, where φ_m is as in (2.5). Here, \det^* denotes the pseudo-determinant of a matrix (the product of its non-zero eigenvalues) and \mathcal{S}^d is the space of symmetric positive semi-definite matrices in $\mathbb{R}^{d \times d}$. The second penalty term is used to impose sparsity of the row and column sums of $\Theta^{(m)}$, in addition to sparsity in the off-diagonal entries themselves. The motivation for such an approach is that zero row sums of $\Theta^{(m)}$ contain information on the absence of edges containing the node m ; see (2.8).

Alternatively, in view of the characterization in (2.10), one may consider a sparse estimate of the positive semi-definite matrix Θ defined in (2.9) by the modified graphical lasso problem

$$(7.2) \quad \arg \min_{\Theta \in \mathcal{S}_1^d} \left\{ -\log \det^* \Theta + \text{tr}(\widehat{\Sigma} \Theta) + \rho \sum_{i \neq j} \sum |\Theta_{ij}| \right\},$$

where \mathcal{S}_1^d is the cone of symmetric, positive semi-definite matrices with rank $d - 1$ and row sums equal to zero. The estimator $\widehat{\Sigma}$ is defined as a transformation of the extremal variogram estimator through $\widehat{\Sigma} = P(-\widehat{\Gamma}/2)P$, where $P = I_d - \mathbf{1}\mathbf{1}^\top/d$ as in Section 2.3. While this is a more symmetric approach, the difficulty is the semi-definiteness of Θ .

For any $m \in V$, the matrix $\Theta^{(m)}$ uniquely defines the variogram Γ , and hence characterizes the Hüsler–Reiss model. The solution to (7.1), an estimate of $\Theta^{(m)}$, can therefore be transformed to a variogram estimate $\widehat{\Gamma}_\rho^{(m)}$. Similarly, the solution to (7.2) is an estimate of Θ and can be uniquely transformed into a variogram estimate $\widehat{\Gamma}_\rho$ through the inverse Farris transform as described in Section 2.3. Interestingly, if the input $\widehat{\Gamma}$ of these optimization problems is the same, e.g., the empirical variogram, then (7.1) and (7.2) result in the same estimated model.

PROPOSITION 2. *Let $\widehat{\Gamma}$ be an arbitrary estimator of the extremal variogram matrix and suppose that (7.1) and (7.2) are solved with inputs $\widehat{\Sigma}^{(m)} = \varphi_m(\widehat{\Gamma})$ and $\widehat{\Sigma} = P(-\widehat{\Gamma}/2)P$, respectively, and with common penalty parameter $\rho > 0$. Then the corresponding estimated models are all the same, i.e.,*

$$\widehat{\Gamma}_\rho^{(1)} = \dots = \widehat{\Gamma}_\rho^{(d)} = \widehat{\Gamma}_\rho.$$

While the above approaches are attractive, preliminary simulations and theoretical investigations indicate that they do in general not lead to consistent recovery of the sparsity structure of the matrices $\Theta^{(m)}$ and Θ . Replacing the vanilla L^1 penalties by adaptively weighted or non-convex versions might provide a way out, but a full investigation of this approach is beyond the scope of the present paper.

The structure learning methods presented in this paper output an estimated graph $\widehat{G} = (V, \widehat{E})$. They do not automatically provide an estimator of the Hüsler–Reiss parameter matrix Γ on this graph structure. A natural estimator $\widehat{\Gamma}^0$ that has the sparsity pattern of \widehat{G} and agrees with the input estimator $\widehat{\Gamma}$ on the edges of \widehat{G} is the solution to the matrix completion problem

$$\widehat{\Gamma}_{ij}^0 = \widehat{\Gamma}_{ij}, \quad (i, j) \in \widehat{E}, \quad \widehat{\Theta}_{ij}^0 = 0, \quad (i, j) \notin \widehat{E},$$

where $\widehat{\Theta}^0$ is the Hüsler–Reiss precision matrix corresponding to $\widehat{\Gamma}^0$. Hentschel (2021) show that if the graph \widehat{G} is connected, there is a unique solution to this completion problem, hence yielding a unique Hüsler–Reiss model fit for each estimated, connected graph. Studying the statistical properties of the resulting parameter estimates provides an interesting direction for future research.

Acknowledgments. The authors would like to thank Nicola Gnecco and Yanbo Tang for helpful comments and Yan Zhang for comments on the R implementation. Sebastian Engelke was supported by an Eccellenza grant of the Swiss National Science Foundation, Michaël Lalancette was supported by an Ontario Graduate Scholarship, and Stanislav Volgushev was supported by a discovery grant from NSERC of Canada.

REFERENCES

- Albert, R. and Barabási, A.-L. (2002). Statistical mechanics of complex networks. *Rev. Mod. Phys.*, 74:47–97.
- Améndola, C., Klüppelberg, C., Lauritzen, S., and Tran, N. M. (2022). Conditional independence in max-linear Bayesian networks. *Ann. Appl. Probab.*, 32(1):1–45.
- Arlot, S. and Celisse, A. (2010). A survey of cross-validation procedures for model selection. *Stat. Surv.*, 4:40–79.
- Asadi, P., Davison, A. C., and Engelke, S. (2015). Extremes on river networks. *Ann. Appl. Stat.*, 9:2023–2050.
- Asenova, S., Mazo, G., and Segers, J. (2021). Inference on extremal dependence in the domain of attraction of a structured Hüsler–Reiss distribution motivated by a Markov tree with latent variables. *Extremes*, 24:461–500.
- Asenova, S. and Segers, J. (2021). Extremes of markov random fields on block graphs. *arXiv preprint arXiv:2112.04847*.
- Beirlant, J., Goegebeur, Y., Segers, J., and Teugels, J. L. (2004). *Statistics of extremes: theory and applications*, volume 558. John Wiley & Sons.
- Bühlmann, P. and van de Geer, S. (2011). *Statistics for high-dimensional data*. Springer Series in Statistics. Springer, Heidelberg. Methods, theory and applications.
- Cléménçon, S., Jalalzai, H., Sabourin, A., Lhaut, S., and Segers, J. (2021). Concentration bounds for the empirical angular measure with statistical learning applications. *arXiv preprint arXiv:2104.03966*.
- Coles, S. G. and Tawn, J. A. (1991). Modelling extreme multivariate events. *J. R. Stat. Soc. Ser. B. Stat. Methodol.*, 53(2):377–392.
- Csorgo, M. and Revesz, P. (1978). Strong approximations of the quantile process. *Ann. Stat.*, pages 882–894.
- Davison, A. C., Padoan, S. A., and Ribatet, M. (2012). Statistical modeling of spatial extremes. *Stat. Sci.*, 27:161–186.
- de Haan, L. and Ferreira, A. (2006). *Extreme Value Theory*. Springer.
- Dombry, C., Engelke, S., and Oesting, M. (2016). Exact simulation of max-stable processes. *Biometrika*, 103(2):303–317.
- Drees, H., Resnick, S., and de Haan, L. (2000). How to make a Hill plot. *Ann. Stat.*, 28(1):254 – 274.
- Drton, M. and Maathuis, M. H. (2017). Structure learning in graphical modeling. *Annu. Rev. Stat. Appl.*, 4:365–393.
- Durrett, R. (2010). *Probability: theory and examples*, volume 31 of *Cambridge Series in Statistical and Probabilistic Mathematics*. Cambridge University Press, Cambridge, fourth edition.
- Einmahl, J. H. J., Krajina, A., and Segers, J. (2008). A method of moments estimator of tail dependence. *Bernoulli*, 14:1003–1026.
- Einmahl, J. H. J., Krajina, A., and Segers, J. (2012). An M-estimator for tail dependence in arbitrary dimensions. *Ann. Stat.*, 40:1764–1793.
- Engelke, S., de Fondeville, R., and Oesting, M. (2019). Extremal behaviour of aggregated data with an application to downscaling. *Biometrika*, 106:127–144.
- Engelke, S. and Hitz, A. S. (2020). Graphical models for extremes (with discussion). *J. R. Stat. Soc. Ser. B. Stat. Methodol.*, 82:871–932.
- Engelke, S. and Ivanovs, J. (2021). Sparse structures for multivariate extremes. *Annu. Rev. Stat. Appl.*, 8:241–270.
- Engelke, S., Malinowski, A., Kabluchko, Z., and Schlather, M. (2015). Estimation of Hüsler–Reiss distributions and Brown–Resnick processes. *J. R. Stat. Soc. Ser. B. Stat. Methodol.*, 77(1):239–265.
- Engelke, S. and Volgushev, S. (2020). Structure learning for extremal tree models. *arXiv preprint arXiv:2012.06179*.
- Farris, J. S., Kluge, A. G., and Eckardt, M. J. (1970). A numerical approach to phylogenetic systematics. *Syst. Zool.*, 19(2):172–189.
- Fougères, A.-L., de Haan, L., and Mercadier, C. (2015). Bias correction in multivariate extremes. *Ann. Stat.*, 43(2):903–934.
- Friedman, J., Hastie, T., and Tibshirani, R. (2008). Sparse inverse covariance estimation with the graphical lasso. *Biostatistics*, 9(3):432–441.
- Gissibl, N. and Klüppelberg, C. (2018). Max-linear models on directed acyclic graphs. *Bernoulli*, 24:2693–2720.
- Gnecco, N., Meinshausen, N., Peters, J., and Engelke, S. (2021). Causal discovery in heavy-tailed models. *Ann. Stat.*, 49(3):1755–1778.
- Goix, N., Sabourin, A., and Cléménçon, S. (2015). Learning the dependence structure of rare events: a non-asymptotic study. In *Conf. Learn. Theory*, pages 843–860. PMLR.

- Hentschel, M. (2021). Statistical inference for Hüsler–Reiss graphical models. Master’s thesis, Universität Mannheim.
- Huang, X. (1992). *Statistics of bivariate extreme value theory*. PhD thesis, Erasmus University Rotterdam.
- Hüsler, J. and Reiss, R.-D. (1989). Maxima of normal random vectors: between independence and complete dependence. *Stat. Probab. Lett.*, 7(4):283–286.
- Joe, H. (2006). Generating random correlation matrices based on partial correlations. *J. Multivariate Anal.*, 97(10):2177–2189.
- Keef, C., Tawn, J. A., and Lamb, R. (2013). Estimating the probability of widespread flood events. *Environmetrics*, 24:13–21.
- Klüppelberg, C. and Lauritzen, S. (2019). *Bayesian networks for max-linear models*, pages 79–97. Springer International Publishing, Cham.
- Koltchinskii, V. (2006). Local rademacher complexities and oracle inequalities in risk minimization. *Ann. Stat.*, 34(6):2593–2656.
- Lalancette, M., Engelke, S., and Volgushev, S. (2021). Rank-based estimation under asymptotic dependence and independence, with applications to spatial extremes. *Ann. Stat.*, 49(5):2552–2576.
- Lauritzen, S. (1996). *Graphical models*. Clarendon Press.
- Lhaut, S., Sabourin, A., and Segers, J. (2021). Uniform concentration bounds for frequencies of rare events. *arXiv preprint arXiv:2110.05826*.
- Liu, H., Han, F., Yuan, M., Lafferty, J., and Wasserman, L. (2012). High-dimensional semiparametric gaussian copula graphical models. *Ann. Stat.*, 40(4):2293–2326.
- Liu, H., Xu, M., Gu, H., Gupta, A., Lafferty, J., and Wasserman, L. (2011). Forest density estimation. *J. Mach. Learn. Res.*, 12:907–951.
- Loh, P.-L. and Wainwright, M. J. (2013). Structure estimation for discrete graphical models: Generalized covariance matrices and their inverses. *Ann. Stat.*, 41:3022–3049.
- Massart, P. (2000). About the constants in talagrand’s concentration inequalities for empirical processes. *Ann. Probab.*, pages 863–884.
- Meinshausen, N. and Bühlmann, P. (2006). High-dimensional graphs and variable selection with the lasso. *Ann. Stat.*, 34(3):1436–1462.
- Mhalla, L., Chavez-Demoulin, V., and Dupuis, D. J. (2020). Causal mechanism of extreme river discharges in the upper Danube basin network. *J. R. Stat. Soc. Ser. C. Appl. Stat.*, 69(4):741–764.
- Papastathopoulos, I. and Strokorb, K. (2016). Conditional independence among max-stable laws. *Stat. Probab. Lett.*, 108:9–15.
- Radulović, D., Wegkamp, M., and Zhao, Y. (2017). Weak convergence of empirical copula processes indexed by functions. *Bernoulli*, 23(4B):3346–3384.
- Ravikumar, P., Wainwright, M. J., Raskutti, G., and Yu, B. (2011). High-dimensional covariance estimation by minimizing l_1 -penalized log-determinant divergence. *Electron. J. Stat.*, 5:935–980.
- Rootzén, H., Segers, J., and Wadsworth, J. L. (2018). Multivariate peaks over thresholds models. *Extremes*, 21(1):115–145.
- Rootzén, H. and Tajvidi, N. (2006). Multivariate generalized Pareto distributions. *Bernoulli*, 12:917–930.
- Röttger, F., Engelke, S., and Zwiernik, P. (2021). Total positivity in multivariate extremes. *arXiv preprint arXiv:2112.14727*.
- Segers, J. (2020). One- versus multi-component regular variation and extremes of Markov trees. *Adv. Appl. Probab.*, 52:855–878.
- Tawn, J. A. (1990). Modelling multivariate extreme value distributions. *Biometrika*, 77:245–253.
- Tibshirani, R. J. (2013). The lasso problem and uniqueness. *Electron. J. Stat.*, 7:1456–1490.
- Tran, N. M., Buck, J., and Klüppelberg, C. (2021). Estimating a latent tree for extremes. *arXiv preprint arXiv:2102.06197*.
- van der Vaart, A. W. and Wellner, J. A. (1996). *Weak convergence and empirical processes with applications to statistics*. Springer.
- Wang, H., Li, B., and Leng, C. (2009). Shrinkage tuning parameter selection with a diverging number of parameters. *J. R. Stat. Soc. Ser. B. Stat. Methodol.*, 71(3):671–683.
- Ying, J., Cardoso, J. M., and Palomar, D. (2021). Minimax estimation of Laplacian constrained precision matrices. In *Int. Conf. Artif. Intell. Stat.*, pages 3736–3744. PMLR.
- Yuan, M. and Lin, Y. (2007). Model selection and estimation in the gaussian graphical model. *Biometrika*, 94(1):19–35.
- Zhao, P. and Yu, B. (2006). On model selection consistency of lasso. *J. Mach. Learn. Res.*, 7:2541–2563.
- Zhou, C. (2010). Are banks too big to fail? Measuring systemic importance of financial institutions. *Int. J. Cent. Bank.*, 6:205–250.

SUPPLEMENTARY MATERIAL

This Supplementary Material is divided into five sections. Section [S1](#) contains additional numerical results that complement Sections [5](#) and [6](#). The rest of the Supplementary Material is dedicated to the proofs of all the results in the paper. We start with the theory related to graph recovery and precision matrix estimation (Sections [S2](#) and [S3](#)), followed by the proof of Theorem [3](#) and related auxiliary results (Sections [S4](#) and [S5](#)).

CONTENTS OF THE SUPPLEMENTARY MATERIAL

S1	Additional numerical results	27
	S1.1 Simulation results for the Barabasi–Albert model in dimension $d = 50$	27
	S1.2 Connectedness of the estimated graphs	28
	S1.3 Estimated graphs	29
	S1.4 Country codes for exchange rate data in Section 6	29
S2	Proofs of extremal graph recovery results	30
	S2.1 Proof of Theorem 1	30
	S2.2 Proof of Theorem 2	31
	S2.3 Sparsistency results for neighborhood selection and graphical lasso	31
	S2.4 Proof of Proposition 2	32
S3	Sparsistency results for neighborhood selection and graphical lasso: proofs	33
	S3.1 Proof of Proposition S1	33
	S3.2 Proof of Proposition S2	38
S4	Proof of Theorem 3	38
	S4.1 Preliminaries, additional notation and structure of the proof	39
	S4.2 The bias terms B	41
	S4.3 The stochastic error terms A	42
	S4.4 Proof of Theorem 3	56
S5	Auxiliary results and proofs	58
	S5.1 Proof of Proposition 1	58
	S5.2 Densities of Hüsler–Reiss Pareto distributions	60
	S5.3 The moments $e_m^{(m),\ell}$	62
	S5.4 Verifying the integral representations of different moments	62
	S5.5 Bounds on the measures R_{ij}	67
	S5.6 Technical results from empirical process theory	68
	S5.7 Discussion of max-stable distributions	69

S1. Additional numerical results.

S1.1. *Simulation results for the Barabasi–Albert model in dimension $d = 50$.* The results of our experiments on the Barabasi–Albert model of dimension $d = 50$ are presented in Figure [S1](#). The conclusions are similar to the 100-dimensional case: with neighborhood selection as base learner, the algorithm seems to have a consistent behavior as k increases, as opposed to the graphical lasso case.

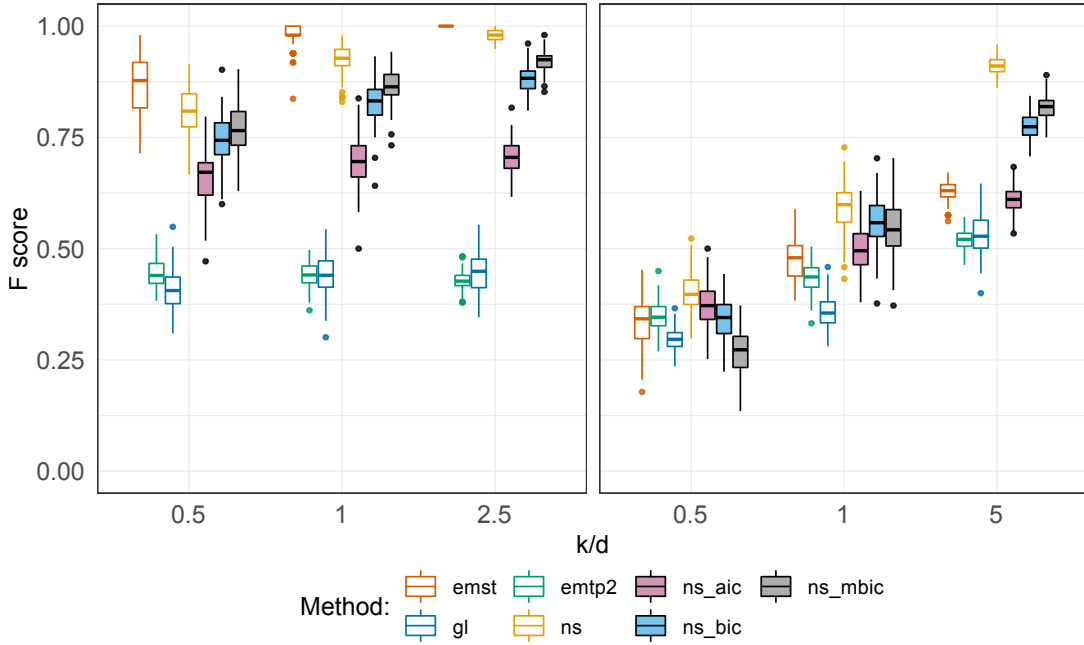


FIG S1. Boxplots of 100 repetitions of the F -scores of different methods fitted to data from the model $BA(d, q)$ of degree $q = 1$ (left) and $q = 2$ (right) and in dimension $d = 50$.

S1.2. Connectedness of the estimated graphs. The graph estimated by the `EGlearn` algorithm with neighborhood selection as its base learner is not guaranteed to be connected in general. In Section 5, we suggested that when the selected graph is not connected, one can compute a path of solutions using $\rho_{m,\ell}^{\text{ns}} \equiv \rho$, for a grid of values ρ , and select the sparsest connected graph in the path.

To quantify the effect of this strategy, we study the models $BA(50, 1)$ and $BA(50, 2)$ as in Section 5. For each model, we simulate 100 samples of size n such that $k := \lfloor n^{0.7} \rfloor$ is equal to $d/2$, d and to $5d$. For each model and sample, a path of estimated graphs is obtained according to `EGlearn` with neighborhood selection as base learner and a suitable grid of penalties ρ . We then calculate the ratio of the maximum F -score among connected graphs in the path to the unconstrained maximum F -score. The average ratio for each setup is presented in Table S1, with standard deviation. In addition, we calculate the proportions of samples where the oracle and the AIC, BIC and MBIC graphs (as defined in Section 5) are connected; see the last four columns of Table S1.

The BIC and MBIC graphs are frequently disconnected if the sample size is small, whereas the AIC, being more conservative, tends to avoid that problem. More importantly, the performance of the algorithm is generally stable over a certain range of tuning parameters, and the loss incurred by only optimizing over the connected graphs is negligible. The largest loss of performance in terms of F -score is of the order of 14% in the $BA(50, 1)$ model with small sample size $k = d/2$. This graph is a tree, the most sparse connected graph structure, which explains why it is well approximated by certain disconnected estimates. For the other, denser model, the performance loss is always less than 1%.

		<i>F</i> -score ratio	oracle	AIC	BIC	MBIC
BA(50, 1)	$k = d/2$	0.862 (0.075)	0.03	0.59	0.01	0
	$k = d$	0.890 (0.074)	0.05	0.92	0.44	0.18
	$k = 5d$	0.997 (0.012)	0.90	1	1	0.99
BA(50, 2)	$k = d/2$	0.996 (0.011)	0.88	0.90	0.01	0
	$k = d$	0.996 (0.012)	0.81	1	0.65	0.07
	$k = 5d$	1 (0)	1	1	1	1

TABLE S1

Average ratio of the best *F*-score among connected graphs in the path obtained by *EGlearn* with neighborhood selection compared to the best *F*-score in the whole path, based on 100 simulations. Standard deviations in parentheses. The last four columns contain the proportions of samples where the oracle, AIC, BIC and MBIC graphs are connected.

S1.3. *Estimated graphs.* Figure S2 contains graphs obtained by running *EGlearn* on the Danube data set with neighborhood selection as the base learner. The empirical variogram is calculated with $k = 69$, and the three graphs correspond to penalty parameters ρ equal to 0.06, 0.09 and 0.12, respectively. Figure S3 contains the estimated graphs calculated similarly for the currency exchange data set with $k = 319$ and ρ equal to 0.35, 0.45 and 0.53, respectively. In both cases, the third graph corresponds to the most sparse connected graph in the estimated path.

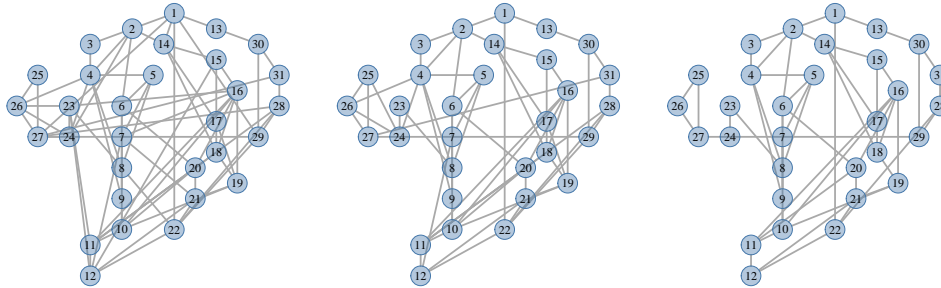


FIG S2. Estimated graphs for the Danube data obtained from *EGlearn* with neighborhood selection and penalty parameter ρ equal to 0.06, 0.09 and 0.12, respectively.

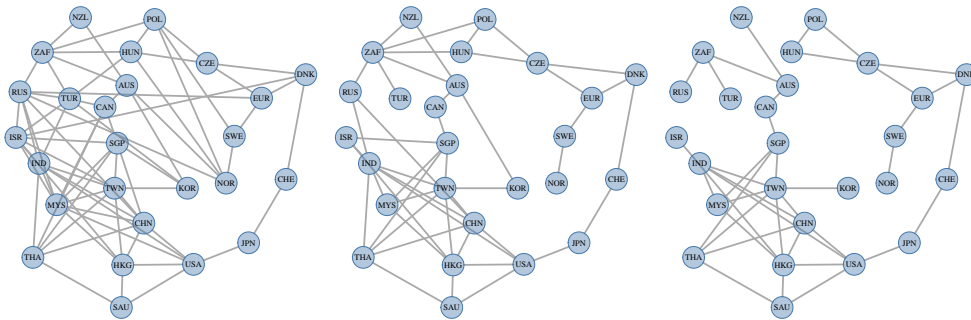


FIG S3. Estimated graphs for the currency exchange data obtained from *EGlearn* with neighborhood selection and penalty parameter ρ equal to 0.35, 0.45 and 0.53, respectively.

S1.4. *Country codes for exchange rate data in Section 6.* Table S2 shows the three-letter country codes of the exchange rates into British Pound sterling.

Code	Foreign Exchange Rate (into GBP)	Code	Foreign Exchange Rate (into GBP)
AUS	Australian Dollar	NOR	Norwegian Krone
CAN	Canadian Dollar	POL	Polish Zloty
CHN	Chinese Yuan	RUS	Russian Ruble
CZE	Czech Koruna	SAU	Saudi Riyal
DNK	Danish Krone	SGP	Singapore Dollar
EUR	Euro	ZAF	South African Rand
HKG	Hong Kong Dollar	KOR	South Korean Won
HUN	Hungarian	SWE	Swedish Krona
IND	Indian Rupee	CHE	Swiss Franc
ISR	Israeli Shekel	TWN	Taiwan Dollar
JPN	Japanese Yen	THA	Thai Baht
MYS	Malaysian ringgit	TUR	Turkish Lira
NZL	New Zealand Dollar	USA	US Dollar

TABLE S2
Three-letter country codes.

S2. Proofs of extremal graph recovery results.

S2.1. *Proof of Theorem 1.* When running the neighborhood selection algorithm on $\Sigma_{\setminus m, \setminus m}^{(m)}$, $m \in V$, recall that $\rho_{m,1}^{\text{ns}}, \dots, \rho_{m,d-1}^{\text{ns}}$ are used as penalty parameters. Let

$$\begin{aligned}
\lambda_{m,\ell} &:= \lambda_{\min}(\Sigma_{S_{m,\ell}, S_{m,\ell}}^{(m)}), \\
\kappa_{m,\ell} &:= \left\| \left\| \Sigma_{S_{m,\ell}^c, S_{m,\ell}}^{(m)} \right\| \right\|_{\infty}, \\
\vartheta_{m,\ell} &:= \left\| \left\| (\Sigma_{S_{m,\ell}, S_{m,\ell}}^{(m)})^{-1} \right\| \right\|_{\infty}, \\
s_{m,\ell} &:= |S_{m,\ell}|, \\
C_{m,\ell}^{\text{ns}} &:= \frac{2}{3} \min \left\{ \frac{\lambda_{m,\ell}}{2s_{m,\ell}}, \frac{\eta_{m,\ell}^{\text{ns}}}{4\vartheta_{m,\ell}(1 + \kappa_{m,\ell}\vartheta_{m,\ell})s_{m,\ell}}, \right. \\
&\quad \left. \frac{\min_{i \in S_{m,\ell}} \frac{|B_{i\ell}|}{B_{\ell\ell}} - \vartheta_{m,\ell}\rho_{m,\ell}^{\text{ns}}}{2\vartheta_{m,\ell}(1 + \kappa_{m,\ell}\vartheta_{m,\ell})}, \frac{\rho_{m,\ell}^{\text{ns}}\eta_{m,\ell}^{\text{ns}}}{8(1 + \kappa_{m,\ell}\vartheta_{m,\ell})^2} \right\}.
\end{aligned}$$

By Proposition S1, we have

$$\{(i, j) \in (V \setminus \{m\})^2 : \tilde{Z}^{(m)} = 1\} = \{(i, j) \in (V \setminus \{m\})^2 \cap E\}$$

provided that

$$\|\widehat{\Sigma}^{(m)} - \Sigma^{(m)}\|_{\infty} < \frac{3}{2} \min_{\ell \neq m} C_{m,\ell}^{\text{ns}}.$$

From the definition of $\Sigma^m, \widehat{\Sigma}^{(m)}$ through $\Gamma, \widehat{\Gamma}$, it follows that

$$\max_{m \in V} \|\widehat{\Sigma}^{(m)} - \Sigma^{(m)}\|_{\infty} \leq \frac{3}{2} \|\widehat{\Gamma} - \Gamma\|_{\infty}.$$

The EGlearn algorithm correctly learns the presence (resp. absence) of an edge (i, j) if a 1 (resp. a 0) rightfully appears in position (i, j) of $\tilde{Z}^{(m)}$ for at least $\lfloor d/2 \rfloor$ values of $m \notin \{i, j\}$. This is clearly the case for each pair (i, j) if at least $\lfloor d/2 \rfloor + 2$ of the neighborhood selections perfectly succeed, which is guaranteed if $\|\widehat{\Gamma} - \Gamma\|_{\infty} < \min_{\ell \neq m} C_{m,\ell}^{\text{ns}}$ for at least $\lfloor d/2 \rfloor + 2$ values of m . Noting that the assumed bound C^{ns} lower bounds each $C_{m,\ell}^{\text{ns}}$, the first statement of the theorem is proved.

For a proof of the second part, let

$$\lambda := \sqrt{\frac{3}{c} \log d + \sigma}$$

with c as in Theorem 3, and $\sigma \rightarrow \infty$ but $\sigma = o(k/(\log k)^8)$. Then, by assumption on d and k , we have eventually $\lambda \leq \sqrt{k}/(\log n)^4$, so that Theorem 3 applies. It states that with probability at least $1 - M \exp\{3 \log d - c\lambda^2\} = 1 - o(1)$,

$$\|\widehat{\Gamma} - \Gamma\|_\infty \lesssim \left(\frac{k}{n}\right)^\xi (\log(n/k))^2 + \frac{\sqrt{\log d + \sigma}}{\sqrt{k}}.$$

By assumption,

$$\left(\frac{k}{n}\right)^\xi (\log(n/k))^2 + \frac{\sqrt{\log d}}{\sqrt{k}} = o(C^{\text{ns}}),$$

so if σ is chosen to diverge slowly enough, we have $\mathbb{P}(\|\widehat{\Gamma} - \Gamma\|_\infty < C^{\text{ns}}) \rightarrow 1$. \square

S2.2. Proof of Theorem 2. When running the graphical lasso algorithm on $\Sigma_{\setminus m, \setminus m}^{(m)}$, $m \in V$, recall that ρ_m^{gl} is used as penalty parameter. Let

$$\kappa_{\Sigma, m} := \|\Sigma^{(m)}\|_\infty, \quad \kappa_{\Omega, m} := \|(\Omega_{S_m, S_m}^{(m)})^{-1}\|_\infty, \quad \chi_m := 6\kappa_{\Sigma, m}\kappa_{\Omega, m} \left(1 \vee \frac{9\kappa_{\Sigma, m}^2 \kappa_{\Omega, m}}{\eta_m^{\text{gl}}}\right),$$

$$s_m := \max_{\ell \in [d-1]} s_{m, \ell},$$

$$C_m^{\text{gl}} := \frac{2}{3} \min \left\{ \min_{i \in [d-1]} \Sigma_{ii}^{(m)}, \frac{\eta_m^{\text{gl}} \rho_m^{\text{gl}}}{8}, \frac{1}{\chi_m s_m} - \rho_m^{\text{gl}}, \frac{\theta_{\min}^{\text{gl}}}{4\kappa_{\Omega, m}} - \rho_m^{\text{gl}} \right\}.$$

By Proposition S2, we have

$$\{(i, j) \in (V \setminus \{m\})^2 : \widetilde{Z}^{(m)} = 1\} = \{(i, j) \in (V \setminus \{m\})^2 \cap E\}$$

provided that

$$\|\widehat{\Sigma}^{(m)} - \Sigma^{(m)}\|_\infty < \frac{3}{2} C_m^{\text{gl}}.$$

Similarly to the proof of Theorem 1, deduce that whenever $\|\widehat{\Gamma} - \Gamma\|_\infty < C_m^{\text{gl}}$ for at least $\lfloor d/2 \rfloor + 2$ values of m , EGlearn correctly recovers the extremal graph G . Moreover, $C_m^{\text{gl}} \leq C_m^{\text{gl}}$ for each $m \in V$, which completes the proof of the first part. The proof of the second statement is identical to that of the second statement in Theorem 1. \square

S2.3. Sparsistency results for neighborhood selection and graphical lasso. Let A be a p -dimensional covariance matrix, $B := A^{-1}$, \widehat{A} be an estimator and $\varepsilon := \|\widehat{A} - A\|_\infty$. Recall the definition of the graph $G(B)$ associated to B , i.e., the graph with edge set $\{(i, j) : i \neq j, B_{ij} \neq 0\}$.

We start by discussing the neighborhood selection algorithm. Define the neighborhood of a node ℓ in the graph $G(B)$ by $\text{ne}(\ell) := \{i \in [p] \setminus \ell : B_{i\ell} \neq 0\}$. Let

$$\lambda_\ell := \lambda_{\min}(A_{\text{ne}(\ell), \text{ne}(\ell)}),$$

$$\kappa_\ell := \|\|A_{\text{ne}(\ell)^c, \text{ne}(\ell)}\|\|_\infty,$$

$$\vartheta_\ell := \|\|(A_{\text{ne}(\ell), \text{ne}(\ell)})^{-1}\|\|_\infty,$$

$$s_\ell := |\text{ne}(\ell)|,$$

$$\eta_\ell := 1 - \|\|A_{\text{ne}(\ell)^c, \text{ne}(\ell)}(A_{\text{ne}(\ell), \text{ne}(\ell)})^{-1}\|\|_\infty.$$

PROPOSITION S1. Assume that $\min_{\ell \in [p]} \eta_\ell > 0$ and

$$\varepsilon < \min_{\ell \in [p]} \min \left\{ \frac{\lambda_\ell}{2s_\ell}, \frac{\eta_\ell}{4\vartheta_\ell(1 + \kappa_\ell\vartheta_\ell)s_\ell}, \frac{\min_{i \in \text{ne}(\ell)} \frac{|B_{i\ell}|}{B_{\ell\ell}} - \vartheta_\ell\rho_\ell}{2\vartheta_\ell(1 + \kappa_\ell\vartheta_\ell)}, \frac{\rho_\ell\eta_\ell}{8(1 + \kappa_\ell\vartheta_\ell)^2} \right\}.$$

Then the graph $G_{NS}(\hat{A})$ obtained through the neighborhood selection in Algorithm 2 with penalty parameters ρ_1, \dots, ρ_p is equal to $G(B)$.

We now discuss the graphical lasso. Define the maximal edge degree $s := \max_{\ell \in [p]} s_\ell$, with s_ℓ as earlier, S to be the augmented edge set $\{(i, j) : B_{ij} \neq 0\}$, including the self loops (i, i) , and S^c to be its complement in V^2 . Let $\Omega := A \otimes A$,

$$\begin{aligned} \kappa_A &:= \|A\|_\infty, \quad \kappa_\Omega := \|(\Omega_{SS})^{-1}\|_\infty, \quad \chi := 6\kappa_A\kappa_\Omega \left(1 \vee \frac{9\kappa_A^2\kappa_\Omega}{\alpha}\right), \\ \alpha &:= 1 - \|\Omega_{S^cS}(\Omega_{SS})^{-1}\|_\infty. \end{aligned}$$

PROPOSITION S2. Assume that $\alpha > 0$ and

$$\varepsilon < \min \left\{ \min_{i \in [p]} A_{ii}, \frac{\alpha\rho}{8}, \frac{1}{\chi s} - \rho, \frac{1}{4\kappa_\Omega} \min_{i \neq j, B_{ij} \neq 0} |B_{ij}| - \rho \right\}.$$

Then the graph $G_{GL}(\hat{A})$ obtained through the graphical lasso with penalty parameter ρ is equal to $G(B)$.

REMARK S1. For both algorithms, $s\varepsilon \rightarrow 0$ is sufficient for model selection consistency as the sample size increases, if everything else is constant and the relevant incoherence condition is satisfied.

S2.4. *Proof of Proposition 2.* Denote by f_m the bijective function that maps Θ to $\Theta^{(m)}$. It is proved in Röttger et al. (2021) that

$$-\log \det^* \Theta + \text{tr}(\hat{\Sigma}\Theta) = -\log \det f_m(\Theta) + \text{tr}(\hat{\Sigma}^{(m)} f_m(\Theta)) + d.$$

Moreover, for any i, j not equal to m , $f_m(\Theta)_{ij} = \Theta_{ij}$. This implies, first, that

$$\sum_{i \neq j} \sum |f_m(\Theta)_{ij}| = \sum_{i \neq m} \sum_{j \notin \{i, m\}} |\Theta_{ij}|.$$

It also implies that

$$2 \sum_i \left| \sum_j f_m(\Theta)_{ij} \right| = 2 \sum_{i \neq m} \left| \sum_{j \neq m} \Theta_{ij} \right| = 2 \sum_{i \neq m} |-\Theta_{im}| = \sum_{i \neq m} |\Theta_{im}| + \sum_{j \neq m} |\Theta_{mj}|,$$

since Θ has row sums zero, that is $\Theta_{im} = -\sum_{j \neq m} \Theta_{ij}$. The two equations above combine into

$$\begin{aligned} \sum_{i \neq j} \sum |f_m(\Theta)_{ij}| + 2 \sum_i \left| \sum_j f_m(\Theta)_{ij} \right| &= \sum_{i \neq m} \left(\sum_{j \notin \{i, m\}} |\Theta_{ij}| + |\Theta_{im}| \right) + \sum_{j \neq m} |\Theta_{mj}| \\ &= \sum_{i \neq m} \sum_{j \neq i} |\Theta_{ij}| + \sum_{j \neq m} |\Theta_{mj}| \\ &= \sum_{i \neq j} \sum |\Theta_{ij}|. \end{aligned}$$

Conclude that since the objective functions in (7.1) and (7.2) differ only by an additive constant term, the solution $\hat{\Theta}$ of (7.2) also minimizes

$$-\log \det f_m(\Theta) + \text{tr}(\hat{\Sigma}^{(m)} f_m(\Theta)) + \rho \sum_{i \neq j} \sum |f_m(\Theta)_{ij}| + 2\rho \sum_i \left| \sum_j f_m(\Theta)_{ij} \right|.$$

This completes the proof. \square

S3. Sparsistency results for neighborhood selection and graphical lasso: proofs.

S3.1. *Proof of Proposition S1.* First note that if each of the lasso regressions therein succeeds in recovering the corresponding neighborhood, then clearly Algorithm 2 recovers the right graph.

We hereby fix an arbitrary index $\ell \in [p]$. Now, note that the assumed bound on ε implies

$$(S3.1) \quad s_\ell \varepsilon \leq \lambda_\ell / 2,$$

$$(S3.2) \quad \vartheta_\ell s_\ell \varepsilon \leq 1/2,$$

$$(S3.3) \quad 2\vartheta_\ell(1 + \kappa_\ell \vartheta_\ell) s_\ell \varepsilon \leq \eta_\ell / 2,$$

$$(S3.4) \quad 2\vartheta_\ell(1 + \kappa_\ell \vartheta_\ell) \varepsilon + \vartheta_\ell \rho_\ell < \min_{i \in \text{ne}(\ell)} \frac{|B_{i\ell}|}{B_{\ell\ell}},$$

$$(S3.5) \quad 2(1 + \kappa_\ell \vartheta_\ell)^2 \varepsilon < \frac{\rho_\ell \eta_\ell}{4}.$$

For the remainder of the proof, ℓ will be kept fix and hence will be partially removed from the notation. In particular, the subscripts of $\lambda_\ell, \kappa_\ell, \vartheta_\ell, s_\ell, \eta_\ell, \rho_\ell$ will be omitted. Our goal is to show then that

$$(S3.6) \quad \hat{\theta} := \arg \min_{\theta \in \mathbb{R}^{p-1}} \left\{ -2\hat{A}_{\ell, \setminus \ell} \theta + \theta^\top \hat{A}_{\setminus \ell, \ell} \theta + \rho \|\theta\|_1 \right\}$$

has the same support (i.e., the set of indices where it is nonzero) as $B_{\setminus \ell, \ell}$.

Partition $[p]$ into the three subsets $\{\ell\}$, $\text{ne}(\ell)$ and $\text{ne}(\ell)^c \setminus \{\ell\}$. We shall index elements of vectors and rows/columns of matrices by $\ell, 1$ and 2 , respectively, to denote those subsets, e.g.,

$$\hat{A}_{11} := (\hat{A}_{ij})_{i \in \text{ne}(\ell), j \in \text{ne}(\ell)}$$

$$\hat{A}_{21} := (\hat{A}_{ij})_{i \in \text{ne}(\ell)^c \setminus \{\ell\}, j \in \text{ne}(\ell)}$$

$$\hat{A}_{1\ell} := (\hat{A}_{i\ell})_{i \in \text{ne}(\ell)}$$

$$\hat{A}_{2\ell} := (\hat{A}_{i\ell})_{i \in \text{ne}(\ell)^c \setminus \{\ell\}};$$

similarly define the population versions $A_{11}, A_{21}, A_{1\ell}$ and $A_{2\ell}$. We use the same notation for partitioning the matrix B . We now show that (S3.1) to (S3.5) imply the bounds

$$(S3.7) \quad \left\| \hat{A}_{21} (\hat{A}_{11})^{-1} \right\|_\infty \leq 1 - \eta/2$$

$$(S3.8) \quad \left\| (\hat{A}_{11})^{-1} \hat{A}_{1\ell} + \frac{B_{1\ell}}{B_{\ell\ell}} \right\|_\infty + \frac{\rho}{2} \left\| (\hat{A}_{11})^{-1} \right\|_\infty < \min_{i \in \text{ne}(\ell)} \frac{|B_{i\ell}|}{B_{\ell\ell}}$$

$$(S3.9) \quad \left\| \hat{A}_{21} (\hat{A}_{11})^{-1} \hat{A}_{1\ell} - \hat{A}_{2\ell} \right\|_\infty < \frac{\rho\eta}{4}.$$

Subsequently, by adapting the arguments of Zhao and Yu (2006), we will show that the invertibility of \hat{A}_{11} , along with (S3.7) to (S3.9), imply the result.

Preliminaries to the proofs of (S3.7) to (S3.9): Let us start by obtaining a few useful bounds and identities.

We first prove that under the assumptions made, the matrix \hat{A}_{11} is invertible. Observe that

$$\lambda_{\min}(\hat{A}_{11}) = \min_{b: \|b\|_2=1} b^\top \hat{A}_{11} b \geq \lambda - \sup_{b: \|b\|_2=1} b^\top (\hat{A}_{11} - A_{11}) b \geq \lambda - s \|\hat{A}_{11} - A_{11}\|_\infty = \lambda - s\varepsilon \geq \lambda/2,$$

by (S3.1). In the second inequality, we have used the known result that the spectral norm of any square matrix is upper bounded by its dimension times its maximum norm. Most importantly, we have established that \hat{A}_{11} is invertible.

Now, by sub-multiplicativity of operator norms,

$$\begin{aligned} \left\| \left(\widehat{A}_{11} \right)^{-1} - \left(A_{11} \right)^{-1} \right\|_{\infty} &= \left\| \left(\widehat{A}_{11} \right)^{-1} \left(A_{11} - \widehat{A}_{11} \right) \left(A_{11} \right)^{-1} \right\|_{\infty} \\ &\leq \left\| \left(A_{11} \right)^{-1} \right\|_{\infty} \left\| \left(\widehat{A}_{11} \right)^{-1} \right\|_{\infty} \left\| \widehat{A}_{11} - A_{11} \right\|_{\infty} \\ &\leq \vartheta \left(\vartheta + \left\| \left(\widehat{A}_{11} \right)^{-1} - \left(A_{11} \right)^{-1} \right\|_{\infty} \right) s\varepsilon. \end{aligned}$$

Rearranging yields

$$(S3.10) \quad \left\| \left(\widehat{A}_{11} \right)^{-1} - \left(A_{11} \right)^{-1} \right\|_{\infty} \leq \frac{\vartheta^2 s\varepsilon}{1 - \vartheta s\varepsilon} \leq 2\vartheta^2 s\varepsilon,$$

since the L^{∞}/L^{∞} -operator norm of a square matrix is also upper bounded by its dimension times its maximum norm. The last inequality is due to (S3.2). For further use, note that this implies

$$(S3.11) \quad \left\| \left(\widehat{A}_{11} \right)^{-1} \right\|_{\infty} \leq \vartheta + \left\| \left(\widehat{A}_{11} \right)^{-1} - \left(A_{11} \right)^{-1} \right\|_{\infty} \leq \vartheta + 2\vartheta^2 s\varepsilon \leq 2\vartheta,$$

where in the last inequality we applied (S3.2) again.

Using (S3.10), it is possible to obtain a sharper bound on the maximum norm difference between $(A_{11})^{-1}$ and $(\widehat{A}_{11})^{-1}$. Indeed, note that for any matrices T_1, T_2 , we have

$$(S3.12) \quad \|T_1 T_2\|_{\infty} \leq \|T_1\|_{\infty} \|T_2\|_1,$$

which reduces to $\|T_1\|_{\infty} \|T_2\|_1$ if T_2 is a column vector. Similarly,

$$(S3.13) \quad \|T_1 T_2\|_{\infty} \leq \|T_1\|_{\infty} \|T_2\|_{\infty}.$$

Repeatedly using those facts, along with symmetry,

$$\begin{aligned} \left\| \left(\widehat{A}_{11} \right)^{-1} - \left(A_{11} \right)^{-1} \right\|_{\infty} &= \left\| \left(\widehat{A}_{11} \right)^{-1} \left(A_{11} - \widehat{A}_{11} \right) \left(A_{11} \right)^{-1} \right\|_{\infty} \\ &\leq \left\| \left(\widehat{A}_{11} \right)^{-1} \left(A_{11} - \widehat{A}_{11} \right) \right\|_{\infty} \left\| \left(A_{11} \right)^{-1} \right\|_1 \\ &\leq \left\| \left(\widehat{A}_{11} \right)^{-1} \right\|_{\infty} \left\| A_{11} - \widehat{A}_{11} \right\|_{\infty} \left\| \left(A_{11} \right)^{-1} \right\|_1 \\ (S3.14) \quad &\leq 2\vartheta^2 \varepsilon, \end{aligned}$$

where in the last step we used the fact that the L^1/L^1 - and L^{∞}/L^{∞} -operator norms of a symmetric matrix (in this case, $(A_{11})^{-1}$) are equal, along with (S3.11).

We now prove that

$$(S3.15) \quad \left(A_{11} \right)^{-1} A_{1\ell} = -\frac{B_{1\ell}}{B_{\ell\ell}}.$$

If $\mathbf{W} \sim N(0, A)$, it is known that $-B_{1\ell}/B_{\ell\ell}$ is the vector of non-zero coefficients for optimal linear prediction of W_{ℓ} using $\mathbf{W}_{\setminus\ell}$. Since removing the non-predictor variables does not change the prediction, we have

$$-\frac{B_{1\ell}}{B_{\ell\ell}} = -\frac{B_{1\ell}^*}{B_{\ell\ell}^*}$$

where

$$B^* := \begin{bmatrix} A_{11} & A_{1\ell} \\ A_{\ell 1} & A_{\ell\ell} \end{bmatrix}^{-1}.$$

By the inversion formula for block matrices,

$$-B_{1\ell}^* = \frac{1}{A_{\ell\ell}} \left(A_{11} - \frac{A_{1\ell}A_{\ell 1}}{A_{\ell\ell}} \right)^{-1} A_{1\ell}, \quad B_{\ell\ell}^* = \frac{1}{A_{\ell\ell}} \left(1 - \frac{A_{\ell 1}(A_{11})^{-1}A_{1\ell}}{A_{\ell\ell}} \right)^{-1},$$

so letting $\lambda := \frac{A_{\ell 1}(A_{11})^{-1}A_{1\ell}}{A_{\ell\ell}} \in (0, 1)$,

$$-\frac{B_{1\ell}^*}{B_{\ell\ell}^*} = (1 - \lambda) \left(A_{11} - \frac{A_{1\ell}A_{\ell 1}}{A_{\ell\ell}} \right)^{-1} A_{1\ell}.$$

Applying Woodbury's matrix inversion formula, we find

$$\begin{aligned} \left(A_{11} - \frac{A_{1\ell}A_{\ell 1}}{A_{\ell\ell}} \right)^{-1} &= (A_{11})^{-1} - (A_{11})^{-1} A_{1\ell} \left(-A_{\ell\ell} + A_{\ell 1}(A_{11})^{-1}A_{1\ell} \right)^{-1} A_{\ell 1}(A_{11})^{-1} \\ &= (A_{11})^{-1} - (A_{11})^{-1} A_{1\ell} \frac{1}{A_{\ell\ell}(\lambda - 1)} A_{\ell 1}(A_{11})^{-1}. \end{aligned}$$

Simple matrix algebra yields

$$-\frac{B_{1\ell}^*}{B_{\ell\ell}^*} = (1 - \lambda)(A_{11})^{-1} A_{1\ell} \left(1 - \frac{1}{A_{\ell\ell}(\lambda - 1)} A_{\ell 1}(A_{11})^{-1} A_{1\ell} \right) = (1 - \lambda)(A_{11})^{-1} A_{1\ell} \left(1 - \frac{\lambda}{\lambda - 1} \right) = (A_{11})^{-1} A_{1\ell},$$

which finally establishes (S3.15).

Similarly, we prove that

$$(S3.16) \quad A_{21}(A_{11})^{-1} A_{1\ell} = A_{2\ell}.$$

Indeed, notice that the Schur complement of A_{11} in A ,

$$A_{(2,\ell),(2,\ell)|1} := \begin{bmatrix} A_{22} & A_{2\ell} \\ A_{\ell 2} & A_{\ell\ell} \end{bmatrix} - \begin{bmatrix} A_{21} \\ A_{\ell 1} \end{bmatrix} (A_{11})^{-1} [A_{12} \ A_{1\ell}],$$

is the conditional covariance matrix of the random vector $\mathbf{W}_{\text{ne}(\ell)^c}$ given $\mathbf{W}_{\text{ne}(\ell)}$. The off-diagonal block of $A_{(2,\ell),(2,\ell)|1}$, that is, $A_{2\ell} - A_{21}(A_{11})^{-1}A_{1\ell}$, is therefore the conditional covariance between W_ℓ and the other variables not in its neighborhood, given the variables in its neighborhood. By definition of the neighborhood, this is zero, hence (S3.16) holds.

Proof of (S3.7): Using (S3.10), we have

$$\begin{aligned} \left\| \widehat{A}_{21}(\widehat{A}_{11})^{-1} - A_{21}(A_{11})^{-1} \right\|_\infty &\leq \left\| \widehat{A}_{21}(\widehat{A}_{11})^{-1} - A_{21}(\widehat{A}_{11})^{-1} \right\|_\infty + \left\| A_{21}(\widehat{A}_{11})^{-1} - A_{21}(A_{11})^{-1} \right\|_\infty \\ &\leq \left\| (\widehat{A}_{11})^{-1} \right\|_\infty \left\| \widehat{A}_{21} - A_{21} \right\|_\infty + \left\| A_{21} \right\|_\infty \left\| (\widehat{A}_{11})^{-1} - (A_{11})^{-1} \right\|_\infty \\ &\leq 2\vartheta s\varepsilon + \kappa 2\vartheta^2 s\varepsilon \\ &= 2\vartheta(1 + \kappa\vartheta)s\varepsilon, \end{aligned}$$

where the third inequality follows by applying (S3.10) and (S3.11). Now by the reverse triangle inequality,

$$\left\| \widehat{A}_{21}(\widehat{A}_{11})^{-1} \right\|_\infty \leq \left\| A_{21}(A_{11})^{-1} \right\|_\infty + \left\| \widehat{A}_{21}(\widehat{A}_{11})^{-1} - A_{21}(A_{11})^{-1} \right\|_\infty \leq 1 - \eta + 2\vartheta(1 + \kappa\vartheta)s\varepsilon.$$

(S3.7) then follows from (S3.3).

Proof of (S3.8): First, by (S3.15),

$$\begin{aligned} \left\| (\widehat{A}_{11})^{-1} \widehat{A}_{1\ell} + \frac{B_{1\ell}}{B_{\ell\ell}} \right\|_\infty &= \left\| (\widehat{A}_{11})^{-1} \widehat{A}_{1\ell} - (A_{11})^{-1} A_{1\ell} \right\|_\infty \\ &\leq \left\| (\widehat{A}_{11})^{-1} \widehat{A}_{1\ell} - (\widehat{A}_{11})^{-1} A_{1\ell} \right\|_\infty + \left\| (\widehat{A}_{11})^{-1} A_{1\ell} - (A_{11})^{-1} A_{1\ell} \right\|_\infty \end{aligned}$$

$$\begin{aligned}
&\leq \left\| \left\| (\widehat{A}_{11})^{-1} \right\| \right\|_{\infty} \left\| \widehat{A}_{1\ell} - A_{1\ell} \right\|_{\infty} + \left\| \left((\widehat{A}_{11})^{-1} - (A_{11})^{-1} \right) \right\|_{\infty} \|A_{1\ell}\|_1 \\
&\leq 2\vartheta\varepsilon + 2\vartheta^2\varepsilon\kappa \\
&= 2\vartheta(1 + \kappa\vartheta)\varepsilon,
\end{aligned}$$

where we first used (S3.12) and (S3.13), then (S3.11) and (S3.14). Noting that

$$\frac{\rho}{2} \left\| \left\| (\widehat{A}_{11})^{-1} \right\| \right\|_{\infty} \leq \frac{\rho}{2} 2\vartheta = \vartheta\rho,$$

(S3.8) follows from (S3.4).

Proof of (S3.9): First, by (S3.16),

$$\left\| \widehat{A}_{21}(\widehat{A}_{11})^{-1}\widehat{A}_{1\ell} - \widehat{A}_{2\ell} \right\|_{\infty} \leq \left\| \widehat{A}_{21}(\widehat{A}_{11})^{-1}\widehat{A}_{1\ell} - A_{21}(A_{11})^{-1}A_{1\ell} \right\|_{\infty} + \left\| \widehat{A}_{2\ell} - A_{2\ell} \right\|_{\infty},$$

the second term of which is clearly upper bounded by ε . The first term above is upper bounded by

$$\begin{aligned}
&\left\| \widehat{A}_{21}(\widehat{A}_{11})^{-1}\widehat{A}_{1\ell} - \widehat{A}_{21}(A_{11})^{-1}A_{1\ell} \right\|_{\infty} + \left\| \widehat{A}_{21}(A_{11})^{-1}A_{1\ell} - A_{21}(A_{11})^{-1}A_{1\ell} \right\|_{\infty} \\
&\leq \left\| \left\| \widehat{A}_{21} \right\| \right\|_{\infty} \left\| (\widehat{A}_{11})^{-1}\widehat{A}_{1\ell} - (A_{11})^{-1}A_{1\ell} \right\|_{\infty} + \left\| \widehat{A}_{21} - A_{21} \right\|_{\infty} \left\| (A_{11})^{-1}A_{1\ell} \right\|_1 \\
&\leq (\kappa + s\varepsilon)2\vartheta(1 + \kappa\vartheta)\varepsilon + \kappa\vartheta\varepsilon \\
&\leq 2(1 + \kappa\vartheta)^2\varepsilon - \varepsilon,
\end{aligned}$$

where we used (S3.12) and (S3.13) and the result in the proof of (S3.8) above where we bound $\|(\widehat{A}_{11})^{-1}\widehat{A}_{1\ell} - (A_{11})^{-1}A_{1\ell}\|_{\infty}$. The final bound was obtained by applying (S3.2) and rearranging. Hence (S3.9) follows from (S3.5).

Proof that (S3.6) recovers the support of $B_{\setminus\ell,\ell}$: Note that

$$\nabla_{\theta} \left\{ -2\widehat{A}_{\ell,\setminus\ell}\theta + \theta^{\top} \widehat{A}_{\setminus\ell,\ell}\theta \right\} = 2\widehat{A}_{\setminus\ell,\ell}\theta - 2\widehat{A}_{\setminus\ell,\ell}$$

and that the subdifferential of the 1-norm at a point $\theta \in \mathbb{R}^{p-1}$ is given by the set of all $x \in [-1, 1]^{p-1}$ such that

$$\theta_j \neq 0 \implies x_j = \text{sign}(\theta_j).$$

Considering the optimization problem in (S3.6), the KKT conditions state that any point $\widehat{\theta}$ satisfying

$$(S3.17) \quad (2\widehat{A}_{\setminus\ell,\setminus\ell}\widehat{\theta} - 2\widehat{A}_{\setminus\ell,\ell})_{\widehat{\mathcal{J}}} = -\rho \text{sign}(\widehat{\theta}_{\widehat{\mathcal{J}}})$$

$$(S3.18) \quad \left\| (2\widehat{A}_{\setminus\ell,\setminus\ell}\widehat{\theta} - 2\widehat{A}_{\setminus\ell,\ell})_{\widehat{\mathcal{J}}^c} \right\|_{\infty} \leq \rho$$

where $\widehat{\mathcal{J}} := \{j \in [p-1] : \widehat{\theta}_j \neq 0\}$, is a solution. Following the arguments in the proof of Proposition 1 in Zhao and Yu (2006), we shall identify one such solution that has the right support. We will subsequently show that it is unique, utilizing arguments similar to (but not implied by) what is found in Section 2.1 of Tibshirani (2013).

Let $\theta^* := -B_{\setminus\ell,\ell}/B_{\ell\ell}$ and θ_1^*, θ_2^* denote its subvectors indexed by $\text{ne}(\ell)$ and $\text{ne}(\ell)^c \setminus \{\ell\}$, respectively¹; we will use the same notation for $\widehat{\theta}$ defined below. The candidate solution $\widehat{\theta}$ is defined by $\widehat{\theta}_2 = 0$ and

$$\widehat{\theta}_1 := (\widehat{A}_{11})^{-1} \left(\widehat{A}_{1\ell} - \frac{\rho}{2} \text{sign}(\theta_1^*) \right),$$

where the sign function is applied to θ_1^* coordinate-wise. First note that by (S3.8),

$$\left\| \widehat{\theta}_1 - \theta_1^* \right\|_{\infty} < \min_{i \in \text{ne}(\ell)} |\theta_i^*|,$$

¹For simplicity, we slightly abuse the notation here. In fact, θ_1^* and θ_2^* are the subvectors that, in the product $A_{\setminus\ell,\setminus\ell}\theta^*$, are multiplied by the columns of A corresponding to variables in $\text{ne}(\ell)$ and in $\text{ne}(\ell)^c \setminus \{\ell\}$, respectively.

hence $\text{sign}(\theta_1^*) = \text{sign}(\hat{\theta}_1)$. Thus, we find

$$2\hat{A}_{\text{ne}(\ell),\setminus\ell}\hat{\theta} - 2\hat{A}_{1\ell} = 2\hat{A}_{11}\hat{\theta}_1 - 2\hat{A}_{1\ell} = -\rho \text{sign}(\theta_1^*) = -\rho \text{sign}(\hat{\theta}_1),$$

i.e., (S3.17) is satisfied. Next, by (S3.7) and (S3.9) we have

$$\begin{aligned} \|2\hat{A}_{\text{ne}(\ell)^c\setminus\{\ell\},\setminus\ell}\hat{\theta} - 2\hat{A}_{2\ell}\|_\infty &= \|2\hat{A}_{21}\hat{\theta}_1 - 2\hat{A}_{2\ell}\|_\infty \\ &= \left\| 2\hat{A}_{21}(\hat{A}_{11})^{-1}\hat{A}_{1\ell} - 2\hat{A}_{2\ell} - \rho\hat{A}_{21}(\hat{A}_{11})^{-1}\text{sign}(\theta_1^*) \right\|_\infty \\ &\leq 2\left\| \hat{A}_{21}(\hat{A}_{11})^{-1}\hat{A}_{1\ell} - \hat{A}_{2\ell} \right\|_\infty + \rho\left\| \hat{A}_{21}(\hat{A}_{11})^{-1} \right\|_\infty \\ &< \frac{\rho\eta}{2} + \rho\left(1 - \frac{\eta}{2}\right) \\ &= \rho, \end{aligned}$$

i.e., (S3.18) is satisfied. Therefore, we have proved the existence of a solution $\hat{\theta}$ to (S3.6) which has the same sign pattern (hence the same support) as θ^* .

It remains to show that this solution is unique. We first prove a weaker statement: $\hat{A}_{\setminus\ell,\setminus\ell}\tilde{\theta}$ is unique across all solutions $\tilde{\theta}$ to (S3.6). Indeed, suppose that $\tilde{\theta}^{(1)}$ and $\tilde{\theta}^{(2)}$ are two distinct solutions such that $\hat{A}_{\setminus\ell,\setminus\ell}\tilde{\theta}^{(1)} \neq \hat{A}_{\setminus\ell,\setminus\ell}\tilde{\theta}^{(2)}$. Let W be a (possibly rectangular) matrix such that $\hat{A}_{\setminus\ell,\setminus\ell} = W^\top W$; for instance, W can be obtained from a Cholesky decomposition. By assumption, $W\tilde{\theta}^{(1)} \neq W\tilde{\theta}^{(2)}$. Both points being a solution means that the objective function in (S3.6) attains its minimum value at both points: if

$$Q(\theta) := -2\hat{A}_{\setminus\ell,\setminus\ell}\theta + \|W\theta\|_2^2 + \rho\|\theta\|_1,$$

then $Q(\tilde{\theta}^{(1)}) = Q(\tilde{\theta}^{(2)}) = \min_\theta Q(\theta) =: v_{\min}$, say. Then, evaluating Q at a point $\alpha\tilde{\theta}^{(1)} + (1-\alpha)\tilde{\theta}^{(2)}$, for some $\alpha \in (0, 1)$, yields

$$\begin{aligned} &-2\hat{A}_{\setminus\ell,\setminus\ell}(\alpha\tilde{\theta}^{(1)} + (1-\alpha)\tilde{\theta}^{(2)}) + \|\alpha W\tilde{\theta}^{(1)} + (1-\alpha)W\tilde{\theta}^{(2)}\|_2^2 + \rho\|\alpha\tilde{\theta}^{(1)} + (1-\alpha)\tilde{\theta}^{(2)}\|_1 \\ &< \alpha\{-2\hat{A}_{\setminus\ell,\setminus\ell}\tilde{\theta}^{(1)} + \|W\tilde{\theta}^{(1)}\|_2^2 + \rho\|\tilde{\theta}^{(1)}\|_1\} + (1-\alpha)\{-2\hat{A}_{\setminus\ell,\setminus\ell}\tilde{\theta}^{(2)} + \|W\tilde{\theta}^{(2)}\|_2^2 + \rho\|\tilde{\theta}^{(2)}\|_1\} \\ &= \alpha Q(\tilde{\theta}^{(1)}) + (1-\alpha)Q(\tilde{\theta}^{(2)}) \\ &= v_{\min}, \end{aligned}$$

where the strict inequality is a consequence of the strict convexity of the squared Euclidean norm and the convexity of the 1-norm. This is a contradiction since v_{\min} was assumed to be the minimum value. Hence $\hat{A}_{\setminus\ell,\setminus\ell}\tilde{\theta}$ must be unique across all solutions $\tilde{\theta}$ of (S3.6).

Now, using this preliminary uniqueness result, we notice that for any solution $\tilde{\theta}$, we have

$$\left\| 2\hat{A}_{\text{ne}(\ell)^c\setminus\{\ell\},\setminus\ell}\tilde{\theta} - 2\hat{A}_{2\ell} \right\|_\infty = \left\| 2\hat{A}_{\text{ne}(\ell)^c\setminus\{\ell\},\setminus\ell}\hat{\theta} - 2\hat{A}_{2\ell} \right\|_\infty < \rho,$$

hence $\tilde{\theta}_2 = 0$. Therefore,

$$2\hat{A}_{11}\tilde{\theta}_1 - 2\hat{A}_{1\ell} = 2\hat{A}_{\text{ne}(\ell),\setminus\ell}\tilde{\theta} - 2\hat{A}_{1\ell} = 2\hat{A}_{\text{ne}(\ell),\setminus\ell}\hat{\theta} - 2\hat{A}_{1\ell} = -\rho \text{sign}(\theta_1^*),$$

which uniquely defines $\tilde{\theta}_1$ by the invertibility of \hat{A}_{11} . Deduce that $\tilde{\theta} = \hat{\theta}$. \square

S3.2. *Proof of Proposition S2.* First note that the assumed bound on ε implies

$$(S3.19) \quad \varepsilon \leq \frac{\alpha\rho}{8},$$

$$(S3.20) \quad 2\kappa_\Omega(\varepsilon + \rho) \leq \min \left\{ \frac{1}{3\kappa_A s}, \frac{1}{3\kappa_A^3 \kappa_\Omega s} \right\},$$

$$(S3.21) \quad 6\kappa_A^3 \kappa_\Omega^2 s(\varepsilon + \rho) \leq \frac{\alpha}{9} \leq \frac{1}{1 + 8/\alpha},$$

$$(S3.22) \quad 2\kappa_\Omega(\varepsilon + \rho) \leq \frac{1}{2} \min_{i \neq j, B_{ij} \neq 0} |B_{ij}|.$$

Without loss of generality, assume that $\rho > 0$. Otherwise, (S3.19) implies that $\hat{A} = A$, in which case the result is trivial.

The proof is heavily based on that of Theorems 1 and 2 of Ravikumar et al. (2011). Note that by assumption, each diagonal element of \hat{A} satisfies $\hat{A}_{ii} \geq A_{ii} - \varepsilon > 0$, $i \in [p]$. Then by Lemma 3 of that paper, the positivity of ρ ensures that the solution \hat{B} exists, is unique and satisfies

$$-\hat{B}^{-1} + \hat{A} + \rho Z = 0,$$

for some matrix Z in the sub-differential of the off-diagonal norm at the point \hat{B} , as defined in Ravikumar et al. (2011). The strategy is now to consider the solution \tilde{B} of the graphical lasso optimization problem with the additional constraint that $B_{S^c} = 0$, which is also guaranteed to exist and to be unique by (S3.19). Define $\Delta := \|\tilde{B} - B\|_\infty$. By (S3.20), the condition of Lemma 6 of Ravikumar et al. (2011) is satisfied. It then follows from that result that $\|\Delta\|_\infty \leq 2\kappa_\Omega(\varepsilon + \rho)$. Lemma 5 from that paper now implies that the matrix $R(\Delta)$, as defined therein, satisfies

$$\|R(\Delta)\|_\infty \leq \frac{3}{2} \kappa_A^3 s \|\Delta\|_\infty^2 \leq 6\kappa_A^3 \kappa_\Omega^2 s(\varepsilon + \rho)^2 \leq \frac{\varepsilon + \rho}{1 + 8/\alpha} \leq \frac{(\alpha/8 + 1)\rho}{1 + 8/\alpha} = \frac{\alpha\rho}{8},$$

where the last three inequalities are due to the previously obtained bound on $\|\Delta\|_\infty$, to (S3.21) and to (S3.19), respectively. Now that $\varepsilon \vee \|R(\Delta)\|_\infty \leq \alpha\rho/8$, we may apply Lemma 4 of Ravikumar et al. (2011) and find that in fact, $\hat{B} = \tilde{B}$. It follows, by definition of \tilde{B} , that $\hat{B}_{ij} = 0$ for all $(i, j) \in S^c$ and that for $(i, j) \in S$, $i \neq j$,

$$|\hat{B}_{ij} - B_{ij}| \leq \|\Delta\|_\infty \leq \frac{|B_{ij}|}{2}$$

by (S3.22). That is, the element-wise error is too small for \hat{B}_{ij} to reach 0. We have therefore guaranteed that the sparsity pattern of \hat{B} is the same as that of B . \square

S4. Proof of Theorem 3. We start by introducing useful additional notation and auxiliary variables that will be useful throughout this proof. For $\ell \in \{1, 2\}$, let $e_i^{(m), \ell} := \mathbb{E}[(\log Y_i^{(m)})^\ell]$ and $e_{ij}^{(m)} := \mathbb{E}[(\log Y_i^{(m)})(\log Y_j^{(m)})]$. Then we have

$$(S4.1) \quad \Gamma_{ij}^{(m)} = e_i^{(m), 2} + e_j^{(m), 2} - 2e_{ij}^{(m)} - (e_i^{(m), 1} - e_j^{(m), 1})^2, \quad i \neq j, m \in V.$$

Similarly

$$\hat{\Gamma}_{ij}^{(m)} = \hat{e}_i^{(m), 2} + \hat{e}_j^{(m), 2} - 2\hat{e}_{ij}^{(m)} - (\hat{e}_i^{(m), 1} - \hat{e}_j^{(m), 1})^2, \quad i \neq j, m \in V,$$

where

$$\begin{aligned} \hat{e}_i^{(m), \ell} &:= \frac{1}{k} \sum_{t=1}^n \left\{ \log \left(\frac{k}{n\hat{F}_i(U_{ti})} \right) \right\}^\ell \mathbf{1} \left\{ \hat{F}_m(U_{tm}) \leq k/n \right\}, \\ \hat{e}_{ij}^{(m)} &:= \frac{1}{k} \sum_{t=1}^n \log \left(\frac{k}{n\hat{F}_j(U_{tj})} \right) \log \left(\frac{k}{n\hat{F}_i(U_{ti})} \right) \mathbf{1} \left\{ \hat{F}_m(U_{tm}) \leq k/n \right\}, \end{aligned}$$

$U_{ti} := 1 - F_i(X_{ti})$, $1 \leq t \leq n$, are independent and uniformly distributed, and \widehat{F}_i is the (right-continuous) empirical distribution function of $(U_{ti})_{1 \leq t \leq n}$, satisfying $\widehat{F}_i(U_{ti}) = 1 - \widetilde{F}_i(X_{ti})$.

Let $i \neq j$ and m be arbitrary. An expression for the estimation error is given by

$$(S4.2) \quad \begin{aligned} \widehat{\Gamma}_{ij}^{(m)} - \Gamma_{ij}^{(m)} &= (\widehat{e}_i^{(m),2} - e_i^{(m),2}) + (\widehat{e}_j^{(m),2} - e_j^{(m),2}) - 2(\widehat{e}_{ij}^{(m)} - e_{ij}^{(m)}) \\ &\quad - 2(e_i^{(m),1} - e_j^{(m),1})((\widehat{e}_i^{(m),1} - e_i^{(m),1}) - (\widehat{e}_j^{(m),1} - e_j^{(m),1})) \\ &\quad - ((\widehat{e}_i^{(m),1} - e_i^{(m),1}) - (\widehat{e}_j^{(m),1} - e_j^{(m),1}))^2, \end{aligned}$$

the last two terms stemming from the identity $y^2 - x^2 = 2x(y - x) + (y - x)^2$. In order to prove the result, it is sufficient to bound the differences

$$\widehat{e}_i^{(m),\ell} - e_i^{(m),\ell}, \quad \widehat{e}_m^{(m),\ell} - e_m^{(m),\ell}, \quad \widehat{e}_{im}^{(m)} - e_{im}^{(m)}, \quad \widehat{e}_{ij}^{(m)} - e_{ij}^{(m)}$$

for all distinct triples (i, j, m) and $\ell \in \{1, 2\}$. The terms $\widehat{e}_m^{(m),\ell} - e_m^{(m),\ell}$ are entirely deterministic, since it is known that the observations X_{tm} that are used for the estimator $\widehat{\Gamma}^{(m)}$ have ranks $n - k + 1, \dots, n$ (by continuity, it can be assumed that there are no ties in the data). They are on the order of $(\log k)^\ell/k$, as is proved in Section S5.3. The rest of the proof thus focuses on the other three differences.

S4.1. *Preliminaries, additional notation and structure of the proof.* Recall that \widehat{F}_i is the empirical distribution function of $(U_{ti})_{1 \leq t \leq n}$ and denote its left-continuous inverse by \widehat{F}_i^- , where $f^-(t) := \inf\{x : f(x) \geq t\}$. Consider the rescaled tail quantile processes

$$(S4.3) \quad u_n^{(i)}(x) := \frac{n}{k} \widehat{F}_i^-(kx/n).$$

Similarly to R and its margins R_J , $J \subset V$, let

$$(S4.4) \quad \widehat{R}_J^0(\mathbf{x}_J) := \frac{1}{k} \sum_{t=1}^n \mathbb{1} \left\{ U_{ti} \leq \frac{k}{n} x_i, i \in J \right\}, \quad \widehat{R}_J(\mathbf{x}_J) := \widehat{R}_J^0(\widehat{\mathbf{x}}_J), \quad \mathbf{x}_J \in [0, \infty)^{|J|},$$

where $\widehat{\mathbf{x}}_J := (u_n^{(i)}(x_i))_{i \in J}$. The function \widehat{R}_J can be seen as the tail empirical copula of the random vector \mathbf{U}_J . As an intermediate between R_J and \widehat{R}_J , let

$$R_{J,n}(\mathbf{x}_J) := \frac{n}{k} \mathbb{P} \left(\mathbf{U}_J \leq \frac{k}{n} \mathbf{x}_J \right) = \frac{n}{k} \mathbb{P} \left(F_J(\mathbf{X}_J) > 1 - \frac{k}{n} \mathbf{x}_J \right),$$

the pre-asymptotic version of R_J .

The function R_J can be seen as a measure on $[0, \infty)^{|J|}$ and for measurable sets $A_i \subset \mathbb{R}$, we will write $R_J((A_i)_{i \in J})$ to denote $R_J(\otimes_{i \in J} A_i)$. If in place of one of the A_i there is a number a_i , it will be understood that $A_i = [0, a_i]$. For example, $R_{ij}([x, \infty), y) = R_{ij}([x, \infty) \times [0, y])$. We use the same conventions for the functions $R_{J,n}$, \widehat{R}_J^0 and \widehat{R}_J , as well as $G_{J,n}$ and \bar{R}_J to be defined later.

The functions R_J , $R_{J,n}$, \widehat{R}_J^0 and \widehat{R}_J enjoy certain properties which will be used throughout the proof, as well as throughout Section S5: they are non-decreasing in each component and are upper bounded by their minimum argument. Beyond component-wise monotonicity, the induced measures, as described above, are non-negative. The functions R_J moreover inherit the homogeneity property of multivariate Pareto distributions ($R_J(q\mathbf{x}_J) = qR_J(\mathbf{x}_J)$, $q \geq 0$).

From now on, fix a number $a \in (0, 1)$. It is proved in Lemma S7 that for all distinct triples (i, j, m) and $\ell \in \{1, 2\}$, we have

$$\begin{aligned} \widehat{e}_i^{(m),\ell} - e_i^{(m),\ell} &= \int_a^1 \frac{(\widehat{R}_{im}(x, 1) - R_{im}(x, 1))(-2 \log x)^{\ell-1}}{x} dx \\ &\quad - \int_1^{n/k} \frac{(\widehat{R}_{im}([x, \infty), 1) - R_{im}([x, \infty), 1))(-2 \log x)^{\ell-1}}{x} dx \end{aligned}$$

$$(S4.5) \quad + O\left(\left(\frac{k}{n}\right)^\xi \log(n/k) + \frac{(\log(n/k) + \log(1/a))^2}{k} + a(\log(n/k) + \log(1/a))\right),$$

$$(S4.6) \quad \begin{aligned} \widehat{e}_{im}^{(m)} - e_{im}^{(m)} &= \int_a^1 \int_a^1 \frac{\widehat{R}_{im}(x, y) - R_{im}(x, y)}{xy} dx dy \\ &\quad - \int_a^1 \int_1^{n/k} \frac{\widehat{R}_{im}([x, \infty), y) - R_{im}([x, \infty), y)}{xy} dx dy \\ &\quad + O\left(\left(\frac{k}{n}\right)^\xi \log(n/k) + \frac{(\log(n/k) + \log(1/a))^2}{k} + a(\log(n/k) + \log(1/a))\right), \end{aligned}$$

$$(S4.7) \quad \begin{aligned} \widehat{e}_{ij}^{(m)} - e_{ij}^{(m)} &= \int_a^1 \int_a^1 \frac{\widehat{R}_{ijm}(x, y, 1) - R_{ijm}(x, y, 1)}{xy} dx dy \\ &\quad - \int_a^1 \int_1^{n/k} \frac{\widehat{R}_{ijm}([x, \infty), y, 1) - R_{ijm}([x, \infty), y, 1)}{xy} dx dy \\ &\quad - \int_1^{n/k} \int_a^1 \frac{\widehat{R}_{ijm}(x, [y, \infty), 1) - R_{ijm}(x, [y, \infty), 1)}{xy} dx dy \\ &\quad + \int_1^{n/k} \int_1^{n/k} \frac{\widehat{R}_{ijm}([x, \infty), [y, \infty), 1) - R_{ijm}([x, \infty), [y, \infty), 1)}{xy} dx dy \\ &\quad + O\left(\left(\frac{k}{n}\right)^\xi \log(n/k) + \frac{(\log(n/k) + \log(1/a))^2}{k} + a(\log(n/k) + \log(1/a))\right) \end{aligned}$$

almost surely, where the error terms are not stochastic. We shall separately bound each of the eight integrals above. Denote these integrals, in order of appearance in (S4.5) to (S4.7), by $\mathcal{I}_i^{(m), \ell, -}$, $\mathcal{I}_i^{(m), \ell, +}$, $\mathcal{I}_{im}^{(m), --}$, $\mathcal{I}_{im}^{(m), +-}$, $\mathcal{I}_{ij}^{(m), --}$, $\mathcal{I}_{ij}^{(m), +-}$, $\mathcal{I}_{ij}^{(m), -+}$ and $\mathcal{I}_{ij}^{(m), ++}$.

The processes $\widehat{R}_J - R_J$ can be decomposed into the stochastic error $\widehat{R}_J - R_{J,n}$ and the difference $R_{J,n} - R_J$ between the tail at finite and infinite levels. Replacing $\widehat{R}_J - R_J$ by $(\widehat{R}_J - R_{J,n}) + (R_{J,n} - R_J)$, each integral $\mathcal{I}^{(m), \cdot}$ is written as

$$\mathcal{I}^{(m), \cdot} =: A^{(m), \cdot} + B^{(m), \cdot},$$

where the A terms are stochastic and the B terms represent deterministic bias.

We proceed as follows. In Section S4.2, it is shown that Assumption 1 is sufficient to bound all the bias terms, up to a constant, by $(k/n)^\xi (\log(n/k) + \log(1/a))^2$. Subsequently, we prove in Section S4.3 concentration results for the stochastic terms which are then leveraged in Section S4.4 to complete the proof.

Before moving on, we highlight some consequences of Assumption 1 and Proposition 1 in terms of the functions $R_{J,n}$ and R_J . For any distinct triple (i, j, m) and $q \in (0, 1]$,

$$(S4.8) \quad \sup_{x \leq n/k, y \leq 1} |R_{ij,n}(x, y) - R_{ij}(x, y)| \leq 2K \left(\frac{k}{n}\right)^\xi,$$

$$(S4.9) \quad \sup_{x \leq n/k, y \leq n/k, z \leq 1} |R_{ijm,n}(x, y, z) - R_{ijm}(x, y, z)| \leq K \left(\frac{k}{n}\right)^\xi,$$

$$(S4.10) \quad 1 - R_{ijm}(q^{-1}, q^{-1}, 1) \leq 1 - R_{im}(q^{-1}, 1) + 1 - R_{jm}(q^{-1}, 1) \leq 2Kq^\xi;$$

to obtain the first inequality in (S4.10), apply the inequality

$$P([0, q^{-1}] \times [0, q^{-1}]) \geq P([0, q^{-1}] \times [0, \infty)) + P([0, \infty) \times [0, q^{-1}]) - 1,$$

valid for probability measures P on $[0, \infty)^2$, with $P = R_{ijm}(\cdot \times [0, 1])$.

S4.2. *The bias terms B .* (S4.8) directly implies

$$\begin{aligned} |B_i^{(m), \ell, -}| &\leq \int_a^1 \frac{|R_{im,n}(x, 1) - R_{im}(x, 1)| (-2 \log x)^{\ell-1}}{x} dx \\ &\leq 2K \left(\frac{k}{n}\right)^\xi \int_a^1 \frac{(-2 \log x)^{\ell-1}}{x} dx \\ &\lesssim \left(\frac{k}{n}\right)^\xi (\log(1/a))^\ell, \end{aligned}$$

$$\begin{aligned} |B_i^{(m), \ell, +}| &\leq \int_1^{n/k} \frac{|R_{im,n}([x, \infty), 1) - R_{im}([x, \infty), 1)| (2 \log x)^{\ell-1}}{x} dx \\ &\leq 2K \left(\frac{k}{n}\right)^\xi \int_1^{n/k} \frac{(2 \log x)^{\ell-1}}{x} dx \\ &\lesssim \left(\frac{k}{n}\right)^\xi (\log(n/k))^\ell, \end{aligned}$$

$$\begin{aligned} |B_{im}^{(m), --}| &\leq \int_a^1 \int_a^1 \frac{|R_{im,n}(x, y) - R_{im}(x, y)|}{xy} dx dy \\ &\leq 2K \left(\frac{k}{n}\right)^\xi \int_a^1 \int_a^1 \frac{1}{xy} dx dy \\ &\lesssim \left(\frac{k}{n}\right)^\xi (\log(1/a))^2, \end{aligned}$$

$$\begin{aligned} |B_{im}^{(m), +-}| &\leq \int_a^1 \int_1^{n/k} \frac{|R_{im,n}([x, \infty), y) - R_{im}([x, \infty), y)|}{xy} dx dy \\ &\leq 2K \left(\frac{k}{n}\right)^\xi \int_a^1 \int_1^{n/k} \frac{1}{xy} dx dy \\ &\lesssim \left(\frac{k}{n}\right)^\xi (\log(n/k)) (\log(1/a)). \end{aligned}$$

Note further that by (S4.9), $B_{ij}^{(m), --}$ admits the same bound as $B_{im}^{(m), --}$. Similarly, $B_{ij}^{(m), +-}$, and by symmetry $B_{ij}^{(m), -+}$, admit the same bound as $B_{im}^{(m), +-}$. Finally, since

$$R_{ijm}([x, \infty), [y, \infty), 1) = 1 - R_{jm}(y, 1) - R_{im}(x, 1) + R_{ijm}(x, y, 1)$$

and the same relation holds for $R_{ijm,n}$, (S4.8) and (S4.9) also imply that

$$\sup_{x \leq n/k, y \leq n/k} |R_{ijm,n}([x, \infty), [y, \infty), 1) - R_{ijm}([x, \infty), [y, \infty), 1)| \leq 5K \left(\frac{k}{n}\right)^\xi.$$

Deduce that

$$|B_{ij}^{(m), ++}| \leq \int_1^{n/k} \int_1^{n/k} \frac{|R_{ijm,n}([x, \infty), [y, \infty), 1) - R_{ijm}([x, \infty), [y, \infty), 1)|}{xy} dx dy$$

$$\begin{aligned} &\leq 5K \left(\frac{k}{n}\right)^\xi \int_1^{n/k} \int_1^{n/k} \frac{1}{xy} dx dy \\ &\lesssim \left(\frac{k}{n}\right)^\xi (\log(n/k))^2. \end{aligned}$$

S4.3. *The stochastic error terms A.* It remains to bound the stochastic error terms A_i , which entirely depend on the processes $\widehat{R}_J - R_{J,n}$. Recall how, for $\mathbf{x}_J \in [0, \infty)^{|J|}$, we define $\widehat{\mathbf{x}}_J$ in (S4.4). Consider further the relation $\widehat{R}_J(\mathbf{x}_J) = \widehat{R}_J^0(\widehat{\mathbf{x}}_J)$. We shall rely on the decomposition

$$\begin{aligned} \widehat{R}_J(\mathbf{x}_J) - R_{J,n}(\mathbf{x}_J) &= (\widehat{R}_J^0(\widehat{\mathbf{x}}_J) - R_{J,n}(\widehat{\mathbf{x}}_J)) + (R_{J,n}(\widehat{\mathbf{x}}_J) - R_{J,n}(\mathbf{x}_J)) \\ (S4.11) \quad &= (G_{J,n}(\widehat{\mathbf{x}}_J) - G_{J,n}(\mathbf{x}_J)) + G_{J,n}(\mathbf{x}_J) + (R_{J,n}(\widehat{\mathbf{x}}_J) - R_{J,n}(\mathbf{x}_J)), \end{aligned}$$

where

$$(S4.12) \quad G_{J,n} := \widehat{R}_J^0 - R_{J,n}.$$

Accordingly, each A_i term is further decomposed into three integrals $A_{i,1}$, $A_{i,2}$ and $A_{i,3}$. For instance,

$$\begin{aligned} A_{ij}^{(m),--} &= A_{ij,1}^{(m),--} + A_{ij,2}^{(m),--} + A_{ij,3}^{(m),--} \\ &:= \int_a^1 \int_a^1 \frac{G_{ijm,n}(u_n^{(i)}(x), u_n^{(j)}(y), u_n^{(m)}(1)) - G_{ijm,n}(x, y, 1)}{xy} dx dy \\ &\quad + \int_a^1 \int_a^1 \frac{G_{ijm,n}(x, y, 1)}{xy} dx dy \\ (S4.13) \quad &\quad + \int_a^1 \int_a^1 \frac{R_{ijm,n}(u_n^{(i)}(x), u_n^{(j)}(y), u_n^{(m)}(1)) - R_{ijm,n}(x, y, 1)}{xy} dx dy. \end{aligned}$$

The first of the three terms in (S4.11) is proportional to a standard empirical process evaluated at a set corresponding to the difference between \mathbf{x}_J and $\widehat{\mathbf{x}}_J$. It will be uniformly bounded by using well known concentration inequalities for empirical processes appearing in [Koltchinskii \(2006\)](#) and [Massart \(2000\)](#). The second term, $G_{J,n}$, is now a rescaled sum of n independent and identically distributed (iid) processes which, when integrated as in (S4.13), becomes a sum of iid, bounded random variables. We will be able to control this sum via Bernstein's inequality. Finally, the third term relates to the difference between \mathbf{x}_J and $\widehat{\mathbf{x}}_J$. It can be controlled by weighted approximation results on the uniform quantile processes given in [Lemmas S1](#) and [S2](#). Two bounds are then proved on the corresponding term in (S4.13), the stronger of which only holds under [Assumption 2](#). This gives rise to the two desired results.

S4.3.1. *Technical preliminaries on uniform quantile processes.* Before tackling each term in (S4.13), we prove a few properties of the rescaled quantile functions $u_n^{(i)}$ which will be used throughout. In [Lemma S1](#), we first prove an approximation of $u_n^{(i)}$ by a certain Gaussian process. We then establish various properties of $u_n^{(i)}$ and its approximation in [Corollary S1](#) and [Lemma S2](#).

LEMMA S1. *For any fixed $i \in V$, define the random function $u_n^{(i)}$ as in (S4.3) and let $0 < \nu < 1/2$. There exist random functions $w_n^{(i)}$ defined on a possibly enriched probability space and universal constants $A, B, C \in (0, \infty)$ such that for any $z > 0$,*

$$\mathbb{P}\left(\sup_{x \in [0, n/k]} |u_n^{(i)}(x) - w_n^{(i)}(x)| > k^{-1}(A \log n + z)\right) \leq B e^{-Cz}.$$

Moreover, the functions $w_n^{(i)}$, along with constants $\widetilde{A}, \widetilde{B}, \widetilde{C}$ possibly depending on ν , can be chosen such that for any $z > 0$,

$$\mathbb{P}\left(\max\left\{\sup_{0 \leq x \leq 1} \frac{|w_n^{(i)}(x) - x|}{x^\nu}, \sup_{1 \leq x \leq n/k} \frac{|w_n^{(i)}(x) - x|}{x^{1-\nu}}\right\} > k^{-1/2}(\widetilde{A} + z)\right) \leq \widetilde{B} e^{-\widetilde{C}z}.$$

Proof. By definition, the quantile function \widehat{F}_i^- appearing in $u_n^{(i)}(x)$ is the right-continuous function

$$\widehat{F}_i^-(x) = U_{ni, \lfloor nx \rfloor},$$

where $U_{ni, j}$ is the j th order statistic from the sample U_{1i}, \dots, U_{ni} . We use the convention $U_{ni, 0} = 0$. Similarly define the left-continuous quantile function

$$\widehat{F}_i^+(x) = U_{ni, \lceil nx \rceil}.$$

Theorem 1 from [Csorgo and Revesz \(1978\)](#) states that for every $z > 0$,

$$\mathbb{P}\left(\sup_{x \in [0, 1]} |(\widehat{F}_i^+(x) - x) - n^{-1/2} B_n(x)| > n^{-1}(A^+ \log n + z)\right) \leq B^+ e^{-C^+ z},$$

for positive constants A^+, B^+, C^+ and a sequence of Brownian bridges B_n . We first establish a similar tail bound for the right-continuous quantile function. Using $\lfloor y \rfloor \geq \lceil y \rceil - 1 = \lceil y - 1 \rceil$, note that

$$\widehat{F}_i^+(x) \geq \widehat{F}_i^-(x) \geq U_{ni, \lceil nx - 1 \rceil} = \widehat{F}_i^+(x - 1/n),$$

so for every $x \in [0, 1]$, using the convention $\widehat{F}_i^+(x) = \widehat{F}_i^+(0)$ if $x < 0$,

$$\begin{aligned} 0 \leq \widehat{F}_i^+(x) - \widehat{F}_i^-(x) &\leq \widehat{F}_i^+(x) - \widehat{F}_i^+(x - 1/n) \\ &\leq 2 \sup_{x \in [0, 1]} |(\widehat{F}_i^+(x) - x) - n^{-1/2} B_n(x)| + \left| \left(x + n^{-1/2} B_n(x)\right) - \left(x - \frac{1}{n} + n^{-1/2} B_n(x - 1/n)\right) \right| \\ &\leq 2 \sup_{x \in [0, 1]} |(\widehat{F}_i^+(x) - x) - n^{-1/2} B_n(x)| + \frac{1}{n} + n^{-1/2} |B_n(x) - B_n(x - 1/n)|. \end{aligned}$$

Thus

$$\sup_{x \in [0, 1]} |(\widehat{F}_i^-(x) - x) - n^{-1/2} B_n(x)| \leq 3 \sup_{x \in [0, 1]} |(\widehat{F}_i^+(x) - x) - n^{-1/2} B_n(x)| + \frac{1}{n} + n^{-1/2} |B_n(x) - B_n(x - 1/n)|.$$

Using the covariance function of the standard Brownian bridge, $n^{-1/2}(B_n(x) - B_n(x - 1/n))$ is normally distributed with mean 0 and variance upper bounded by $4/n^2$. Thus, its absolute value is upper bounded by \sqrt{z}/n with probability greater than $1 - e^{-z/4}$. Therefore,

$$\mathbb{P}\left(\sup_{x \in [0, 1]} |(\widehat{F}_i^-(x) - x) - n^{-1/2} B_n(x)| > n^{-1}(3A^+ \log n + 3z + 1 + \sqrt{z})\right) \leq B^+ e^{-C^+ z} + e^{-z/4}$$

which implies, for the right choice of A, B, C ,

$$(S4.14) \quad \mathbb{P}\left(\sup_{x \in [0, 1]} |(\widehat{F}_i^-(x) - x) - n^{-1/2} B_n(x)| > n^{-1}(A \log n + z)\right) \leq B e^{-Cz}.$$

Now define

$$w_n^{(i)}(x) := x + n^{-1/2} \frac{n}{k} B_n(kx/n).$$

Then

$$u_n^{(i)}(x) - w_n^{(i)}(x) = \frac{n}{k} \widehat{F}_i^-(kx/n) - x - n^{-1/2} \frac{n}{k} B_n(kx/n) = \frac{n}{k} \left(\widehat{F}_i^-(kx/n) - \frac{kx}{n} - n^{-1/2} B_n(kx/n) \right)$$

Thus for $w_n^{(i)}$ defined above

$$\mathbb{P}\left(\sup_{x \in [0, n/k]} |u_n^{(i)}(x) - w_n^{(i)}(x)| > k^{-1}(A \log n + z)\right)$$

$$\begin{aligned}
&= \mathbb{P}\left(\sup_{x \in [0, n/k]} \frac{n}{k} \left| \widehat{F}_i^-(kx/n) - \frac{kx}{n} - n^{-1/2} B_n(kx/n) \right| > k^{-1}(A \log n + z)\right) \\
&= \mathbb{P}\left(\sup_{x \in [0, 1]} \left| \widehat{F}_i^-(x) - x - n^{-1/2} B_n(x) \right| > n^{-1}(A \log n + z)\right) \\
&\leq B e^{-Cz}
\end{aligned}$$

by (S4.14), which proves the first claim.

We now prove the second claim. Let

$$Z_n(x) := n^{-1/2} \frac{n}{k} B_n(kx/n).$$

Observe that

$$\begin{aligned}
\{Z_n(x)\}_{x \in [0, n/k]} &\stackrel{\mathcal{D}}{=} \left\{ n^{-1/2} \frac{n}{k} W_n(kx/n) - n^{-1/2} x W_n(1) \right\}_{x \in [0, n/k]} \\
&\stackrel{\mathcal{D}}{=} \left\{ k^{-1/2} W_n(x) - k^{-1/2} kx/n W_n(n/k) \right\}_{x \in [0, n/k]},
\end{aligned}$$

where W_n are standard Wiener processes on $[0, \infty)$. If the sequences of suprema $\sup_{0 < x \leq 1} k^{1/2} |Z_n(x)| / x^\nu$ and $\sup_{1 \leq x \leq n/k} k^{1/2} |Z_n(x)| / x^{1-\nu}$ are uniformly tight, their distributions have finite medians independent of n . Hence by Proposition A.2.1 of [van der Vaart and Wellner \(1996\)](#), there exist constants $\tilde{A}, \tilde{B}, \tilde{C}$, depending only on those medians, such that

$$\mathbb{P}\left(\max\left\{\sup_{0 < x \leq 1} \frac{k^{1/2} |Z_n(x)|}{x^\nu}, \sup_{1 \leq x \leq \frac{n}{k}} \frac{k^{1/2} |Z_n(x)|}{x^{1-\nu}}\right\} > \tilde{A} + z\right) \leq \tilde{B} e^{-\tilde{C}z^2}.$$

and the result follows.

To establish tightness, note that since $\nu < 1/2$,

$$\sup_{0 < x \leq 1} \frac{k^{1/2} |Z_n(x)|}{x^\nu} \leq \sup_{0 < x \leq 1} \frac{|W_n(x)|}{x^\nu} + \frac{k}{n} |W_n(n/k)| = O_{\mathbb{P}}\left(1 + \sqrt{\frac{k}{n}}\right) = O_{\mathbb{P}}(1)$$

and

$$\sup_{1 \leq x \leq \frac{n}{k}} \frac{k^{1/2} |Z_n(x)|}{x^{1-\nu}} \leq \sup_{1 \leq x < \infty} \frac{|W_n(x)|}{x^{1-\nu}} + \left(\frac{k}{n}\right)^{1-\nu} |W_n(n/k)| = O_{\mathbb{P}}\left(1 + \left(\frac{k}{n}\right)^{1/2-\nu} \sqrt{\log \log \frac{n}{k}}\right) = O_{\mathbb{P}}(1),$$

where we used the law of the iterated logarithm at 0 and at ∞ , respectively, for Wiener processes (see for instance [Durrett, 2010](#), Section 8.11). Note that the probability bounds on the suprema above, and hence the bounds on their medians, are uniform in n but may depend on ν , hence the dependence of the constants $\tilde{A}, \tilde{B}, \tilde{C}$ on this parameter. \square

Let $w_n^{(i)}$ be as in the proof of Lemma S1. For $a \in (0, 1)$ and $\nu_1, \nu_2 \in [0, 1]$, let

$$\tilde{\Delta}_n^{(i)}(a, \nu_1, \nu_2) = \max\left\{\sup_{a \leq x \leq 1} \frac{|w_n^{(i)}(x) - x|}{x^{\nu_1}}, \sup_{1 \leq x \leq n/k} \frac{|w_n^{(i)}(x) - x|}{x^{1-\nu_2}}\right\}$$

and

$$\tilde{\Delta}_n^{(i)}(a, \nu) = \tilde{\Delta}_n^{(i)}(a, \nu, \nu).$$

Similarly, let

$$\widehat{\Delta}_n^{(i)}(a, \nu_1, \nu_2) = \max\left\{\sup_{a \leq x \leq 1} \frac{|u_n^{(i)}(x) - x|}{x^{\nu_1}}, \sup_{1 \leq x \leq n/k} \frac{|u_n^{(i)}(x) - x|}{x^{1-\nu_2}}\right\}$$

and

$$\widehat{\Delta}_n^{(i)}(a, \nu) = \widetilde{\Delta}_n^{(i)}(a, \nu, \nu).$$

It is established in Lemma S1 that there are constants $\widetilde{A}, \widetilde{B}, \widetilde{C}$ only depending on $\nu \in (0, 1/2)$ such that

$$\mathbb{P}\left(\widetilde{\Delta}_n^{(i)}(0, \nu) > k^{-1/2}(\widetilde{A} + z)\right) \leq \widetilde{B}e^{-\widetilde{C}z^2}.$$

Lemma S1 also allows to obtain a certain bound for the terms $\widehat{\Delta}_n^{(i)}$.

COROLLARY S1. *Let $\widehat{\Delta}_n^{(i)}$ be as above. There exist constants $\widehat{A}, \widehat{B}, \widehat{C}$ depending only on $\nu \in (1/2)$ such that for all $z \geq 0$,*

$$\mathbb{P}\left(\widehat{\Delta}_n^{(i)}(0, 0, \nu) > \widehat{A}\left(\frac{1}{\sqrt{k}} + \frac{\log n}{k}\right) + \sqrt{\frac{z}{k}} + \frac{z}{k}\right) \leq \widehat{B}e^{-\widehat{C}z}.$$

PROOF. Write

$$\begin{aligned} \widehat{\Delta}_n^{(i)}(0, 0, \nu) &\leq \widetilde{\Delta}_n^{(i)}(0, 0, \nu) + |\widehat{\Delta}_n^{(i)}(0, 0, \nu) - \widetilde{\Delta}_n^{(i)}(0, 0, \nu)| \\ &\leq \widetilde{\Delta}_n^{(i)}(0, \nu) + \max\left\{\sup_{0 \leq x \leq 1} |u_n^{(i)}(x) - w_n^{(i)}(x)|, \sup_{1 \leq x \leq n/k} \frac{|u_n^{(i)}(x) - w_n^{(i)}(x)|}{x^{1-\nu}}\right\} \\ &\leq \widetilde{\Delta}_n^{(i)}(0, \nu) + \sup_{0 \leq x \leq n/k} |u_n^{(i)}(x) - w_n^{(i)}(x)|, \end{aligned}$$

where the second inequality follows from the fact that for two functions f and g defined on the same domain, $|\sup_x f(x) - \sup_x g(x)| \leq \sup_x |f(x) - g(x)|$.

By Lemma S1, the first term above is larger than $(\widetilde{A} + \sqrt{z})/\sqrt{k}$ with probability at most $\widetilde{B}e^{-\widetilde{C}z}$ and the second one is larger than $(A \log n + z)/k$ with probability at most $B e^{-Cz}$. The result follows by the right choice of $\widehat{A}, \widehat{B}, \widehat{C}$. \square

LEMMA S2. *With $w_n^{(i)}$ as above, there exists a universal positive constant c' such that for all $a \in (0, 1)$,*

$$\mathbb{P}\left(\sup_{a \leq x \leq n/k} \frac{|w_n^{(i)}(x) - x|}{x} > 1/2\right) \leq 6 \exp\left\{-c'k\left(1 \wedge \frac{a}{\log \log(1/a)}\right)\right\}.$$

PROOF. From the proof of Lemma S1, there is a standard Brownian motion W such that $\{w_n^{(i)}(x) - x\}_{x \in [a, n/k]}$ is equal in distribution to the zero-mean Gaussian process

$$\{Z_n(x)\}_{x \in [a, n/k]} := \left\{W(x)/\sqrt{k} - \sqrt{k}x/nW(n/k)\right\}_{x \in [a, n/k]}.$$

Assume first that $a \leq e^{-2}$. We are therefore interested in

$$\begin{aligned} \sup_{x \in [a, n/k]} \frac{|Z_n(x)|}{x} &\leq \frac{1}{\sqrt{k}} \left(\sup_{x \in [a, n/k]} \frac{|W(x)|}{x} + \frac{k}{n} W(n/k) \right) \\ &\leq \frac{1}{\sqrt{k}} \left(\sup_{x \in [a, e^{-2}]} \sqrt{\frac{\log \log(1/x)}{x}} \frac{|W(x)|}{\sqrt{x \log \log(1/x)}} + \sup_{x \in [e^{-2}, n/k]} \frac{|W(x)|}{x} + \frac{k}{n} W(n/k) \right) \\ \text{(S4.15)} \quad &\leq \frac{1}{\sqrt{k}} \left(\sqrt{\frac{\log \log(1/a)}{a}} \sup_{x \in [0, e^{-2}]} \frac{|W(x)|}{\sqrt{x \log \log(1/x)}} + \sup_{x \in [e^{-2}, \infty)} \frac{|W(x)|}{x} + \frac{k}{n} W(n/k) \right). \end{aligned}$$

By the laws of the iterated logarithm at 0 and at infinity, respectively, the above two suprema of Gaussian processes are tight random variables. It follows that they have finite medians and hence, by Proposition A.2.1 of [van der Vaart and](#)

Wellner (1996), that they have sub-Gaussian tails. The same can be said of the uniformly (in n) tight random variable $\frac{k}{n}W(n/k)$. Therefore,

$$\begin{aligned} \mathbb{P}\left(\sup_{x \in [a, n/k]} \frac{|Z_n(x)|}{x} > 1/2\right) &\leq \mathbb{P}\left(\sup_{x \in [0, e^{-2}]} \frac{|W(x)|}{\sqrt{x \log \log(1/x)}} > \frac{\sqrt{ka}}{6\sqrt{\log \log(1/a)}}\right) \\ &\quad + \mathbb{P}\left(\sup_{x \in [e^{-2}, \infty)} \frac{|W(x)|}{x} > \frac{\sqrt{k}}{6}\right) + \mathbb{P}\left(\frac{k}{n}W(n/k) > \frac{\sqrt{k}}{6}\right) \\ &\leq 2 \exp\left\{-c_1 \frac{ka}{\log \log(1/a)}\right\} + 2e^{-c_2 k} + 2e^{-c_3 k}, \end{aligned}$$

for some universal positive constants c_1, c_2, c_3 . The result follows for some c' depending on those three constants only.

If, instead, $a > e^{-2}$, then the sum of the last two terms of (S4.15) is a valid bound in itself. The rest of the proof goes through and we obtain the bound $4e^{-c'k}$. \square

In particular, Lemma S2 lower bounds the probability that for all $x \in [a, n/k]$, $x/2 \leq w_n^{(i)}(x) \leq 2x$, which will be repeatedly used in Section S4.3.4.

The following sections are respectively dedicated to each of the three terms of the decomposition introduced in (S4.11).

S4.3.2. Increments of empirical processes. We first consider the terms $A_{\cdot,1}$. In this section we prove that for any $\nu \in (0, 1/2)$ there exists a constant $C_1 < \infty$ (which can also depend on the constant K from Assumption 1) such that for any $\varepsilon \leq 1$,

$$\begin{aligned} \mathbb{P}\left(\max |A_{\cdot,1}| > C_1(\log(n/k) + \log(1/a))^2 \left\{ \left(\frac{\log(n/k)}{k}\right)^{1/2} \left((k/n)^\xi + \varepsilon\right)^{1/2} \right. \right. \\ \left. \left. + \frac{\log(n/k)}{k} + \frac{\lambda}{\sqrt{k}} \left((k/n)^\xi + \varepsilon\right)^{1/2} + \frac{\lambda^2}{k} \right\}\right) \\ \leq d^3 e^{-\lambda^2} + \mathbb{P}\left(\max_{i \in V} \widehat{\Delta}_n^{(i)}(a, 0, \nu) > \varepsilon\right). \end{aligned}$$

Consider the following decompositions. For all $x, y \in [a, 1]$, the numerator in the integral $A_{ij,1}^{(m),--}$ satisfies

$$\begin{aligned} &|G_{ijm,n}(u_n^{(i)}(x), u_n^{(j)}(y), u_n^{(m)}(1)) - G_{ijm,n}(x, y, 1)| \\ &\leq |G_{ijm,n}(u_n^{(i)}(x), u_n^{(j)}(y), [1 \wedge u_n^{(m)}(1), 1 \vee u_n^{(m)}(1)])| + |G_{ijm,n}(u_n^{(i)}(x), [y \wedge u_n^{(j)}(y), y \vee u_n^{(j)}(y)], 1)| \\ &\quad + |G_{ijm,n}([x \wedge u_n^{(i)}(x), x \vee u_n^{(i)}(x)], y, 1)|. \end{aligned}$$

The numerators in $A_{im,1}^{(m),--}$ and $A_{i,1}^{(m),\ell,-}$ satisfy a similar bound with only the first two terms, up to a logarithmic factor that is everywhere bounded by $\log(1/a)$ in the case of $A_{i,1}^{(m),2,-}$.

For all $x \in [1, n/k]$, $y \in [a, 1]$, the numerator in the integral $A_{ij,1}^{(m),+-}$ satisfies

$$\begin{aligned} &|G_{ijm,n}([u_n^{(i)}(x), \infty), u_n^{(j)}(y), u_n^{(m)}(1)) - G_{ijm,n}([x, \infty), y, 1)| \\ &\leq |G_{ijm,n}([u_n^{(i)}(x), \infty), u_n^{(j)}(y), [1 \wedge u_n^{(m)}(1), 1 \vee u_n^{(m)}(1)])| \\ &\quad + |G_{ijm,n}([u_n^{(i)}(x), \infty), [y \wedge u_n^{(j)}(y), y \vee u_n^{(j)}(y)], 1)| + |G_{ijm,n}([x \wedge u_n^{(i)}(x), x \vee u_n^{(i)}(x)], y, 1)|. \end{aligned}$$

The numerators in $A_{im,1}^{(m),+-}$ and $A_{i,1}^{(m),\ell,+}$ satisfy a similar bound with only the first two terms, up to a logarithmic factor that is everywhere bounded by $\log(n/k)$ in the case of $A_{i,1}^{(m),2,+}$, as well as the numerators in $A_{ij,1}^{(m),-+}$ by symmetry.

For all $x, y \in [1, n/k]$, the numerator in the integral $A_{ij,1}^{(m),++}$ satisfies

$$\begin{aligned} & |G_{ijm,n}([u_n^{(i)}(x), \infty), [u_n^{(j)}(y), \infty), u_n^{(m)}(1)] - G_{ijm,n}([x, \infty), [y, \infty), 1)| \\ & \leq |G_{ijm,n}([u_n^{(i)}(x), \infty), [u_n^{(j)}(y), \infty), [1 \wedge u_n^{(m)}(1), 1 \vee u_n^{(m)}(1)]| \\ & \quad + |G_{ijm,n}([u_n^{(i)}(x), \infty), [y \wedge u_n^{(j)}(y), y \vee u_n^{(j)}(y)], 1)| + |G_{ijm,n}([x \wedge u_n^{(i)}(x), x \vee u_n^{(i)}(x)], [y, \infty), 1)|. \end{aligned}$$

Define, for any $\varepsilon \in (0, 1]$, $\mathcal{F}(\varepsilon) := \cup_{i,j,m} \mathcal{F}_{ijm}(\varepsilon)$ where

$$\mathcal{F}_{ijm}(\varepsilon) := \left\{ \frac{n}{k} \mathbb{1}_{\frac{k}{n} S} : S \in \mathcal{S}_{ijm}^- \cup \mathcal{S}_{ijm}^+ \right\},$$

and where the classes of sets \mathcal{S}_{ijm}^- and \mathcal{S}_{ijm}^+ are defined as

$$\begin{aligned} \mathcal{S}_{ijm}^- & := \{ \{w \in [0, \infty)^d : x - \varepsilon \leq w_i \leq x + \varepsilon, a_j \leq w_j \leq b_j, a_m \leq w_m \leq b_m\} : \\ & \quad a \leq x \leq 1, a_j, b_j, a_m, b_m \in [0, \infty] \}, \end{aligned}$$

and

$$\begin{aligned} \mathcal{S}_{ijm}^+ & := \{ \{w \in [0, \infty)^d : x - x^{1-\nu} \varepsilon \leq w_i \leq x + x^{1-\nu} \varepsilon, a_j \leq w_j \leq b_j, 0 \leq w_m \leq 1\} : \\ & \quad 1 \leq x \leq n/k, a_j, b_j, \in [0, \infty] \}. \end{aligned}$$

Recalling the definition of $\widehat{\Delta}_n^{(i)}(a, 0, \nu)$, it follows from the definition of the class $\mathcal{F}(\varepsilon)$ that whenever

$$\widehat{\Delta}_n^{(i)}(a, 0, \nu) = \max_{i \in V} \max \left\{ \sup_{a \leq x \leq 1} |u_n^{(i)}(x) - x|, \sup_{1 \leq x \leq n/k} \frac{|u_n^{(i)}(x) - x|}{x^{1-\nu}} \right\} \leq \varepsilon,$$

the numerator inside any of the integrals $A_{\cdot,1}$ can be expressed as a sum of at most three terms of the form $(P_n f_1 - P f_1) + (P_n f_2 - P f_2) + (P_n f_3 - P f_3)$, for functions $f_1, f_2, f_3 \in \mathcal{F}(\varepsilon)$. Here, P_n is the empirical distribution of the random vectors U_1, \dots, U_n whereas P is their true distribution. In the case of the terms $A_{i,1}^{(m),2,\pm}$, the sum is multiplied by a logarithmic term. In this case, all the integrals $A_{\cdot,1}$ are upper bounded, in absolute value, by

$$3(\log(n/k) + \log(1/a))^2 \sup_{f \in \mathcal{F}(\varepsilon)} |P_n f - P f|.$$

What we have established so far is that each such term $A_{\cdot,1}$ satisfies, for any $t > 0$,

$$\begin{aligned} \mathbb{P}(|A_{\cdot,1}| \geq t) & \leq \mathbb{P}\left(3(\log(n/k) + \log(1/a))^2 \sup_{f \in \mathcal{F}(\varepsilon)} |P_n f - P f| \geq t\right) \\ & \quad + \mathbb{P}\left(\max_{i \in V} \max \left\{ \sup_{a \leq x \leq 1} |u_n^{(i)}(x) - x|, \sup_{1 \leq x \leq n/k} \frac{|u_n^{(i)}(x) - x|}{x^{1-\nu}} \right\} > \varepsilon\right). \end{aligned}$$

For any triple (i, j, m) , $\mathcal{F}_{ijm}(\varepsilon)$ clearly admits the constant envelope function of the form n/k . Moreover it is a VC-subgraph class that satisfies (S5.17) with universal constants A and V (see for instance [van der Vaart and Wellner \(1996\)](#), Theorem 2.6.7). Moreover, the variance of any single function f in $\mathcal{F}_{ijm}(\varepsilon)$ is bounded by

$$\begin{aligned} P f^2 & \leq \left(\frac{n}{k}\right)^2 \left\{ \sup_{a \leq x \leq 1} \mathbb{P}\left(U_i \in \frac{k}{n}[x - \varepsilon, x + \varepsilon]\right) \vee \sup_{1 \leq x \leq n/k} \mathbb{P}\left(U_i \in \frac{k}{n}[x - x^{1-\nu} \varepsilon, x + x^{1-\nu} \varepsilon], U_m \leq \frac{k}{n}\right) \right\} \\ & \leq \frac{n}{k} \left\{ 2\varepsilon \vee \sup_{1 \leq x \leq n/k} R_{im,n}([x - x^{1-\nu} \varepsilon, x + x^{1-\nu} \varepsilon], 1) \right\} \\ & \leq \frac{n}{k} \left\{ 2\varepsilon + \sup_{1 \leq x \leq n/k} R_{im}([x - x^{1-\nu} \varepsilon, x + x^{1-\nu} \varepsilon], 1) + 2K \left(\frac{k}{n}\right)^\xi \right\} \\ & \lesssim \frac{n}{k} \left\{ \varepsilon + \left(\frac{k}{n}\right)^\xi \right\} \end{aligned}$$

where the last two inequalities follow from (S4.8) and Lemma S9, respectively. By (S5.18) we therefore have

$$\begin{aligned} \mathbb{E} \left[\sup_{f \in \mathcal{F}_{ijm}(\varepsilon)} |P_n f - P f| \right] &\lesssim k^{-1/2} \left((k/n)^\xi + \varepsilon \right)^{1/2} \log \left((n/k)^{1/2} \left((k/n)^\xi + \varepsilon \right)^{-1/2} \right)^{1/2} \\ &\quad + k^{-1} \log \left((n/k)^{1/2} \left((k/n)^\xi + \varepsilon \right)^{-1/2} \right) \\ &\lesssim \left(\frac{\log(n/k)}{k} \right)^{1/2} \left((k/n)^\xi + \varepsilon \right)^{1/2} + \frac{\log(n/k)}{k}. \end{aligned}$$

It follows from (S5.19) that there exists a constant c such that for each triple (i, j, m) and each $\lambda > 0$,

$$\mathbb{P} \left(\sup_{f \in \mathcal{F}_{ijm}(\varepsilon)} |P_n f - P f| \geq c \left\{ \left(\frac{\log(n/k)}{k} \right)^{1/2} \left((k/n)^\xi + \varepsilon \right)^{1/2} + \frac{\log(n/k)}{k} + \frac{\lambda}{\sqrt{k}} \left((k/n)^\xi + \varepsilon \right)^{1/2} + \frac{\lambda^2}{k} \right\} \right) \leq e^{-\lambda^2}.$$

Combined with the union bound, this completes the proof.

S4.3.3. Sums of iid processes. We now deal with the terms $A_{:,2}$ involving integrated empirical processes, such as in (S4.13). In this section, we show that there exists a positive constant c_2 such that for all $\lambda > 0$,

$$\mathbb{P} \left(\max |A_{:,2}| > \left(1 + \left(\frac{k}{n} \right)^\xi (\log(n/k))^2 (\log(n/k) + \log(1/a))^2 \right)^{1/2} \frac{\lambda}{\sqrt{k}} + (\log(n/k) + \log(1/a))^2 \frac{\lambda^2}{k} \right) \leq 16d^3 e^{-c_2 \lambda^2/2}.$$

Starting with $A_{ij,2}^{(m),--}$, we have by definition of $G_{ijm,n}$

$$\begin{aligned} A_{ij,2}^{(m),--} &= \int_a^1 \int_a^1 \frac{G_{ijm,n}(x, y, 1)}{xy} dx dy \\ &= \int_a^1 \int_a^1 \frac{\sum_{t=1}^n \left(\frac{1}{k} \mathbb{1} \{ U_{ti} \leq \frac{k}{n} x, U_{tj} \leq \frac{k}{n} y, U_{tm} \leq \frac{k}{n} \} - \frac{1}{k} \mathbb{P}(U_i \leq \frac{k}{n} x, U_j \leq \frac{k}{n} y, U_m \leq \frac{k}{n}) \right)}{xy} dx dy \\ &= \sum_{t=1}^n (V_{t,ijm}^{(m),--} - \mathbb{E}[V_{t,ijm}^{(m),--}]), \end{aligned}$$

where $V_{t,ijm}^{(m),--}$, $1 \leq t \leq n$, are independent copies of the random variable

$$\begin{aligned} V_{ijm}^{(m),--} &:= \frac{1}{k} \int_a^1 \int_a^1 \frac{\mathbb{1} \{ U_i \leq \frac{k}{n} x, U_j \leq \frac{k}{n} y, U_m \leq \frac{k}{n} \}}{xy} dx dy \\ &= \frac{1}{k} \log \left(\frac{k}{nU_i} \wedge a^{-1} \right) \log \left(\frac{k}{nU_j} \wedge a^{-1} \right) \mathbb{1} \left\{ U_i \leq \frac{k}{n}, U_j \leq \frac{k}{n}, U_m \leq \frac{k}{n} \right\}. \end{aligned}$$

Recall that by assumption $a < 1$. We may then write

$$V_{ijm}^{(m),--} = \frac{1}{k} \log(W_i) \log(W_j) \mathbb{1} \{ W_i, W_j > 1 \},$$

with

$$W_i := \left(\frac{k}{nU_i} \wedge a^{-1} \right) \mathbb{1} \{ U_m \leq \frac{k}{n} \}$$

and W_j defined the same way. We easily notice that $0 \leq V_{ijm}^{(m),--} \leq (\log(1/a))^2/k$. Moreover, an application of Lemma S6 (particularly (S5.8)) gives

$$\mathbb{V}\text{ar}(V_{ijm}^{(m),--}) \leq \mathbb{E}[(V_{ijm}^{(m),--})^2]$$

$$\begin{aligned}
&= \frac{4}{k^2} \int_a^1 \int_a^1 \frac{\frac{k}{n} R_{ijm,n}(x, y, 1) |(\log x)(\log y)|}{xy} dx dy \\
&\leq \frac{4}{kn} \int_0^1 \int_0^1 \frac{|(\log x)(\log y)|}{\sqrt{xy}} dx dy \\
&= \frac{64}{kn},
\end{aligned}$$

where we used once again that $R_{ijm,n}(x, y, 1) \leq x \wedge y \leq \sqrt{xy}$, along with the formula $\int_0^1 \log(x)/\sqrt{x} dx = -4$. We may therefore apply Bernstein's inequality for bounded random variables ([van der Vaart and Wellner, 1996](#), Lemma 2.2.9) with $v = 64/k$, $M = (\log(1/a))^2/k$, which yields

$$\mathbb{P}(|A_{ij,2}^{(m),--}| > \lambda) \leq 2 \exp \left\{ - \frac{k\lambda^2}{2(64 + \lambda(\log(1/a))^2/3)} \right\}.$$

Now considering $A_{ij,2}^{(m),+-}$, we use the same approach and see that

$$A_{ij,2}^{(m),+-} = \sum_{t=1}^n (V_{t,ijm}^{(m),+-} - \mathbb{E}[V_{t,ijm}^{(m),+-}]),$$

where

$$V_{ijm}^{(m),+-} = -\frac{1}{k} \log(W_i) \log(W_j) \mathbb{1}\{W_i < 1, W_j > 1\}$$

and W_i, W_j are as before. This time, $0 \leq V_{ijm}^{(m),+-} \leq (\log(n/k)) \log(1/a)/k$. An application of Lemma [S6](#) (this time, [\(S5.9\)](#)) gives

$$\begin{aligned}
\text{Var}(V_{ijm}^{(m),+-}) &\leq \mathbb{E}[(V_{ijm}^{(m),+-})^2] \\
&= \frac{4}{k^2} \int_a^1 \int_1^{n/k} \frac{\frac{k}{n} R_{ijm,n}([x, \infty), y, 1) |(\log x)(\log y)|}{xy} dx dy \\
&\leq \frac{4}{kn} \int_a^1 \int_1^{n/k} \frac{(R_{ijm}([x, \infty), y, 1) + 3K(k/n)^\xi) |(\log x)(\log y)|}{xy} dx dy,
\end{aligned}$$

by [\(S4.8\)](#) and [\(S4.9\)](#). By [\(S4.10\)](#), $R_{ijm}([x, \infty), y, 1) \leq R_{im}([x, \infty), 1) \wedge R_{jm}(y, 1) \leq Kx^{-\xi} \wedge y \leq Kx^{-\xi/2}y^{1/2}$. The integral above is thus bounded by

$$\begin{aligned}
&K \int_0^1 \int_1^\infty \frac{(\log x)(-\log y)}{x^{1+\xi/2}y^{1/2}} dx dy + 3K \left(\frac{k}{n}\right)^\xi \int_a^1 \int_1^{n/k} \frac{(\log x)(-\log y)}{xy} dx dy \\
&\leq \frac{16K}{\xi^2} + 3K \left(\frac{k}{n}\right)^\xi (\log(n/k))^2 (\log(1/a))^2 \leq C_2 \left(1 + \left(\frac{k}{n}\right)^\xi (\log(n/k))^2 (\log(1/a))^2\right),
\end{aligned}$$

for a suitably chosen constant C_2 depending on K and ξ only. Bernstein's inequality, with

$$v = \frac{4C_2}{k} \left(1 + \left(\frac{k}{n}\right)^\xi (\log(n/k))^2 (\log(1/a))^2\right)$$

and $M = (\log(n/k)) \log(1/a)/k$, therefore implies that for a positive constant c_2 depending on C_2 only,

$$\mathbb{P}(|A_{ij,2}^{(m),+-}| > \lambda) \leq 2 \exp \left\{ - c_2 \frac{k\lambda^2}{1 + (k/n)^\xi (\log(n/k))^2 (\log(1/a))^2 + \lambda(\log(n/k)) \log(1/a)} \right\}.$$

By symmetry, $A_{ij,2}^{(m),-+}$ admits the same bound.

As for $A_{ij,2}^{(m),++}$, we write it as

$$A_{ij,2}^{(m),++} = \sum_{t=1}^n (V_{t,ijm}^{(m),++} - \mathbb{E}[V_{t,ijm}^{(m),++}]),$$

where

$$V_{ijm}^{(m),++} = \frac{1}{k} \log(W_i) \log(W_j) \mathbb{1}\{W_i, W_j < 1\}$$

and W_i, W_j are as before. Again, $0 \leq V_{ijm}^{(m),++} \leq (\log(n/k))^2/k$. An application of Lemma S6 (this time, (S5.10)) gives

$$\begin{aligned} \text{Var}(V_{ijm}^{(m),++}) &\leq \mathbb{E}[(V_{ijm}^{(m),++})^2] \\ &= \frac{4}{k^2} \int_1^{n/k} \int_1^{n/k} \frac{\frac{k}{n} R_{ijm,n}([x, \infty), [y, \infty), 1) (\log x)(\log y)}{xy} dx dy \\ &\leq \frac{4}{kn} \int_1^{n/k} \int_1^{n/k} \frac{(R_{ijm}([x, \infty), [y, \infty), 1) + 5K(k/n)^\xi) (\log x)(\log y)}{xy} dx dy, \end{aligned}$$

by (S4.8) and (S4.9). By (S4.10), $R_{ijm}([x, \infty), [y, \infty), 1) \leq R_{im}([x, \infty), 1) \wedge R_{jm}([y, \infty), 1) \leq Kx^{-\xi} \wedge Ky^{-\xi} \leq Kx^{-\xi/2}y^{-\xi/2}$. The integral above is thus bounded by

$$\begin{aligned} &K \int_1^\infty \int_1^\infty \frac{(\log x)(\log y)}{(xy)^{1+\xi/2}} dx dy + 5K \left(\frac{k}{n}\right)^\xi \int_1^{n/k} \int_1^{n/k} \frac{(\log x)(\log y)}{xy} dx dy \\ &\leq \frac{16K}{\xi^4} + 5K \left(\frac{k}{n}\right)^\xi (\log(n/k))^4 \leq C_2 \left(1 + \left(\frac{k}{n}\right)^\xi (\log(n/k))^4\right), \end{aligned}$$

after possibly enlarging the constant C_2 . Hence by a similar application of Bernstein's inequality for bounded random variables as before,

$$\mathbb{P}(|A_{ij,2}^{(m),++}| > \lambda) \leq 2 \exp \left\{ -c_2 \frac{k\lambda^2}{1 + (k/n)^\xi (\log(n/k))^4 + \lambda(\log(n/k))^2} \right\},$$

after possibly decreasing the (still positive) constant c_2 .

Finally, the terms $A_{i,2}^{(m),\ell,-}$, $A_{i,2}^{(m),\ell,+}$, $A_{im,2}^{(m),--}$ and $A_{im,2}^{(m),+-}$ can be shown to satisfy similar tail bounds by the same strategy, using (S5.6) and (S5.7) instead of (S5.8) to (S5.10) for $A_{i,2}^{(m),\ell,-}$ and $A_{i,2}^{(m),\ell,+}$.

The conclusion of this section is that the positive constant c_2 can be chosen sufficiently small (only depending on K and ξ) such that all the terms $A_{\cdot,2}$ satisfy

$$\mathbb{P}(|A_{\cdot,2}| > \lambda) \leq 2 \exp \left\{ -c_2 \frac{k\lambda^2}{1 + (k/n)^\xi (\log(n/k))^2 (\log(n/k) + \log(1/a))^2 + \lambda(\log(n/k) + \log(1/a))^2} \right\},$$

for all $\lambda > 0$. The denominator in the exponential above is clearly upper bounded by

$$2 \max \left\{ 1 + (k/n)^\xi (\log(n/k))^2 (\log(n/k) + \log(1/a))^2, \lambda(\log(n/k) + \log(1/a))^2 \right\},$$

so the whole exponential is upper bounded by

$$\max \left\{ 2 \exp \left\{ -c_2 \frac{k\lambda^2}{2(1 + (k/n)^\xi (\log(n/k))^2 (\log(n/k) + \log(1/a))^2)} \right\}, 2 \exp \left\{ -c_2 \frac{k\lambda}{2(\log(n/k) + \log(1/a))^2} \right\} \right\}.$$

Deduce that at least one of

$$\mathbb{P} \left(|A_{\cdot,2}| > \left(1 + \left(\frac{k}{n}\right)^\xi (\log(n/k))^2 (\log(n/k) + \log(1/a))^2 \right)^{1/2} \frac{\lambda}{\sqrt{k}} \right) \leq 2e^{-c_2\lambda^2/2}$$

or

$$\mathbb{P}\left(|A_{\cdot,2}| > (\log(n/k) + \log(1/a))^2 \frac{\lambda^2}{k}\right) \leq 2e^{-c_2\lambda^2/2}$$

holds. Therefore

$$\mathbb{P}\left(|A_{\cdot,2}| > \left(1 + \left(\frac{k}{n}\right)^\xi (\log(n/k))^2 (\log(n/k) + \log(1/a))^2\right)^{1/2} \frac{\lambda}{\sqrt{k}} + (\log(n/k) + \log(1/a))^2 \frac{\lambda^2}{k}\right) \leq 2e^{-c_2\lambda^2/2},$$

and a union bound allows to conclude.

S4.3.4. Increments of rescaled copulae. It remains to bound the terms $A_{\cdot,3}$, corresponding to increments of the measures $R_{J,n}$ when the rescaled quantile functions $u_n^{(i)}$ are applied to their arguments. In this section, we prove that under Assumption 1, there exists a constant C_3 such that for any $\lambda, \tau > 0$,

$$\begin{aligned} & \mathbb{P}\left(\max |A_{\cdot,3}| > 3\tau(\log(n/k) + \log(1/a))^2 + C_3(\log(n/k) + \log(1/a))^2 \left(\frac{\tilde{A} + \lambda}{\sqrt{k}} + \left(\frac{k}{n}\right)^\xi\right)\right) \\ & \leq \mathbb{P}\left(\max_i \tilde{\Delta}_n^{(i)}(a, \nu) > \frac{\tilde{A} + \lambda}{\sqrt{k}}\right) + \mathbb{P}\left(\max_i \sup_{x \in [0, n/k]} |u_n^{(i)}(x) - w_n^{(i)}(x)| > \tau\right) \\ & \quad + \mathbb{P}\left(\max_i \sup_{a \leq x \leq n/k} \frac{|w_n^{(i)}(x) - x|}{x} > 1/2\right), \end{aligned}$$

where the constant \tilde{A} is as in Lemma S1. Moreover, if Assumption 2 is also satisfied, C_3 can be modified in a way that only depends on ε and $K(\beta)$ and such that the slightly larger probability

$$\mathbb{P}\left(\max |A_{\cdot,3}| > 3\tau(\log(n/k) + \log(1/a))^2 + C_3\left(\frac{\tilde{A} + \lambda}{\sqrt{k}} + \left(\frac{k}{n}\right)^\xi (\log(n/k) + \log(1/a))^2\right)\right)$$

admits the same upper bound.

By Assumption 1, the measure $R_{J,n}$ in any integrand can be replaced by R_J at the cost of adding a deterministic error of the order of $(k/n)^\xi$. After being integrated, such an error is of order at most $(k/n)^\xi (\log(n/k) + \log(1/a))^2$. We will use this fact on multiple occasions by bounding the increments of R_J instead of $R_{J,n}$.

Next we observe that by Lipschitz continuity of $R_{J,n}$ the quantities $u_n^{(i)}(x), u_n^{(j)}(y), u_n^{(m)}(1)$ appearing in the arguments of R_J inside $A_{\cdot,3}$ can be replaced by $w_n^{(i)}(x), w_n^{(j)}(y), w_n^{(m)}(1)$ with an error that is controlled by Lemma S1, uniformly over x, y, i, j, m . For example

$$\begin{aligned} & \max_{i,j,m} \sup_{x,y \in [0, n/k]} \left| R_{ijm,n}(u_n^{(i)}(x), u_n^{(j)}(y), u_n^{(m)}(1)) - R_{ijm,n}(w_n^{(i)}(x), w_n^{(j)}(y), w_n^{(m)}(1)) \right| \\ & \leq 3 \max_i \sup_{x \in [0, n/k]} |u_n^{(i)}(x) - w_n^{(i)}(x)|. \end{aligned}$$

Define

$$\tilde{A}_{ij,3}^{(m),--} := \int_a^1 \int_a^1 \frac{|R_{ijm,n}(w_n^{(i)}(x), w_n^{(j)}(y), w_n^{(m)}(1)) - R_{ijm,n}(x, y, 1)|}{xy} dx dy,$$

and similarly define other terms $\tilde{A}_{\cdot,3}$ replacing the different $A_{\cdot,3}$. The difference between those quantities and the original $A_{\cdot,3}$ terms that they replace can be uniformly controlled as

$$\max |A_{\cdot,3} - \tilde{A}_{\cdot,3}| \leq 3(\log(n/k) + \log(1/a))^2 \max_i \sup_{x \in [0, n/k]} |u_n^{(i)}(x) - w_n^{(i)}(x)|,$$

some of those bounds using the fact that

$$(S4.16) \quad \int \frac{(\log x)^{\ell-1}}{x} dx = \frac{(\log x)^\ell}{\ell} + \text{constant}.$$

We then obtain that for all $\tau > 0$,

$$\mathbb{P}\left(\max |A_{\cdot,3} - \tilde{A}_{\cdot,3}| > 3\tau(\log(n/k) + \log(1/a))^2\right) \leq \mathbb{P}\left(\max_i \sup_{x \in [0, n/k]} |u_n^{(i)}(x) - w_n^{(i)}(x)| > \tau\right).$$

Hence it remains to bound the terms $\tilde{A}_{\cdot,3}$ which are defined in the same way as $A_{\cdot,3}$ but with $w_n^{(i)}(x), w_n^{(j)}(y), w_n^{(m)}(1)$ replacing $u_n^{(i)}(x), u_n^{(j)}(y), u_n^{(m)}(1)$.

Note that whenever

$$\max_i \sup_{a \leq x \leq n/k} \frac{|w_n^{(i)}(x) - x|}{x} \leq 1/2,$$

we have for all i and $x \in [a, n/k]$ that $x/2 \leq u_n^{(i)}(x) \leq 2x$. We will assume, for the remainder of the section, that this is realized. Lemma S2 allows to lower bound the probability of that event.

Finally, recall the quantities

$$\tilde{\Delta}_n^{(i)}(a, \nu) = \max \left\{ \sup_{x \in [a, 1]} \frac{|w_n^{(i)}(x) - x|}{x^\nu}, \sup_{x \in [1, n/k]} \frac{|w_n^{(i)}(x) - x|}{x^{1-\nu}} \right\}$$

from the discussion after Lemma S1.

S4.3.4.1. The general case. We first prove the weaker bound that does not rely on Assumption 2.

Firstly, for $x, y \in [a, 1]$ and every triple (i, j, m) ,

$$(S4.17) \quad \begin{aligned} R_{ijm,n}(w_n^{(i)}(x), w_n^{(j)}(y), w_n^{(m)}(1)) - R_{ijm,n}(x, y, 1) &= R_{ijm,n}(w_n^{(i)}(x), w_n^{(j)}(y), w_n^{(m)}(1)) - R_{ijm,n}(w_n^{(i)}(x), w_n^{(j)}(y), 1) \\ &\quad + R_{ijm,n}(w_n^{(i)}(x), w_n^{(j)}(y), 1) - R_{ijm,n}(w_n^{(i)}(x), y, 1) \\ &\quad + R_{ijm,n}(w_n^{(i)}(x), y, 1) - R_{ijm,n}(x, y, 1). \end{aligned}$$

Each of the three differences above, by Lipschitz continuity of $R_{ij,m}$, is of course bounded by $\max_i \tilde{\Delta}_n^{(i)}(a, 0) \leq \max_i \tilde{\Delta}_n^{(i)}(a, \nu)$, for arbitrary $1/2 > \nu > 0$. Deduce that

$$|\tilde{A}_{ij,3}^{(m),--}| \leq \int_a^1 \int_a^1 \frac{|R_{ijm,n}(w_n^{(i)}(x), w_n^{(j)}(y), w_n^{(m)}(1)) - R_{ijm,n}(x, y, 1)|}{xy} dx dy \leq (\log(1/a))^2 \max_i \tilde{\Delta}_n^{(i)}(0, \nu).$$

The term $\tilde{A}_{im,3}^{(m),--}$ is bounded using the same strategy, following an expansion similar to (S4.17) but without the first term. As for the term $\tilde{A}_{i,3}^{(m),\ell,-}$, it is also bounded after an expansion similar to the third term in (S4.17), using the indefinite integral (S4.16).

Secondly, for all $x \in [1, n/k], y \in [a, 1]$ and every triple (i, j, m) ,

$$(S4.18) \quad \begin{aligned} R_{ijm,n}([w_n^{(i)}(x), \infty), w_n^{(j)}(y), w_n^{(m)}(1)) - R_{ijm,n}([x, \infty), y, 1) \\ = R_{ijm,n}([w_n^{(i)}(x), \infty), w_n^{(j)}(y), w_n^{(m)}(1)) - R_{ijm,n}([w_n^{(i)}(x), \infty), w_n^{(j)}(y), 1) \\ + R_{ijm,n}([w_n^{(i)}(x), \infty), w_n^{(j)}(y), 1) - R_{ijm,n}([w_n^{(i)}(x), \infty), y, 1) \\ + R_{ijm,n}([w_n^{(i)}(x), \infty), y, 1) - R_{ijm,n}([x, \infty), y, 1). \end{aligned}$$

The first two differences are again uniformly bounded by $\max_i \tilde{\Delta}_n^{(i)}(a, \nu)$ by Lipschitz continuity. As for the third difference in (S4.18), let us replace $R_{ijm,n}$ by R_{ijm} as described at the beginning of this section. We are then left with

$$(S4.19) \quad R_{ijm}([x \wedge w_n^{(i)}(x), x \vee w_n^{(i)}(x)], y, 1) \leq y \frac{|w_n^{(i)}(x) - x|}{x \wedge w_n^{(i)}(x)} \leq 2x^{-\nu} y \max_i \tilde{\Delta}_n^{(i)}(a, \nu),$$

by Lemma S9 and the fact that we are on the event $w_n^{(i)}(x) \geq x/2$. Deduce that

$$\begin{aligned} |\tilde{A}_{ij,3}^{(m),+-}| &\leq \int_1^{n/k} \int_a^1 \frac{|R_{ijm,n}([w_n^{(i)}(x), \infty), w_n^{(j)}(y), w_n^{(m)}(1)] - R_{ijm,n}([x, \infty), y, 1]|}{xy} dx dy \\ &\lesssim (\log(n/k))(\log(1/a)) \max_i \tilde{\Delta}_n^{(i)}(a, \nu) + \left(\frac{k}{n}\right)^\xi (\log(n/k))(\log(1/a)), \end{aligned}$$

where the last term comes from the approximation of $R_{ijm,n}$ by R_{ijm} . By symmetry, $A_{ij,3}^{(m),+-}$ enjoys the same bound. Moreover, $A_{im,3}^{(m),+-}$ is bounded using the same strategy, following an expansion similar to (S4.18) but without the first term. As for the term $A_{i,3}^{(m),\ell,+}$, it is also bounded after an expansion similar to the third term in (S4.18), using (S4.16).

Thirdly, for all $x, y \in [1, n/k]$ and every triple (i, j, m) ,

$$(S4.20) \quad \begin{aligned} &R_{ijm,n}([w_n^{(i)}(x), \infty), [w_n^{(j)}(y), \infty), w_n^{(m)}(1)] - R_{ijm,n}([x, \infty), [y, \infty), 1) \\ &= R_{ijm,n}([w_n^{(i)}(x), \infty), [w_n^{(j)}(y), \infty), w_n^{(m)}(1)] - R_{ijm,n}([w_n^{(i)}(x), \infty), [w_n^{(j)}(y), \infty), 1) \\ &\quad + R_{ijm,n}([w_n^{(i)}(x), \infty), [w_n^{(j)}(y), \infty), 1) - R_{ijm,n}([w_n^{(i)}(x), \infty), [y, \infty), 1) \\ &\quad + R_{ijm,n}([w_n^{(i)}(x), \infty), [y, \infty), 1) - R_{ijm,n}([x, \infty), [y, \infty), 1). \end{aligned}$$

The first difference is upper bounded similarly to before by using the Lipschitz continuity of $R_{ijm,n}$. As for the second term, we once again replace $R_{ijm,n}$ by its limit R_{ijm} and obtain

$$(S4.21) \quad \begin{aligned} &R_{ijm}([w_n^{(i)}(x), \infty), [y \wedge w_n^{(j)}(y), y \vee w_n^{(j)}(y)], 1) \leq R_{ijm}([y \wedge w_n^{(j)}(y), y \vee w_n^{(j)}(y)], 1) \\ &\leq \frac{|w_n^{(j)}(y) - y|}{y \wedge w_n^{(j)}(y)} \leq 2y^{-\nu} \max_i \tilde{\Delta}_n^{(i)}(a, \nu). \end{aligned}$$

The third term of (S4.20) admits the same bound with x replacing y . Deduce that

$$\begin{aligned} |\tilde{A}_{ij,3}^{(m),++}| &\leq \int_1^{n/k} \int_1^{n/k} \frac{|R_{ijm,n}([w_n^{(i)}(x), \infty), [w_n^{(j)}(y), \infty), w_n^{(m)}(1)] - R_{ijm,n}([x, \infty), [y, \infty), 1]|}{xy} dx dy \\ &\lesssim (\log(n/k))^2 \max_i \tilde{\Delta}_n^{(i)}(a, \nu) + \left(\frac{k}{n}\right)^\xi (\log(n/k))^2, \end{aligned}$$

the last term again from replacing $R_{ijm,n}$ by R_{ijm} .

We have therefore proved that, for any $1/2 > \nu > 0$, each term $A_{i,3}$ is upper bounded by a constant multiple of

$$(\log(n/k) + \log(1/a))^2 \max_i \tilde{\Delta}_n^{(i)}(a, \nu) + \left(\frac{k}{n}\right)^\xi (\log(n/k) + \log(1/a))^2.$$

S4.3.4.2. Assuming bounded densities. Let us now suppose that Assumption 2 is satisfied with a certain $\varepsilon \in (0, 4)$. While in the general case above $\nu \in (0, 1/2)$ was arbitrary, let now $\nu = 1/2 - \varepsilon/8$.

The various bounds above on the numerators in the integrals $\tilde{A}_{i,3}$ were for the most part uniform in the integrands x and y . By integrating them over a growing domain, a polylogarithmic factor was paid. We shall now derive more subtle bounds that are proportional to functions $f(x, y)$ such that $f(x, y)/xy$ is integrable over the infinite domain, thus allowing us to remove the extra polylogarithmic factors.

Firstly, for $x, y \in [a, 1]$, consider the three terms in (S4.17) and in each one, replace $R_{ijm,n}$ by R_{ijm} . By Lemma S10 with $\beta = \nu/2$, the third term is then bounded by

$$R_{ij}([x \wedge w_n^{(i)}(x), x \vee w_n^{(i)}(x)], y) \lesssim y^{\nu/2} \frac{|w_n^{(i)}(x) - x|}{x^{\nu/2}} \leq (xy)^{\nu/2} \max_i \tilde{\Delta}_n^{(i)}(a, \nu).$$

The second term admits the same bound up to a factor of $2^{\nu/2}$, since by assumption $w_n^{(i)}(x) \leq 2x$. As for the first term, now using Lemma S10 with $\beta = \nu$, it is upper bounded by both

$$R_{im}(2x, [1 \wedge w_n^{(m)}(1), 1 \vee w_n^{(m)}(1)]) \lesssim x^\nu \max_i \tilde{\Delta}_n^{(i)}(a, \nu)$$

and

$$R_{jm}(2y, [1 \wedge w_n^{(m)}(1), 1 \vee w_n^{(m)}(1)]) \lesssim y^\nu \max_i \tilde{\Delta}_n^{(i)}(a, \nu),$$

hence by

$$(xy)^{\nu/2} \max_i \tilde{\Delta}_n^{(i)}(a, \nu)$$

up to a constant. It then follows that

$$\begin{aligned} |\tilde{A}_{ij,3}^{(m),--}| &\lesssim \max_i \tilde{\Delta}_n^{(i)}(a, \nu) \int_0^1 \int_0^1 (xy)^{\nu/2-1} dx dy + \left(\frac{k}{n}\right)^\xi (\log(1/a))^2 \\ &\lesssim \max_i \tilde{\Delta}_n^{(i)}(a, \nu) + \left(\frac{k}{n}\right)^\xi (\log(1/a))^2. \end{aligned}$$

The bounds on $A_{im,3}^{(m),--}$ and $A_{i,3}^{(m),\ell,-}$ follow from the same argument, noting for the latter that

$$\int_0^1 \frac{(\log x)^{\ell-1}}{x^{1-\nu/2}} dx < \infty.$$

Secondly, for $x \in [1, n/k]$, $y \in [a, 1]$ and every triple (i, j, m) , consider the three terms in (S4.18) and in each one, replace $R_{ijm,n}$ by R_{ijm} . It was already proved in the general case that by Lemma S9, the third term satisfies (see (S4.19))

$$R_{ijm}([x \wedge w_n^{(i)}(x), x \vee w_n^{(i)}(x)], y, 1) \leq R_{ij}([x \wedge w_n^{(i)}(x), x \vee w_n^{(i)}(x)], y) \leq 2x^{-\nu} y \max_i \tilde{\Delta}_n^{(i)}(a, \nu).$$

The second term, by an application of Lemma S11 with $\beta = -\varepsilon$, is upper bounded by

$$R_{ij}([w_n^{(i)}(x), \infty), [y \wedge w_n^{(j)}(y), y \vee w_n^{(j)}(y)]) \lesssim w_n^{(i)}(x)^{-\varepsilon} (y \vee w_n^{(j)}(y))^\varepsilon |w_n^{(j)}(y) - y| \lesssim x^{-\varepsilon} y^{\varepsilon+\nu} \max_i \tilde{\Delta}_n^{(i)}(a, \nu).$$

The first term of (S4.18) is upper bounded by both

$$R_{jm}(w_n^{(j)}(y), [1 \wedge w_n^{(m)}(1), 1 \vee w_n^{(m)}(1)]) \leq w_n^{(j)}(y) |w_n^{(m)}(1) - 1| \lesssim y \max_i \tilde{\Delta}_n^{(i)}(a, \nu),$$

by Lemma S10, and

$$R_{im}([w_n^{(i)}(x), \infty), [1 \wedge w_n^{(m)}(1), 1 \vee w_n^{(m)}(1)]) \lesssim w_n^{(i)}(x)^{-\varepsilon} |w_n^{(m)}(1) - 1| \lesssim x^{-\varepsilon} \max_i \tilde{\Delta}_n^{(i)}(a, \nu),$$

again by Lemma S11 with $\beta = -\varepsilon$. Hence the first term is in fact bounded by

$$x^{-\varepsilon/2} y^{1/2} \max_i \tilde{\Delta}_n^{(i)}(a, \nu)$$

up to a constant. It then follows that

$$\begin{aligned} |\tilde{A}_{ij,3}^{(m),+-}| &\lesssim \max_i \tilde{\Delta}_n^{(i)}(a, \nu) \int_0^1 \int_1^\infty (x^{-1-\nu} + x^{-1-\varepsilon} y^{\varepsilon+\nu-1} + x^{-1-\varepsilon/2} y^{-1/2}) dx dy \\ &\quad + \left(\frac{k}{n}\right)^\xi (\log(n/k)) (\log(1/a)) \\ &\lesssim \max_i \tilde{\Delta}_n^{(i)}(a, \nu) + \left(\frac{k}{n}\right)^\xi (\log(n/k)) (\log(1/a)). \end{aligned}$$

The same holds for $A_{ij,3}^{(m),-+}$ by symmetry. The bounds on $A_{im,3}^{(m),+-}$ and $A_{i,3}^{(m),\ell,+}$ follow from the same argument, noting for the latter that

$$\int_1^\infty \frac{(\log x)^{\ell-1}}{x^{1+\zeta}} dx < \infty$$

for any positive ζ .

Finally, for $x, y \in [1, n/k]$ and every triple (i, j, m) , consider the three terms in (S4.20) and in each one, replace $R_{ijm,n}$ by R_{ijm} . By Lemma S10 with $\beta = 1 + \varepsilon$, the third term of (S4.20) satisfies

$$R_{ijm}([x \wedge w_n^{(i)}(x), x \vee w_n^{(i)}(x)], [y, \infty), 1) \leq R_{im}([x \wedge w_n^{(i)}(x), x \vee w_n^{(i)}(x)], 1) \lesssim \frac{|w_n^{(i)}(x) - x|}{x^{1+\varepsilon}} \lesssim x^{-\nu-\varepsilon} \max_i \tilde{\Delta}_n^{(i)}(a, \nu)$$

but at the same time, Lemma S11 with $\beta = -\varepsilon/2$ yields

$$\begin{aligned} R_{ijm}([x \wedge w_n^{(i)}(x), x \vee w_n^{(i)}(x)], [y, \infty), 1) &\leq R_{ij}([x \wedge w_n^{(i)}(x), x \vee w_n^{(i)}(x)], [y, \infty)) \\ &\lesssim y^{-\varepsilon/2} x^{\varepsilon/2} |w_n^{(i)}(x) - x| \\ &\lesssim x^{1-\nu+\varepsilon/2} y^{-\varepsilon/2} \max_i \tilde{\Delta}_n^{(i)}(a, \nu). \end{aligned}$$

The minimum between the bounds above being smaller than their geometric mean, we then have

$$R_{ijm}([x \wedge w_n^{(i)}(x), x \vee w_n^{(i)}(x)], [y, \infty), 1) \lesssim x^{-\varepsilon/8} y^{-\varepsilon/4} \max_i \tilde{\Delta}_n^{(i)}(a, \nu),$$

recalling that $\nu = 1/2 - \varepsilon/8$, so that $(-\nu - \varepsilon) + (1 - \nu + \varepsilon/2) = 1 - 2\nu - \varepsilon/2 = -\varepsilon/4$. The second term of (S4.20) admits a similar bound since by assumption $w_n^{(i)}(x) \geq x/2$. As for the first term, by Lemma S11 with $\beta = -\varepsilon$ it is bounded by

$$R_{im}([x/2, \infty), [1 \wedge w_n^{(m)}(1), 1 \vee w_n^{(m)}(1)]) \leq x^{-\varepsilon} |w_n^{(m)}(1) - 1| \lesssim x^{-\varepsilon} \max_i \tilde{\Delta}_n^{(i)}(a, \nu),$$

but also by

$$R_{jm}([y/2, \infty), [1 \wedge w_n^{(m)}(1), 1 \vee w_n^{(m)}(1)]) \leq y^{-\varepsilon} |w_n^{(m)}(1) - 1| \lesssim y^{-\varepsilon} \max_i \tilde{\Delta}_n^{(i)}(a, \nu),$$

hence by

$$(xy)^{-\varepsilon/2} \max_i \tilde{\Delta}_n^{(i)}(a, \nu)$$

up to a constant. It then follows that

$$\begin{aligned} |\tilde{A}_{ij,3}^{(m),++}| &\lesssim \max_i \tilde{\Delta}_n^{(i)}(a, \nu) \int_1^\infty \int_1^\infty (x^{-1-\varepsilon/8} y^{-1-\varepsilon/4} + (xy)^{-1-\varepsilon/2}) dx dy + \left(\frac{k}{n}\right)^\xi (\log(n/k))^2 \\ &\lesssim \max_i \tilde{\Delta}_n^{(i)}(a, \nu) + \left(\frac{k}{n}\right)^\xi (\log(n/k))^2. \end{aligned}$$

We have therefore proved that each term $A_{i,3}$ is upper bounded, up to a constant, by

$$\max_i \tilde{\Delta}_n^{(i)}(a, \nu) + \left(\frac{k}{n}\right)^\xi (\log(n/k) + \log(1/a))^2.$$

□

S4.4. *Proof of Theorem 3.* As per the statement of the theorem, pick an arbitrary $\zeta \in (0, 1)$ and assume that $k \geq n^\zeta$. Since the statement is trivial for $\lambda < 1$ (with the right choice of constants), suppose that $1 \leq \lambda \leq \sqrt{k}/(\log n)^4$. Moreover let a satisfy

$$(S4.22) \quad \max \left\{ \frac{\lambda^2 \log n}{k}, \left(\frac{k}{n} \right)^\xi \right\} \leq a \leq \max \left\{ \frac{\lambda}{\sqrt{k} \log n}, \left(\frac{k}{n} \right)^\xi \right\}.$$

Note that by our choice of λ , the interval above is always non-empty. Introduce the notation $l_{n,a} := \log(n/k) + \log(1/a)$ and note that by (S4.22), $l_{n,a} \lesssim \log(n/k)$. Consider the results of Sections S4.3.2 to S4.3.4 with

$$\varepsilon := \widehat{A} \left(\frac{1}{\sqrt{k}} + \frac{\log n}{k} \right) + \frac{\lambda}{\sqrt{k}} + \frac{\lambda^2}{k} \lesssim \frac{\lambda}{\sqrt{k}} \leq \frac{1}{(\log n)^4}$$

and

$$\tau := \frac{A \log n + \lambda^2}{k},$$

for \widehat{A} and A as in Corollary S1 and Lemma S1, respectively. Combining these results with those of Section S4.2, we obtain the following simultaneous upper bound on each integral \mathcal{I} in (S4.5) to (S4.7):

$$(S4.23) \quad \begin{aligned} & C_1 l_{n,a}^2 \left\{ \left(\frac{\log(n/k)}{k} \right)^{1/2} \left(\left(\frac{k}{n} \right)^\xi + \varepsilon \right)^{1/2} + \frac{\log(n/k)}{k} + \frac{\lambda}{\sqrt{k}} \left(\left(\frac{k}{n} \right)^\xi + \varepsilon \right)^{1/2} + \frac{\lambda^2}{k} \right\} \\ & + \left(1 + \left(\frac{k}{n} \right)^\xi (\log(n/k))^2 l_{n,a}^2 \right)^{1/2} \frac{\lambda}{\sqrt{k}} + l_{n,a}^2 \frac{\lambda^2}{k} \\ & + 3\tau l_{n,a}^2 + C_3 l_{n,a}^2 \left(\frac{\widehat{A} + \lambda}{\sqrt{k}} + \left(\frac{k}{n} \right)^\xi \right) \\ & + O \left(\left(\frac{k}{n} \right)^\xi l_{n,a}^2 \right). \end{aligned}$$

Note that $(k/n)^\xi (\log(n/k))^2 l_{n,a}^2 \lesssim (k/n)^\xi (\log(n/k))^4$ can be upper bounded by a constant only depending on ξ . Using this and the fact that $(x+y)^{1/2} \leq x^{1/2} + y^{1/2}$ for $x, y \geq 0$, we find

$$\begin{aligned} & l_{n,a}^2 \left(\frac{\log(n/k)}{k} \right)^{1/2} \left(\left(\frac{k}{n} \right)^\xi + \varepsilon \right)^{1/2} \lesssim l_{n,a}^2 \left(\frac{k}{n} \right)^{\xi/2} \left(\frac{\log(n/k)}{k} \right)^{1/2} + l_{n,a}^2 \left(\frac{\log(n/k)}{k} \right)^{1/2} \varepsilon^{1/2} \\ & \lesssim \frac{1}{\sqrt{k}} + l_{n,a}^2 \left(\frac{\log(n/k)}{k} \right)^{1/2} \lambda^{1/2} k^{-1/4} \lesssim \frac{\lambda}{\sqrt{k}} \end{aligned}$$

since $(\log n)^{5/2} \lesssim k^{1/4}$. By similar arguments using that $\varepsilon \lesssim 1/(\log n)^4$

$$l_{n,a}^2 \left(\left(\frac{k}{n} \right)^\xi + \varepsilon \right)^{1/2} \lesssim 1.$$

Moreover,

$$\tau l_{n,a}^2 \lesssim \frac{(\log n)^3}{k} + l_{n,a}^2 \frac{\lambda^2}{k}.$$

In addition, notice that by our choice of λ ,

$$\frac{\lambda^2}{k} \leq l_{n,a}^2 \frac{\lambda^2}{k} \lesssim \frac{\lambda (\log n)^{-2} \sqrt{k}}{k} \leq \frac{\lambda}{\sqrt{k}}$$

and that since $k \geq n^\zeta$,

$$\frac{(\log n)^3}{k} \lesssim \frac{1}{\sqrt{k}}.$$

Piecing those results together, (S4.23) can be bounded by

$$(S4.24) \quad C' \left\{ \left(\frac{k}{n} \right)^\xi (\log(n/k))^2 + \frac{(\log(n/k))^2(1+\lambda)}{\sqrt{k}} \right\},$$

for the right constant C' . If Assumption 2 is made, the same strategy yields the sharper bound

$$(S4.25) \quad \begin{aligned} & C_1 l_{n,a}^2 \left\{ \left(\frac{\log(n/k)}{k} \right)^{1/2} \left(\left(\frac{k}{n} \right)^\xi + \varepsilon \right)^{1/2} + \frac{\log(n/k)}{k} + \frac{\lambda}{\sqrt{k}} \left(\left(\frac{k}{n} \right)^\xi + \varepsilon \right)^{1/2} + \frac{\lambda^2}{k} \right\} \\ & + \left(1 + \left(\frac{k}{n} \right)^\xi (\log(n/k))^2 l_{n,a}^2 \right)^{1/2} \frac{\lambda}{\sqrt{k}} + l_{n,a}^2 \frac{\lambda^2}{k} \\ & + 3\tau l_{n,a}^2 + C_3 \left(\frac{\tilde{A} + \lambda}{\sqrt{k}} + \left(\frac{k}{n} \right)^\xi l_{n,a}^2 \right) \\ & + O \left(\left(\frac{k}{n} \right)^\xi l_{n,a}^2 \right) \\ & \leq \bar{C}' \left\{ \left(\frac{k}{n} \right)^\xi (\log(n/k))^2 + \frac{1+\lambda}{\sqrt{k}} \right\}, \end{aligned}$$

for the right constant \bar{C}' . It is left to control the deterministic error terms in (S4.5) to (S4.7) arising from the truncation of the integrals. Those terms are upper bounded by a constant multiple of

$$\begin{aligned} \left(\frac{k}{n} \right)^\xi (\log(n/k)) + l_{n,a}^2 k^{-1} + a l_{n,a} & \lesssim \left(\frac{k}{n} \right)^\xi (\log(n/k)) + \frac{1}{\sqrt{k}} + \max \left\{ \frac{\lambda}{\sqrt{k}}, \left(\frac{k}{n} \right)^\xi (\log(n/k)) \right\} \\ & \lesssim \left(\frac{k}{n} \right)^\xi (\log(n/k)) + \frac{1+\lambda}{\sqrt{k}} \end{aligned}$$

so they are absorbed into the bounds above. Note that this time we have used the upper bound on a in (S4.22) in order to bound $a l_{n,a}$.

The probability that each of the two bounds in (S4.24) and (S4.25) holds is at least

$$\begin{aligned} & 1 - d^3 e^{-\lambda^2} - \mathbb{P} \left(\max_{i \in V} \widehat{\Delta}_n^{(i)}(a, 0, \nu) > \widehat{A} \left(\frac{1}{\sqrt{k}} + \frac{\log n}{k} \right) + \frac{\lambda}{\sqrt{k}} + \frac{\lambda^2}{k} \right) - 16d^3 e^{-c_2 \lambda^2 / 2} - \mathbb{P} \left(\max_i \widetilde{\Delta}_n^{(i)}(a, \nu) > \frac{\tilde{A} + \lambda}{\sqrt{k}} \right) \\ & - \mathbb{P} \left(\max_i \sup_{x \in [0, n/k]} |u_n^{(i)}(x) - w_n^{(i)}(x)| > \frac{A \log n + \lambda^2}{k} \right) - \mathbb{P} \left(\max_i \sup_{a \leq x \leq n/k} \frac{|w_n^{(i)}(x) - x|}{x} > 1/2 \right) \\ & \geq 1 - d^3 e^{-\lambda^2} - \widehat{B} d e^{-\widehat{C} \lambda^2} - 16d^3 e^{-c_2 \lambda^2 / 2} - \widetilde{B} d e^{-\widetilde{C} \lambda^2} - B d e^{-C \lambda^2} - 6d \exp \left\{ -c' k \left(1 \wedge \frac{a}{\log \log(1/a)} \right) \right\} \\ & \geq 1 - M d^3 \exp \left\{ -c \min \left\{ \lambda^2, \frac{ka}{\log \log(1/a)} \right\} \right\}, \end{aligned}$$

for suitable constants M and c , where we have used Corollary S1 and Lemmas S1 and S2. By (S4.22), since $a \geq \lambda^2 (\log n) / k$, we find

$$\frac{ka}{\log \log(1/a)} \geq \frac{\lambda^2 \log n}{\log \log k} \geq \lambda^2,$$

so that the probability above is equal to

$$1 - M d^3 e^{-c \lambda^2}.$$

Combining this with (S4.2) and (S4.5) to (S4.7) finally concludes the proof, upon noting that the factor $e_i^{(m),1} - e_j^{(m),1}$ appearing in (S4.2) is upper bounded by $1 + K/\xi$ (see the proof of Lemma S8) and properly choosing the constants C and \bar{C} in terms of C' and \bar{C}' . \square

S5. Auxiliary results and proofs.

S5.1. *Proof of Proposition 1.* We first show that (4.1) is sufficient for Assumptions 3 and 4, and subsequently prove the converse which turns out to be more involved.

Assumption 1 implies Assumptions 3 and 4: Assume that (4.1) holds for all $q \in (0, 1]$ and all sets $J \subset V$ of size 3. We then have, for any i, j, m ,

$$\begin{aligned} R_{im}(q^{-1}, 1) &= R_{ijm}(q^{-1}, \infty, 1) \\ &\geq R_{ijm}(q^{-1}, q^{-1}, 1) \\ &\geq q^{-1} \mathbb{P}(F_i(X_i) > 0, F_j(X_j) > 0, F_m(X_m) > 1 - q) - Kq^\xi \\ &= 1 - Kq^\xi, \end{aligned}$$

since the marginal distribution of $F_m(X_m)$ is uniform on $(0, 1)$. Thus (4.6) holds with $K_T = K$, $\xi_T = \xi$.

Now, that (4.5) follows from (4.1) when $|J| = 3$ is trivial. For the case where J is a pair, say (i, m) , let $x \leq q^{-1}$, $z \leq 1$. We have

$$\begin{aligned} &\left| q^{-1} \mathbb{P}(F_i(X_i) > 1 - qx, F_m(X_m) > 1 - qz) - R_{im}(x, z) \right| \\ &= \left| q^{-1} \mathbb{P}(F_i(X_i) > 1 - qx, F_j(X_j) > 1 - qq^{-1}, F_m(X_m) > 1 - qz) - R_{im}(x, z) \right| \\ &\leq \left| R_{ijm}(x, q^{-1}, z) - R_{im}(x, z) \right| + Kq^\xi \\ (S5.1) \quad &= R_{ijm}([0, x], [q^{-1}, \infty), [0, z]) + Kq^\xi, \end{aligned}$$

using (4.1) and the representation of R_{ijm} as a non-negative measure. Then, (4.6) implies that the first term above is upper bounded by $R_{ijm}([q^{-1}, \infty), 1) \leq Kq^\xi$. Hence for pairs J , (4.5) (in fact, a stronger version thereof where one component of \mathbf{x} is allowed to grow) holds with $K' = 2K$, $\xi' = \xi$.

Assumptions 3 and 4 imply Assumption 1: Assume that (4.5) and (4.6) hold for all $q \in (0, 1]$ and all pairs and triples $J \subset V$ of indices. As in the statement of the result, let $\xi := \xi' \xi_T / (1 + \xi' + \xi_T)$. Let

$$\psi := \frac{\xi'}{1 + \xi' + \xi_T} \in (0, 1),$$

and note that both $-\psi + (1 - \psi)\xi'$ and $\psi\xi_T$ are equal to ξ .

We wish to bound

$$(S5.2) \quad \left| q^{-1} \mathbb{P}(F_i(X_i) > 1 - qx, F_j(X_j) > 1 - qy, F_m(X_m) > 1 - qz) - R_{ijm}(x, y, z) \right|$$

uniformly over all $x, y \in [0, q^{-1}]$, $z \in [0, 1]$. Let us divide the square $[0, q^{-1}]^2$ of possible values of (x, y) into four quadrants defined by the axes $x = q^{-\psi}$ and $y = q^{-\psi}$. First, for all $x, y, z \leq q^{-\psi}$,

$$\begin{aligned} &\left| q^{-1} \mathbb{P}(F_i(X_i) > 1 - qx, F_j(X_j) > 1 - qy, F_m(X_m) > 1 - qz) - R_{ijm}(x, y, z) \right| \\ &= \left| q^{-1} \mathbb{P}(F_i(X_i) > 1 - q^{1-\psi} q^\psi x, F_j(X_j) > 1 - q^{1-\psi} q^\psi y, F_m(X_m) > 1 - q^{1-\psi} q^\psi z) \right. \\ &\quad \left. - q^{-\psi} R_{ijm}(q^\psi x, q^\psi y, q^\psi z) \right| \\ &= q^{-\psi} \left| q^{\psi-1} \mathbb{P}(F_i(X_i) > 1 - q^{1-\psi} q^\psi x, F_j(X_j) > 1 - q^{1-\psi} q^\psi y, F_m(X_m) > 1 - q^{1-\psi} q^\psi z) \right. \\ &\quad \left. - R_{ijm}(q^\psi x, q^\psi y, q^\psi z) \right| \\ (S5.3) \quad &\leq K' q^{-\psi+(1-\psi)\xi'} = K' q^\xi, \end{aligned}$$

where we applied (4.5) with q replaced by $q^{1-\psi}$, since $q^\psi(x, y, z) \in [0, 1]^3$. This bounds (S5.2) for $x, y \leq q^{-\psi}$.

Second, for $q^{-\psi} \leq x, y \leq q^{-1}, z \leq 1$,

$$\begin{aligned}
z &\geq R_{ijm}(x, y, z) = zR_{ijm}(x/z, y/z, 1) \geq zR_{ijm}(q^{-\psi}, q^{-\psi}, 1) \\
&= zR_{ijm}([0, q^{-\psi}] \times [0, q^{-\psi}] \times [0, 1]) \\
&\geq z(R_{im}([0, q^{-\psi}], [0, 1]) + R_{jm}([0, q^{-\psi}], [0, 1]) - 1) \\
&\geq z(1 - 2K_T(q^\psi)^{\xi_T}) \\
\text{(S5.4)} \quad &\geq z - 2K_T q^\xi,
\end{aligned}$$

using (4.6) to lower bound R_{im} and R_{jm} . Similarly,

$$\begin{aligned}
z &\geq q^{-1}\mathbb{P}(F_i(X_i) > 1 - qx, F_j(X_j) > 1 - qy, F_m(X_m) > 1 - qz) \\
&\geq q^{-1}\mathbb{P}(F_i(X_i) > 1 - qq^{-\psi}, F_j(X_j) > 1 - qq^{-\psi}, F_m(X_m) > 1 - qz) \\
&\geq R_{ijm}(q^{-\psi}, q^{-\psi}, z) - K'q^\xi \\
&= zR_{ijm}(q^{-\psi}/z, q^{-\psi}/z, 1) - K'q^\xi \\
&\geq zR_{ijm}(q^{-\psi}, q^{-\psi}, 1) - K'q^\xi,
\end{aligned}$$

where the third inequality follows from (S5.3). Using the developments leading to (S5.4), this lower bound is itself lower bounded by

$$z - (K' + 2K_T)q^\xi.$$

Deduce that (S5.2) is bounded by $(K' + 2K_T)q^\xi$ for $q^{-\psi} \leq x, y \leq q^{-1}$.

Third, let $q^{-\psi} \leq x \leq q^{-1}, y \leq q^{-\psi}, z \leq 1$; the case where $q^{-\psi} \leq y \leq q^{-1}$ and $x \leq q^{-\psi}$ is handled symmetrically. We will again sandwich the two terms in (S5.2). We first have

$$\begin{aligned}
R_{jm}(y, z) &\geq R_{ijm}(x, y, z) \\
&\geq R_{ijm}(q^{-\psi}, y, z) \\
&= R_{jm}(y, z) - (R_{jm}(y, z) - R_{ijm}(q^{-\psi}, y, z)) \\
&\geq R_{jm}(y, z) - (z - R_{im}(q^{-\psi}, z)) \\
&\geq R_{jm}(y, z) - (1 - R_{im}(q^{-\psi}, 1)) \\
&\geq R_{jm}(y, z) - K_T q^\xi,
\end{aligned}$$

where in the last step we use (4.6). The other term in (S5.2) enjoys similar upper and lower bounds: by (S5.3) and by the preceding lower bound on $R_{ijm}(q^{-\psi}, y, z)$,

$$\begin{aligned}
q^{-1}\mathbb{P}(F_i(X_i) > 1 - qx, F_j(X_j) > 1 - qy, F_m(X_m) > 1 - qz) \\
&\geq q^{-1}\mathbb{P}(F_i(X_i) > 1 - qq^{-\psi}, F_j(X_j) > 1 - qy, F_m(X_m) > 1 - qz) \\
&\geq R_{ijm}(q^{-\psi}, y, z) - K'q^\xi \\
&\geq R_{jm}(y, z) - (K' + K_T)q^\xi.
\end{aligned}$$

Meanwhile,

$$\begin{aligned}
q^{-1}\mathbb{P}(F_i(X_i) > 1 - qx, F_j(X_j) > 1 - qy, F_m(X_m) > 1 - qz) \\
\leq q^{-1}\mathbb{P}(F_j(X_j) > 1 - qy, F_m(X_m) > 1 - qz)
\end{aligned}$$

$$\begin{aligned}
&\leq q^{-\psi} q^{\psi-1} \mathbb{P}(F_j(X_j) > 1 - q^{1-\psi} q^\psi y, F_m(X_m) > 1 - q^{1-\psi} q^\psi z) \\
&\leq q^{-\psi} (R_{jm}(q^\psi y, q^\psi z) + K' q^{(1-\psi)\xi'}) \\
&= R_{jm}(y, z) + K' q^\xi,
\end{aligned}$$

where we have used (4.5) with q replaced by $q^{1-\psi}$, since $q^\psi(y, z) \in [0, 1]^2$. Deduce that (S5.2) is bounded by $(K' + K_T)q^\xi$ for $y \leq q^{-\psi} \leq x \leq q^{-1}$ (and also for $y \leq q^{-\psi} \leq x \leq q^{-1}$ by symmetry).

We have therefore established that for all $x, y \leq q^{-1}$, $z \leq 1$, (S5.2) is upper bounded by $(K' + 2K_T)q^\xi$, i.e., Assumption 1 is satisfied with the desired values K and ξ . \square

S5.2. Densities of Hüsler–Reiss Pareto distributions. Using the known expression for the stable tail dependence function of the bivariate Hüsler–Reiss distribution, we now show that any such distribution satisfies Assumptions 2 and 4.

LEMMA S3. *Suppose that \mathbf{Y} has a Hüsler–Reiss distribution with parameter matrix Γ . For any distinct pair (i, j) , as long as $\lambda := \sqrt{\Gamma_{ij}} > 0$, its bivariate R -function R_{ij} satisfies the following.*

(i) *For any positive ξ , there exists a finite constant K_ξ (which also depends on λ) such that*

$$1 - R_{ij}(q^{-1}, 1) \leq K_\xi q^\xi, \quad q \in (0, 1].$$

(ii) *The function R_{ij} has density*

$$r_{ij}(x, y) = \frac{1}{2\sqrt{2\pi}\lambda\sqrt{xy}} \exp\left\{-\frac{\lambda^2}{2} - \frac{(\log x - \log y)^2}{8\lambda^2}\right\}, \quad (x, y) \in (0, \infty)^2.$$

For any $\beta \in \mathbb{R}$, this density enjoys the upper bound

$$r_{ij}(x, y) \leq \frac{K(\beta)}{x^\beta y^{1-\beta}}, \quad K(\beta) := \frac{\exp\{\lambda^2(2(\beta - 1/2)^2 - 1/2)\}}{2\sqrt{2\pi}\lambda}.$$

PROOF. The pair (Y_i, Y_j) has a bivariate Hüsler–Reiss distribution with dependence parameter λ^2 , so its stable tail dependence function is

$$L_{ij}(x, y) = x\Phi\left(\lambda + \frac{\log x - \log y}{2\lambda}\right) + y\Phi\left(\lambda + \frac{\log y - \log x}{2\lambda}\right),$$

so R_{ij} is given by

$$R_{ij}(x, y) = x\Phi^c\left(\lambda + \frac{\log x - \log y}{2\lambda}\right) + y\Phi^c\left(\lambda + \frac{\log y - \log x}{2\lambda}\right),$$

where Φ^c denotes the standard Gaussian survival function.

Proof of (i): Fix a number $\xi > 0$. First note that if $q \geq e^{-4\lambda^2}$, we trivially have that

$$1 - R_{ij}(q^{-1}, 1) \leq 1 \leq e^{4\lambda^2\xi} q^\xi,$$

so we shall assume without loss of generality that $q \leq e^{-4\lambda^2}$. This implies that $\log q^{-1} \geq 4\lambda^2$, or equivalently

$$\frac{\log q^{-1}}{2\lambda} - \lambda \geq \frac{\log q^{-1}}{4\lambda}.$$

We then have

$$\begin{aligned}
1 - R_{ij}(q^{-1}, 1) &\leq 1 - \Phi^c\left(\lambda + \frac{\log q}{2\lambda}\right) = \Phi^c\left(\frac{\log q^{-1}}{2\lambda} - \lambda\right) \leq \Phi^c\left(\frac{\log q^{-1}}{4\lambda}\right) \\
&\leq \frac{4\lambda}{\sqrt{2\pi} \log q^{-1}} \exp\left\{-\frac{1}{32\lambda^2} (\log q^{-1})^2\right\},
\end{aligned}$$

the last inequality following from well known bounds on the Gaussian tails (Durrett, 2010, Theorem 1.2.3). This is in turn upper bounded by

$$\frac{1}{\sqrt{2\pi\lambda}} q^{(\log q^{-1})/32\lambda^2},$$

which is of smaller order than any power of q since the exponent diverges as $q \downarrow 0$. We can therefore upper bound it by any power q^ξ , up to a multiplicative constant depending on both ξ and λ .

Proof of (ii): The density of R_{ij} is defined as

$$r_{ij}(x, y) := \frac{\partial^2}{\partial x \partial y} R_{ij}(x, y) = -\frac{\partial^2}{\partial x \partial y} L_{ij}(x, y).$$

First, we have

$$\begin{aligned} \frac{\partial}{\partial x} x \Phi\left(\lambda + \frac{\log x - \log y}{2\lambda}\right) &= \Phi\left(\lambda + \frac{\log x - \log y}{2\lambda}\right) + x \phi\left(\lambda + \frac{\log x - \log y}{2\lambda}\right) \frac{1}{2\lambda x} \\ &= \Phi\left(\lambda + \frac{\log x - \log y}{2\lambda}\right) + \frac{1}{2\lambda} \phi\left(\lambda + \frac{\log x - \log y}{2\lambda}\right), \end{aligned}$$

so

$$\begin{aligned} \frac{\partial^2}{\partial x \partial y} x \Phi\left(\lambda + \frac{\log x - \log y}{2\lambda}\right) &= -\frac{1}{2\lambda y} \phi\left(\lambda + \frac{\log x - \log y}{2\lambda}\right) - \frac{1}{4\lambda^2 y} \phi'\left(\lambda + \frac{\log x - \log y}{2\lambda}\right) \\ &= -\frac{1}{4\lambda^2 y} \left(\lambda + \frac{\log y - \log x}{2\lambda}\right) \phi\left(\lambda + \frac{\log x - \log y}{2\lambda}\right), \end{aligned}$$

where we used the expression $\phi'(t) = -t\phi(t)$ for the derivative of the standard Gaussian density ϕ . Now by definition of ϕ , this is equal to

$$\begin{aligned} &-\frac{1}{4\sqrt{2\pi}\lambda^2 y} \left(\lambda + \frac{\log y - \log x}{2\lambda}\right) \exp\left\{-\frac{\lambda^2}{2} - \frac{(\log x - \log y)^2}{8\lambda^2} + \frac{\log y - \log x}{2}\right\} \\ &= -\frac{1}{4\sqrt{2\pi}\lambda^2 \sqrt{xy}} \left(\lambda + \frac{\log y - \log x}{2\lambda}\right) \exp\left\{-\frac{\lambda^2}{2} - \frac{(\log x - \log y)^2}{8\lambda^2}\right\}. \end{aligned}$$

Adding this to

$$\frac{\partial^2}{\partial x \partial y} y \Phi\left(\lambda + \frac{\log y - \log x}{2\lambda}\right) = -\frac{1}{4\sqrt{2\pi}\lambda^2 \sqrt{xy}} \left(\lambda + \frac{\log x - \log y}{2\lambda}\right) \exp\left\{-\frac{\lambda^2}{2} - \frac{(\log x - \log y)^2}{8\lambda^2}\right\},$$

obtained by a symmetric argument, yields the desired density. As for the upper bound, note that for any $\beta \in \mathbb{R}$,

$$r_{ij}(x, y) = \frac{1}{2\sqrt{2\pi}\lambda x^\beta \sqrt{y}} \exp\left\{-\frac{\lambda^2}{2} - \frac{(\log x - \log y)^2}{8\lambda^2} + (\beta - 1/2) \log x\right\}.$$

Writing u and v for $\log x$ and $\log y$, the exponent above is

$$-\frac{\lambda^2}{2} - \frac{(u-v)^2}{8\lambda^2} + (\beta - 1/2)u = \frac{-u^2}{8\lambda^2} + \left((\beta - 1/2) + \frac{v}{4\lambda^2}\right)u - \frac{v^2}{8\lambda^2}$$

which is maximized (in u) at $u = v + 4\lambda^2(\beta - 1/2)$, hence

$$\begin{aligned} -\frac{\lambda^2}{2} - \frac{(u-v)^2}{8\lambda^2} + (\beta - 1/2)u &\leq -\frac{\lambda^2}{2} - 2\lambda^2(\beta - 1/2)^2 + (\beta - 1/2)v + 4\lambda^2(\beta - 1/2)^2 \\ &= (\beta - 1/2)v + \lambda^2(2(\beta - 1/2)^2 - 1/2). \end{aligned}$$

Conclude that

$$r_{ij}(x, y) \leq \frac{1}{2\sqrt{2\pi}\lambda x^\beta y^{1-\beta}} \exp\{\lambda^2(2(\beta - 1/2)^2 - 1/2)\}.$$

□

S5.3. *The moments $e_m^{(m),\ell}$.* Recalling that for any m , $Y_m^{(m)}$ has a unit Pareto distribution, and thus that $\log Y_m^{(m)}$ has a unit exponential distribution, it is evident that $e_m^{(m),1} = 1$ and $e_m^{(m),2} = 2$. As for the empirical versions $\widehat{e}_m^{(m),\ell}$ of those moments, they are in fact deterministic, since the terms $\widehat{F}_m(U_{tm})$ appearing in the sum are exactly the k smallest such terms $\{1/n, \dots, k/n\}$. Precisely, we have the following result.

LEMMA S4. *As long as $k \geq 3$, we have*

$$|\widehat{e}_m^{(m),1} - 1| \leq \frac{3 \log k}{k}, \quad |\widehat{e}_m^{(m),2} - 2| \leq \frac{8(\log k)^2}{k}.$$

PROOF. By definition, we have

$$(S5.5) \quad \widehat{e}_m^{(m),\ell} = \frac{1}{k} \sum_{j=1}^k \{\log(k/j)\}^\ell = \begin{cases} \log k - \frac{1}{k} \sum_{j=1}^k \log j, & \ell = 1 \\ (\log k)^2 - \frac{2 \log k}{k} \sum_{j=1}^k \log j + \frac{1}{k} \sum_{j=1}^k (\log j)^2, & \ell = 2 \end{cases}.$$

Note that

$$\sum_{j=1}^k (\log j)^\ell = \sum_{j=2}^k \int_j^{j+1} (\log j)^\ell dt \in \left[\int_1^k (\log t)^\ell dt, \int_2^{k+1} (\log t)^\ell dt \right].$$

Evaluating those integrals yields

$$k\{\log k - 1\} + 1 \leq \sum_{j=1}^k \log j \leq (k+1)\{\log(k+1) - 1\} - 2(\log 2 - 1)$$

and

$$k\{(\log k)^2 - 2 \log k + 2\} - 2 \leq \sum_{j=1}^k (\log j)^2 \leq (k+1)\{(\log(k+1))^2 - 2 \log(k+1) + 2\} - 2\{(\log 2)^2 - 2 \log 2 + 2\}.$$

Denote by a_ℓ and b_ℓ the lower and upper bound on $\sum_{j=1}^k (\log j)^\ell$ above, $\ell \in \{1, 2\}$. As long as $k \geq 3$, we have by (S5.5) and by simple computations

$$k|\widehat{e}_m^{(m),1} - 1| \leq |a_1 - k \log k + k| \vee |b_1 - k \log k + k| \leq 3 \log k$$

and

$$k|\widehat{e}_m^{(m),2} - 2| \leq |a_2 - 2(\log k)b_1 + k(\log k)^2 - 2k| \vee |b_2 - 2(\log k)a_1 + k(\log k)^2 - 2k| \leq 8(\log k)^2,$$

which is the desired result. \square

S5.4. *Verifying the integral representations of different moments.* We start by deriving general expressions for the moments of logarithms of random vectors which will lead to proving the representations in (S4.5) to (S4.7). The following result is a multivariate version of the so-called ‘‘Darth Vader rule’’.

LEMMA S5. *Let X_1, \dots, X_d be non-negative random variables and $p_1, \dots, p_d > 0$. Then*

$$\mathbb{E} \left[\prod_{j=1}^d X_j^{p_j} \right] = \int_{[0, \infty)^d} \prod_{j=1}^d p_j x_j^{p_j-1} \mathbb{P}(X_1 \geq x_1, \dots, X_d \geq x_d) dx_1 \dots dx_d.$$

Moreover, any number of ‘‘ \geq ’’ can be replaced by ‘‘ $>$ ’’, as this changes the value of the probability, at most, on a Lebesgue-null set.

PROOF. Letting (Ω, \mathcal{F}, P) be the underlying probability space containing all the random variables, we have

$$\begin{aligned}
\mathbb{E} \left[\prod_{j=1}^d X_j^{p_j} \right] &= \int_{\Omega} \prod_{j=1}^d X_j(\omega)^{p_j} P(d\omega) \\
&= \int_{\Omega} \int_{[0, X_1(\omega)^{p_1}] \times \dots \times [0, X_d(\omega)^{p_d}]} du_1 \dots du_d P(d\omega) \\
&= \int_{\Omega} \int_{[0, \infty)^d} \mathbb{1} \left\{ X_1(\omega) \geq u_1^{1/p_1}, \dots, X_d(\omega) \geq u_d^{1/p_d} \right\} du_1 \dots du_d P(d\omega) \\
&= \int_{[0, \infty)^d} \left(\int_{\Omega} \mathbb{1} \left\{ X_1(\omega) \geq u_1^{1/p_1}, \dots, X_d(\omega) \geq u_d^{1/p_d} \right\} P(d\omega) \right) du_1 \dots du_d \\
&= \int_{[0, \infty)^d} \mathbb{P}(X_1 \geq u_1^{1/p_1}, \dots, X_d \geq u_d^{1/p_d}) du_1 \dots du_d,
\end{aligned}$$

where we have used the fact that $X_j(\omega) \geq 0$ for almost every ω to justify the second equality. The change in the order of integration was allowed by Tonelli's theorem. Finally, applying the change of variable $x_j = u_j^{1/p_j}$, $du_j/dx_j = p_j x_j^{p_j-1}$ produces the desired result. \square

LEMMA S6. *Let X and Y be almost surely positive random variables and let S be the distribution function of $(1/X, 1/Y)$, so that for positive x, y , $\mathbb{P}(X \geq x, Y \geq y) = S(1/x, 1/y)$. Then for any $p \in \{1, 2, \dots\}$,*

$$(S5.6) \quad \mathbb{E}[(\log X)^p \mathbb{1}\{X > 1\}] = p \int_0^1 \frac{S(x, \infty) |\log x|^{p-1}}{x} dx,$$

$$(S5.7) \quad \mathbb{E}[(-\log X)^p \mathbb{1}\{X < 1\}] = p \int_1^{\infty} \frac{S([x, \infty), \infty) |\log x|^{p-1}}{x} dx,$$

$$(S5.8) \quad \mathbb{E}[(\log X)(\log Y))^p \mathbb{1}\{X, Y > 1\}] = p^2 \int_0^1 \int_0^1 \frac{S(x, y) |(\log x)(\log y)|^{p-1}}{xy} dx dy,$$

$$(S5.9) \quad \mathbb{E}[(-\log X)(\log Y))^p \mathbb{1}\{X < 1, Y > 1\}] = p^2 \int_0^1 \int_1^{\infty} \frac{S([x, \infty), y) |(\log x)(\log y)|^{p-1}}{xy} dx dy,$$

$$(S5.10) \quad \mathbb{E}[(\log X)(\log Y))^p \mathbb{1}\{X, Y < 1\}] = p^2 \int_1^{\infty} \int_1^{\infty} \frac{S([x, \infty), [y, \infty)) |(\log x)(\log y)|^{p-1}}{xy} dx dy,$$

where $S([x, \infty), y)$ and $S([x, \infty), [y, \infty))$ are shorthand for $S(\infty, y) - S(x, y)$ and $1 - S(x, \infty) - S(\infty, y) + S(x, y)$, respectively.

PROOF. First, by Lemma S5 with $d = 1$, $p_1 = p$,

$$\begin{aligned}
\mathbb{E}[(\log X)^p \mathbb{1}\{X > 1\}] &= p \int_0^{\infty} u^{p-1} \mathbb{P}(\log X \geq u) du \\
&= p \int_0^{\infty} u^{p-1} S(e^{-u}, \infty) du \\
&= p \int_0^1 \frac{S(x, \infty) (-\log x)^{p-1}}{x} dx,
\end{aligned}$$

by the change of variable $x = e^{-u}$. Similarly,

$$\mathbb{E}[(-\log X)^p \mathbb{1}\{X < 1\}] = p \int_0^{\infty} u^{p-1} \mathbb{P}(\log X \leq -u) du$$

$$\begin{aligned}
&= p \int_0^\infty u^{p-1} S([e^u, \infty), \infty) du \\
&= p \int_1^\infty \frac{S([x, \infty), \infty) (\log x)^{p-1}}{x} dx,
\end{aligned}$$

by the change of variable $x = e^u$. This establishes (S5.6) and (S5.7).

(S5.8) to (S5.10) are proved in a similar fashion by using Lemma S5 with $d = 2$, $p_1 = p_2 = p$. First,

$$\begin{aligned}
\mathbb{E}[(\log X)(\log Y))^p \mathbf{1}\{X, Y > 1\}] &= p^2 \int_0^\infty \int_0^\infty (uv)^{p-1} \mathbb{P}(\log X \geq u, \log Y \geq v) dudv \\
&= p^2 \int_0^\infty \int_0^\infty (uv)^{p-1} S(e^{-u}, e^{-v}) dudv \\
&= p^2 \int_0^1 \int_0^1 \frac{S(x, y) ((\log x)(\log y))^{p-1}}{xy} dx dy,
\end{aligned}$$

using the change of variable $x = e^{-u}$, $y = e^{-v}$. Second,

$$\begin{aligned}
\mathbb{E}[(-\log X)(\log Y))^p \mathbf{1}\{X < 1, Y > 1\}] &= p^2 \int_0^\infty \int_0^\infty (uv)^{p-1} \mathbb{P}(\log X \leq -u, \log Y \geq v) dudv \\
&= p^2 \int_0^\infty \int_0^\infty (uv)^{p-1} S([e^u, \infty), e^{-v}) dudv \\
&= p^2 \int_0^1 \int_1^\infty \frac{S([x, \infty), y) (-\log x)(\log y)^{p-1}}{xy} dx dy,
\end{aligned}$$

using the change of variable $x = e^u$, $y = e^{-v}$. Third,

$$\begin{aligned}
\mathbb{E}[(\log X)(\log Y))^p \mathbf{1}\{X, Y < 1\}] &= p^2 \int_0^\infty \int_0^\infty (uv)^{p-1} \mathbb{P}(\log X \leq -u, \log Y \leq -v) dudv \\
&= p^2 \int_0^\infty \int_0^\infty (uv)^{p-1} S([e^u, \infty), [e^v, \infty)) dudv \\
&= p^2 \int_1^\infty \int_1^\infty \frac{S([x, \infty), [y, \infty)) ((\log x)(\log y))^{p-1}}{xy} dx dy,
\end{aligned}$$

using the change of variable $x = e^u$, $y = e^v$. This establishes (S5.8) to (S5.10). \square

LEMMA S7. Under Assumption 1, (S4.5) to (S4.7) hold for any $a \in (0, 1)$.

PROOF. Recall that i, j, m are assumed to be distinct indices. It is already proved in (Engelke and Volgushev, 2020, Section S.7) that the moments of interest satisfy

$$(S5.11) \quad e_i^{(m), \ell} = \int_0^1 \frac{R_{im}(x, 1) (-2 \log x)^{\ell-1}}{x} dx - \int_1^\infty \frac{R_{im}([x, \infty), 1) (-2 \log x)^{\ell-1}}{x} dx,$$

$$(S5.12) \quad e_{im}^{(m)} = \int_0^1 \int_0^1 \frac{R_{im}(x, y)}{xy} dx dy - \int_0^1 \int_1^\infty \frac{R_{im}([x, \infty), y)}{xy} dx dy,$$

$$(S5.13) \quad \begin{aligned} e_{ij}^{(m)} &= \int_0^1 \int_0^1 \frac{R_{ijm}(x, y, 1)}{xy} dx dy - \int_0^1 \int_1^\infty \frac{R_{ijm}([x, \infty), y, 1)}{xy} dx dy \\ &\quad - \int_1^\infty \int_0^1 \frac{R_{ijm}(x, [y, \infty), 1)}{xy} dx dy + \int_1^\infty \int_1^\infty \frac{R_{ijm}([x, \infty), [y, \infty), 1)}{xy} dx dy \end{aligned}$$

and that their empirical versions satisfy

$$(S5.14) \quad \widehat{e}_i^{(m),\ell} = \int_{1/k}^1 \frac{\bar{R}_{im}(x,1)(-2\log x)^{\ell-1}}{x} dx - \int_1^{n/k} \frac{\bar{R}_{im}([x,\infty),1)(-2\log x)^{\ell-1}}{x} dx,$$

$$(S5.15) \quad \widehat{e}_{im}^{(m)} = \int_{1/k}^1 \int_{1/k}^1 \frac{\bar{R}_{im}(x,y)}{xy} dx dy - \int_{1/k}^1 \int_1^{n/k} \frac{\bar{R}_{im}([x,\infty),y)}{xy} dx dy,$$

$$(S5.16) \quad \begin{aligned} \widehat{e}_{ij}^{(m)} &= \int_{1/k}^1 \int_{1/k}^1 \frac{\bar{R}_{ijm}(x,y,1)}{xy} dx dy - \int_{1/k}^1 \int_1^{n/k} \frac{\bar{R}_{ijm}([x,\infty),y,1)}{xy} dx dy \\ &\quad - \int_1^{n/k} \int_{1/k}^1 \frac{\bar{R}_{ijm}(x,[y,\infty),1)}{xy} dx dy + \int_1^{n/k} \int_1^{n/k} \frac{\bar{R}_{ijm}([x,\infty),[y,\infty),1)}{xy} dx dy, \end{aligned}$$

where

$$\bar{R}_J(\mathbf{x}_J) := \frac{1}{k} \sum_{t=1}^n \mathbb{1} \left\{ \widehat{F}_i(U_{ti}) \leq \frac{k}{n} x_i, i \in J \right\}, \quad \mathbf{x}_J := (x_i)_{i \in J} \in [0, \infty)^{|J|}.$$

The integrals in (S5.11) to (S5.13) can be truncated above by using (S4.10), which allows to upper bound the tails of the functions R_J . In particular, we have

$$\int_{n/k}^{\infty} \frac{R_{im}([x,\infty),1)(2\log x)^{\ell-1}}{x} dx \lesssim \int_{n/k}^{\infty} \frac{(\log x)^{\ell-1}}{x^{1+\xi}} dx \lesssim \left(\frac{k}{n}\right)^{\xi} \log(n/k),$$

$$\int_0^1 \int_{n/k}^{\infty} \frac{R_{im}([x,\infty),y)}{xy} dx dy = \int_0^1 \int_{n/k}^{\infty} \frac{R_{im}([x/y,\infty),1)}{x} dx dy \lesssim \int_0^1 \int_{n/k}^{\infty} \frac{(x/y)^{-\xi}}{x} dx dy \lesssim \left(\frac{k}{n}\right)^{\xi},$$

and

$$\begin{aligned} &\iint_{[1,\infty)^2 \setminus [1,n/k]^2} \frac{R_{ijm}([x,\infty),[y,\infty),1)}{xy} dx dy \\ &= \int_{n/k}^{\infty} \int_{n/k}^{\infty} \frac{R_{ijm}([x,\infty),[y,\infty),1)}{xy} dx dy + \int_1^{n/k} \int_{n/k}^{\infty} \frac{R_{ijm}([x,\infty),[y,\infty),1)}{xy} dx dy \\ &\quad + \int_{n/k}^{\infty} \int_1^{n/k} \frac{R_{ijm}([x,\infty),[y,\infty),1)}{xy} dx dy \\ &\leq \int_{n/k}^{\infty} \int_{n/k}^{\infty} \frac{R_{ijm}([x,\infty),[y,\infty),1)}{xy} dx dy + \int_1^{n/k} \int_{n/k}^{\infty} \frac{R_{im}([x,\infty),1)}{xy} dx dy + \int_{n/k}^{\infty} \int_1^{n/k} \frac{R_{jm}([y,\infty),1)}{xy} dx dy \\ &\lesssim \int_{n/k}^{\infty} \int_{n/k}^{\infty} \frac{x^{-\xi} \wedge y^{-\xi}}{xy} dx dy + 2 \int_1^{n/k} \int_{n/k}^{\infty} \frac{x^{-\xi}}{xy} dx dy \\ &\lesssim \left(\frac{k}{n}\right)^{\xi} \log(n/k). \end{aligned}$$

Hence we proved that all integral can be truncated above at n/k while incurring an error of at most $O((k/n)^{\xi} \log(n/k))$. Next we show that the integrals can as well be truncated below.

Recall that $a \in (0, 1)$. Since by their definitions, R_J and \bar{R}_J are both upper bounded by the minimum component of their argument, so is $|\bar{R}_J - R_J|$. We then have for $\ell \in \{1, 2\}$

$$\int_0^a \frac{|\bar{R}_{im}(x,1) - R_{im}(x,1)|(-2\log x)^{\ell-1}}{x} dx \leq \int_0^a (-2\log x)^{\ell-1} dx \lesssim a(1 + \log(1/a)),$$

$$\iint_{[0,1]^2 \setminus [a,1]^2} \frac{|\bar{R}_{im}(x,y) - R_{im}(x,y)|}{xy} dx dy \leq \int_0^a \int_0^a \frac{x \wedge y}{xy} dx dy + 2 \int_a^1 \int_0^a \frac{1}{y} dx dy \lesssim a(1 + \log(1/a)),$$

$$\int_0^a \int_1^{n/k} \frac{|\bar{R}_{im}([x,\infty),y) - R_{im}([x,\infty),y)|}{xy} dx dy \leq \int_0^a \int_1^{n/k} \frac{1}{x} dx dy \leq a \log(n/k),$$

and by symmetry

$$\int_1^{n/k} \int_0^a \frac{|\bar{R}_{im}(x,[y,\infty)) - R_{im}(x,[y,\infty))|}{xy} dx dy$$

admits the same bound. Finally, the integral

$$\iint_{[0,1]^2 \setminus [a,1]^2} \frac{|\bar{R}_{ijm}(x,y,1) - R_{ijm}(x,y,1)|}{xy} dx dy$$

is handled similarly as

$$\iint_{[0,1]^2 \setminus [a,1]^2} \frac{|\bar{R}_{im}(x,y) - R_{im}(x,y)|}{xy} dx dy.$$

We have therefore proved that each of the integrals in (S5.11) to (S5.16) can be truncated below at a point a and above at n/k , up to a deterministic additive error which satisfies the bound $\lesssim (k/n)^\xi \log(n/k) + a(\log(n/k) + \log(1/a))$. It follows that with probability 1,

$$\begin{aligned} \hat{e}_i^{(m),\ell} - e_i^{(m),\ell} &= \int_a^1 \frac{(\bar{R}_{im}(x,1) - R_{im}(x,1))(-2\log x)^{\ell-1}}{x} dx \\ &\quad - \int_1^{n/k} \frac{(\bar{R}_{im}([x,\infty),1) - R_{im}([x,\infty),1))(-2\log x)^{\ell-1}}{x} dx \\ &\quad + O\left(\left(\frac{k}{n}\right)^\xi \log(n/k) + a(\log(n/k) + \log(1/a))\right), \\ \hat{e}_{im}^{(m)} - e_{im}^{(m)} &= \int_a^1 \int_a^1 \frac{\bar{R}_{im}(x,y) - R_{im}(x,y)}{xy} dx dy \\ &\quad - \int_a^1 \int_1^{n/k} \frac{\bar{R}_{im}([x,\infty),y) - R_{im}([x,\infty),y)}{xy} dx dy \\ &\quad + O\left(\left(\frac{k}{n}\right)^\xi \log(n/k) + a(\log(n/k) + \log(1/a))\right), \\ \hat{e}_{ij}^{(m)} - e_{ij}^{(m)} &= \int_a^1 \int_a^1 \frac{\bar{R}_{ijm}(x,y,1) - R_{ijm}(x,y,1)}{xy} dx dy \\ &\quad - \int_a^1 \int_1^{n/k} \frac{\bar{R}_{ijm}([x,\infty),y,1) - R_{ijm}([x,\infty),y,1)}{xy} dx dy \\ &\quad - \int_1^{n/k} \int_a^1 \frac{\bar{R}_{ijm}(x,[y,\infty),1) - R_{ijm}(x,[y,\infty),1)}{xy} dx dy \\ &\quad + \int_1^{n/k} \int_1^{n/k} \frac{\bar{R}_{ijm}([x,\infty),[y,\infty),1) - R_{ijm}([x,\infty),[y,\infty),1)}{xy} dx dy \end{aligned}$$

$$+ O\left(\left(\frac{k}{n}\right)^\xi \log(n/k) + a(\log(n/k) + \log(1/a))\right),$$

where the error terms are deterministic. All that remains to obtain the desired result is to replace the functions \bar{R}_J above by \widehat{R}_J , which amounts to comparing the left- and right-continuous versions of an empirical tail copula. By the result in Appendix C.1 of Radulović et al. (2017), we have

$$\max_{J:|J|\leq 3} \sup_{\mathbf{x}_J \in [0, \infty)^{|J|}} |\bar{R}_J(\mathbf{x}_J) - \widehat{R}_J(\mathbf{x}_J)| \leq \frac{3}{k}$$

almost surely, so replacing \bar{R}_J by \widehat{R}_J in the integrals above adds an error that is at most of the order of $(\log(n/k) + \log(1/a))^2/k$. \square

LEMMA S8. *Under Assumption 1, $\max_{m \in V} \|\Gamma^{(m)}\|_\infty$ admits an upper bound that depends only on K and ξ .*

PROOF. First, as is pointed out in Section S5.3, for $\ell \in \{1, 2\}$, $e_m^{(m), \ell} = \ell$.

The remaining arguments are based on (S4.10), which holds by assumption and states that for all distinct triples (i, j, m) ,

$$R_{ij}([x, \infty), 1) \leq Kx^{-\xi}, \quad R_{ijm}([x, \infty), [y, \infty), 1) \leq K(x \wedge y)^{-\xi}, \quad x, y \geq 1.$$

Equally important is the fact that every function R_J is upper bounded by its minimum argument. The proof consists of plugging those different bounds in (S5.11) to (S5.13) above, which provided expressions for the moments $e_i^{(m), \ell}$, $e_{im}^{(m)}$ and $e_{ij}^{(m)}$. Repeatedly using the inequality $a \wedge b \leq (ab)^{1/2}$ for positive a, b , deduce that

$$\begin{aligned} |e_i^{(m), \ell}| &\leq \int_0^1 (-2 \log x)^{\ell-1} dx + K \int_1^\infty \frac{(-2 \log x)^{\ell-1}}{x^{1+\xi}} dx, \\ |e_{im}^{(m)}| &\leq \int_0^1 \int_0^1 (xy)^{-1/2} dx dy + \sqrt{K} \int_0^1 \int_1^\infty x^{-1-\xi/2} y^{-1/2} dx dy, \\ |e_{ij}^{(m)}| &\leq \int_0^1 \int_0^1 (xy)^{-1/2} dx dy + 2\sqrt{K} \int_0^1 \int_1^\infty x^{-1-\xi/2} y^{-1/2} dx dy + K \int_1^\infty \int_1^\infty (xy)^{-1-\xi/2} dx dy. \end{aligned}$$

Simply plugging those bounds in (S4.1) yields the result. \square

S5.5. *Bounds on the measures R_{ij} .* Recall the representation of R_{ij} as a non-negative measure, for an arbitrary pair $i \neq j$. The following bounds necessarily hold.

LEMMA S9. *Let $0 < a \leq b$ and $y > 0$. Then for every distinct pair (i, j) ,*

$$R_{ij}([a, b], y) \leq y \frac{b-a}{a}.$$

PROOF. The idea is that the rectangle $[a, b] \times [0, y]$ is included in the trapezoid $\{(u, v) \in [0, \infty)^2 : a \leq u \leq b, v \leq yu/a\} = S(b) \setminus S(a)$, where

$$S(x) := \{(u, v) \in [0, \infty)^2 : u \leq x, v \leq yu/a\}.$$

By homogeneity of R_{ij} ,

$$R_{ij}(S(b) \setminus S(a)) = (b-a)R_{ij}(S(1)) \leq (b-a)R_{ij}(1, y/a) \leq y \frac{b-a}{a},$$

since R_{ij} is always upper bounded by its smallest argument. \square

The following bound assumes more but is considerably more flexible, as β can be both smaller and larger than 1.

LEMMA S10. *Under Assumption 2, for every $\beta \in (0, 1 + \varepsilon]$ there exists $K(\beta) < \infty$ such that for any $0 < a \leq b$, $y > 0$ and every distinct pair (i, j) ,*

$$R_{ij}([a, b], y) \leq \frac{K(\beta)}{\beta} y^\beta \frac{b-a}{a^\beta}.$$

PROOF. The bound in Assumption 2 gives

$$R_{ij}([a, b], y) = \int_0^y \int_a^b r_{ij}(u, v) du dv \leq K(\beta) \int_0^y v^{\beta-1} dv \int_a^b u^{-\beta} du \leq \frac{K(\beta)}{\beta} y^\beta \int_a^b a^{-\beta} du = \frac{K(\beta)}{\beta} y^\beta \frac{b-a}{a^\beta}.$$

□

LEMMA S11. *Under Assumption 2, for every $\beta \in [-\varepsilon, 0)$ there exists $K(\beta) < \infty$ such that for any $0 < a \leq b$, $y > 0$ and every distinct pair (i, j) ,*

$$R_{ij}([a, b], [y, \infty)) \leq \frac{K(\beta)}{-\beta} y^\beta b^{-\beta} (b-a).$$

PROOF. Following the proof of Lemma S10,

$$R_{ij}([a, b], [y, \infty)) \leq K(\beta) \int_y^\infty v^{\beta-1} dv \int_a^b u^{-\beta} du \leq \frac{K(\beta)}{-\beta} y^\beta \int_a^b b^{-\beta} du = \frac{K(\beta)}{-\beta} y^\beta b^{-\beta} (b-a).$$

□

S5.6. *Technical results from empirical process theory.* In this section, we collect two fundamental inequalities from empirical process theory that are used in Section S4.3.2. Denote by \mathcal{G} a class of real-valued functions that satisfies $|f(x)| \leq F(x) \leq U$ for every $f \in \mathcal{G}$ and let $\sigma^2 \geq \sup_{f \in \mathcal{G}} P f^2$. Additionally, suppose that for some positive A, V and for all $\varepsilon > 0$,

$$(S5.17) \quad N(\varepsilon, \mathcal{G}, L_2(\mathbb{P}_n)) \leq \left(\frac{A \|F\|_{L^2(\mathbb{P}_n)}}{\varepsilon} \right)^V$$

almost surely. In that case, the symmetrization inequality and inequality (2.2) from Koltchinskii (2006) yield

$$(S5.18) \quad \mathbb{E}[\|\mathbb{P}_n - P\|_{\mathcal{G}}] \leq c_0 \left[\sigma \left(\frac{V}{n} \log \frac{A \|F\|_{L^2(P)}}{\sigma} \right)^{1/2} + \frac{VU}{n} \log \frac{A \|F\|_{L^2(P)}}{\sigma} \right]$$

for a universal constant $c_0 > 0$ provided that $1 \geq \sigma^2 > \text{const} \times n^{-1}$. In fact, the inequality in Koltchinskii (2006) is for $\sigma^2 = \sup_{f \in \mathcal{G}} P f^2$. However, this is not a problem since we can replace \mathcal{G} by $\mathcal{G}\sigma / (\sup_{f \in \mathcal{G}} P f^2)^{1/2}$.

The second inequality (a refined version of Talagrand's concentration inequality) states that for any countable class of measurable functions \mathcal{F} with elements mapping into $[-M, M]$,

$$(S5.19) \quad \mathbb{P} \left(\|\mathbb{P}_n - P\|_{\mathcal{F}} \geq 2\mathbb{E}[\|\mathbb{P}_n - P\|_{\mathcal{F}}] + c_1 n^{-1/2} \left(\sup_{f \in \mathcal{F}} P f^2 \right)^{1/2} \sqrt{t} + n^{-1} c_2 M t \right) \leq e^{-t},$$

for all $t > 0$ and some universal constants $c_1, c_2 > 0$. This is a special case of Theorem 3 in Massart (2000) (in the notation of that paper, set $\varepsilon = 1$).

S5.7. *Discussion of max-stable distributions.* In this section, we take \mathbf{X} to be distributed according to the max-stable distribution associated to an arbitrary multivariate Pareto \mathbf{Y} with stable dependence function L . That is, the copula of \mathbf{X} is given by

$$\mathbb{P}(F(\mathbf{X}) \leq \mathbf{x}) = \exp\{-L(-\log \mathbf{x})\}.$$

We shall demonstrate the following result. Note that the constant $K' = 48$ therein is not particularly sharp, and can be improved at the cost of more detailed calculations.

PROPOSITION S3. *The max-stable random vector \mathbf{X} , assuming that its marginal distributions are continuous, satisfies Assumption 3 with $K' = 48$ and $\xi' = 1$.*

PROOF. First note that for $q > 1/2$ and $\mathbf{x} \in [0, 1]^{|J|}$, we have

$$\left| q^{-1} \mathbb{P}(F_J(\mathbf{X}_J) > 1 - q\mathbf{x}) - R_J(\mathbf{x}) \right| \leq 1 \leq 2q,$$

so we may without loss of generality consider only $q \leq 1/2$.

Now let J be a subset of size 2 or 3. For $q \leq 1/2$, we have

$$(S5.20) \quad \begin{aligned} \mathbb{P}(F_J(\mathbf{X}_J) \not\leq 1 - q\mathbf{x}) &= 1 - \exp\{-L_J(-\log(1 - q\mathbf{x}))\} \\ &\in \left[L_J(-\log(1 - q\mathbf{x})) - \frac{1}{2}L_J(-\log(1 - q\mathbf{x}))^2, L_J(-\log(1 - q\mathbf{x})) \right], \end{aligned}$$

using a Taylor expansion of the exponential around the origin: for $z > 0$, there exists $0 \leq \bar{z} \leq z$ such that $e^{-z} = 1 - z + e^{-\bar{z}}z^2/2 \in [1 - z, 1 - z + z^2/2]$. Here L_J is the stable tail dependence function of the subvector \mathbf{X}_J ; it is obtained by evaluating L at a point the components of which in positions J^c are zero. Using a similar decomposition of $-\log(1 - z)$ around $z = 0$, we find that

$$z \leq -\log(1 - z) \leq z + 2z^2.$$

Now recall that $\mathbf{x} \in [0, 1]^{|J|}$. Using the properties of stable tail dependence functions, namely that L (and L_J) is component-wise monotone, convex, homogeneous and upper bounded by the sum of its arguments, we find

$$L_J(q\mathbf{x}) \leq L_J(-\log(1 - q\mathbf{x})) \leq L_J(q\mathbf{x} + 2q^2\mathbf{1}) = 2L_J\left(\frac{1}{2}q\mathbf{x} + \frac{1}{2}2q^2\mathbf{1}\right) \leq L_J(q\mathbf{x}) + L_J(2q^2\mathbf{1}) \leq L_J(q\mathbf{x}) + 2|J|q^2.$$

Finally, deduce from (S5.20) that

$$q^{-1} \mathbb{P}(F_J(\mathbf{X}_J) \not\leq 1 - q\mathbf{x}) \leq L_J(\mathbf{x}) + 6q,$$

and that

$$\begin{aligned} q^{-1} \mathbb{P}(F_J(\mathbf{X}_J) \not\leq 1 - q\mathbf{x}) &\geq \min \left\{ L_J(\mathbf{x}) - q^{-1} \frac{1}{2} L_J(q\mathbf{x})^2, L_J(\mathbf{x}) + 6q - q^{-1} \frac{1}{2} (L_J(q\mathbf{x}) + 6q^2)^2 \right\} \\ &\geq \min \left\{ L_J(\mathbf{x}) - \frac{9}{2}q, L_J(\mathbf{x}) + 6q - q^{-1} \frac{1}{2} (3q + 3q^2)^2 \right\} \\ &= L_J(\mathbf{x}) - 12q. \end{aligned}$$

We have established an approximation similar to what is desired, but for the probabilities $\mathbb{P}(F_J(\mathbf{X}_J) \not\leq 1 - q\mathbf{x})$ by the functions L_J :

$$(S5.21) \quad \left| q^{-1} \mathbb{P}(F_J(\mathbf{X}_J) \not\leq 1 - q\mathbf{x}) - L_J(\mathbf{x}) \right| \leq 12q.$$

We shall use this result to complete the proof.

For $i \in V$, let $E_i = \{F_i(X_i) > 1 - qx_i\}$. Now, if $J = (i, j)$ has size 2, then

$$\mathbb{P}(F_J(\mathbf{X}_J) > 1 - q\mathbf{x}) = \mathbb{P}(E_i \cap E_j) = qx_i + qx_j - \mathbb{P}(E_i \cup E_j)$$

and

$$R_J(\mathbf{x}) = x_i + x_j - L_J(\mathbf{x}),$$

so the result follows from (S5.21). If $J = (i, j, m)$ has size 3,

$$\begin{aligned} \mathbb{P}(F_J(\mathbf{X}_J) > 1 - q\mathbf{x}) &= \mathbb{P}(E_i \cap E_j \cap E_m) \\ &= \mathbb{P}(E_i \cup E_j \cup E_m) - \mathbb{P}(E_i \cup E_j) - \mathbb{P}(E_i \cup E_m) - \mathbb{P}(E_j \cup E_m) \\ &\quad + \mathbb{P}(E_i) + \mathbb{P}(E_j) + \mathbb{P}(E_m) \\ &= \mathbb{P}(E_i \cup E_j \cup E_m) - \mathbb{P}(E_i \cup E_j) - \mathbb{P}(E_i \cup E_m) - \mathbb{P}(E_j \cup E_m) \\ &\quad + qx_i + qx_j + qx_m, \end{aligned}$$

and similarly

$$R_J(\mathbf{x}) = L_J(\mathbf{x}) - L_{ij}(x_i, x_j) - L_{im}(x_i, x_m) - L_{jm}(x_j, x_m) + x_i + x_j + x_m,$$

so the result again follows by applying (S5.21) to approximate each of the four probabilities above by the corresponding L terms. \square